2020

# Mechanisms of anthocyanin-enrich Riceberry rice extract (Oryza sativa L.) on the regulation of nutrient metabolisms and adipogenesis

Phutthida Kongthitilerd
*Graduate School*

# Mechanisms of anthocyanin-enrich Riceberry rice extract (Oryza sativa L.) on the regulation of nutrient metabolisms and adipogenesis

Miss Phutthida Kongthitilerd



A Dissertation Submitted in Partial Fulfillment of the Requirements
for the Degree of Doctor of Philosophy in Biomedical Sciences
Inter-Department of Biomedical Sciences
GRADUATE SCHOOL
Chulalongkorn University
Academic Year 2020

# กลไกของสารสกัดแอนโทไซยานินจากข้าวไรซ์เบอร์รี่ต่อการควบคุมเมแทบอลิซึมของสารอาหารและอะดิโพเจนเนซิส

น.ส.พุทธิดา คงธิติเลิศ



วิทยานิพนธ์นี้เป็นส่วนหนึ่งของการศึกษาตามหลักสูตรปริญญาวิทยาศาสตรดุษฎีบัณฑิต
สาขาวิชาชีวเวชศาสตร์ สหสาขาวิชาชีวเวชศาสตร์
บัณฑิตวิทยาลัย จุฬาลงกรณ์มหาวิทยาลัย
ปีการศึกษา 2563

| | |
|---|---|
| Thesis Title | Mechanisms of anthocyanin-enrich Riceberry rice extract (Oryza sativa L.) on the regulation of nutrient metabolisms and adipogenesis |
| By | Miss Phutthida Kongthitilerd |
| Field of Study | Biomedical Sciences |
| Thesis Advisor | Professor SIRICHAI ADISAKWATTANA, Ph.D. |
| Thesis Co Advisor | Associate Professor Henrique Cheng, D.V.M, Ph.D. |
| | TANYAWAN SUANTAWEE, Ph.D. |

Accepted by the GRADUATE SCHOOL, Chulalongkorn University in Partial Fulfillment of the Requirement for the Doctor of Philosophy

..... Dean of the GRADUATE SCHOOL
(Associate Professor THUMNOON NHUJAK, Ph.D.)

DISSERTATION COMMITTEE

..... Chairman
(Assistant Professor AMORNPUN SEREEMASPUN, M.D., Ph.D.)

..... Thesis Advisor
(Professor SIRICHAI ADISAKWATTANA, Ph.D.)

..... Thesis Co-Advisor
(Associate Professor Henrique Cheng, D.V.M, Ph.D.)

..... Thesis Co-Advisor
(TANYAWAN SUANTAWEE, Ph.D.)

..... Examiner
(Assistant Professor SATHAPORN NGAMUKOTE, Ph.D.)

..... Examiner
(THITITIP TIPPAYAMONTRI, Ph.D.)

..... External Examiner
(Thavaree Thilavech, Ph.D.)

พุทธิดา คงธิติเลิศ : กลไกของสารสกัดแอนโทไซยานินจากข้าวไรซ์เบอร์รี่ต่อการควบคุมเมแทบอลิซึมของสารอาหารและอะดิโพเจนเนซิส. ( Mechanisms of anthocyanin-enrich Riceberry rice extract (Oryza sativa L.) on the regulation of nutrient metabolisms and adipogenesis) อ.ที่ปรึกษาหลัก : ศ. ดร.สิริชัย อดิศักดิ์วัฒนา, อ.ที่ปรึกษาร่วม : รศ. ดร.เฮนริก เชงD.V.M,ดร.ธันยวัน สวนทวี

ข้าวไรซ์เบอร์รี่เป็นข้าวไม่ขัดสีสายพันธุ์ใหม่ของประเทศไทยที่อุดมไปด้วยสารแอนโทไซยานินและมีคุณประโยชน์ต่อสุขภาพหลากหลาย การศึกษานี้มีวัตถุประสงค์เพื่อศึกษาฤทธิ์ของสารสกัดข้าวไรซ์เบอร์รี่ต่อการเจริญเติบโตและการพัฒนาเป็นเซลล์ไขมันของเซลล์ 3T3-L1 รวมถึงศึกษากลไกของสารสกัดข้าวไรซ์เบอร์รี่และสารพฤกษเคมีในข้าวไรซ์เบอร์รี่ต่อการหลั่งอินซูลินจากเซลล์ตับอ่อนชนิดเบต้า (INS-1 cells) ผลการศึกษาในเซลล์ไขมัน 3T3-L1 พบว่า สารสกัดข้าวไรซ์เบอร์รี่สามารถยับยั้งการเจริญเติบโตของเซลล์ไขมันได้โดยชะลอวัฏจักรของเซลล์อย่างไม่เป็นพิษต่อเซลล์ รวมทั้งยับยั้งการแสดงออกของยีนหลักที่ควบคุมกระบวนการพัฒนาของเซลล์ไขมัน ส่งผลลดจำนวนเซลล์ไขมันและลดระดับไขมันสะสมในเซลล์ได้ นอกจากนี้ยังสามารถชะลอการดูดซึมน้ำตาลเข้าสู่เซลล์ไขมันโดยยับยั้งการแสดงออกของโปรตีนขนส่งน้ำตาลที่ผิวเซลล์ และกระตุ้นการสลายไขมันจากเซลล์ได้อีกด้วย ทั้งนี้สารสกัดข้าวไรซ์เบอร์รี่และสารพฤกษเคมีในข้าวไรซ์เบอร์รี่ไม่มีผลต่อระดับแคลเซียมทั้งในเซลล์ไขมันและเซลล์ตับอ่อน อย่างไรก็ตามผลการศึกษาในเซลล์ตับอ่อน INS-1 พบว่าสารไซยานิดิน-3-รูติโนไซด์ซึ่งสังเคราะห์จากสารรูตินที่พบในสารสกัดข้าวไรซ์เบอร์รี่สามารถกระตุ้นการหลั่งอินซูลินได้ โดยกระตุ้นการนำเข้าของแคลเซียมผ่านทางตัวขนส่งแคลเซียมชนิด L-type voltage-dependent (VDCCs) และกระตุ้นกลไก PLC-$IP_3$ นอกจากนี้ยังส่งเสริมการแสดงออกของยีนที่เกี่ยวข้องกับกระบวนการหลั่งอินซูลินอย่างไม่เป็นพิษต่อเซลล์อีกด้วย ผลการศึกษาข้างต้นใช้เป็นข้อมูลสนับสนุนประโยชน์ของสารแอนโทไซยานินในการป้องกันโรคอ้วน โรคเบาหวาน และภาวะอ้วนลงพุง



สาขาวิชา ชีวเวชศาสตร์ ลายมือชื่อนิสิต .....
ปีการศึกษา 2563 ลายมือชื่อ อ.ที่ปรึกษาหลัก .....
ลายมือชื่อ อ.ที่ปรึกษาร่วม .....
ลายมือชื่อ อ.ที่ปรึกษาร่วม .....

## 5987783320 : MAJOR BIOMEDICAL SCIENCES

KEYWORD: Riceberry rice, Anthocyanin, Adipogenesis, Cyanidin-3-rutinoside, Insulin secretion, Beta cells

Phutthida Kongthitilerd : Mechanisms of anthocyanin-enrich Riceberry rice extract (Oryza sativa L.) on the regulation of nutrient metabolisms and adipogenesis. Advisor: Prof. SIRICHAI ADISAKWATTANA, Ph.D. Co-advisor: Assoc. Prof. Henrique Cheng, D.V.M, Ph.D., TANYAWAN SUANTAWEE, Ph.D.

Riceberry rice, a new pigmented rice variety from Thailand, contained high anthocyanin content and expressed various biological activities. This study aimed to investigate the anti-obesity effects of Riceberry rice extract (RBE) in 3T3-L1 preadipocytes and to identify the mechanism of RBE and its phytochemicals on insulin secretion from pancreatic INS-1 cells. In 3T3-L1 cells, RBE inhibited preadipocyte proliferation by inducing cell cycle arrest without causing cytotoxicity. During adipogenesis, RBE downregulated transcription factor and adipogenic gene expression leading to the decrease in adipocyte number and triglyceride accumulation. Moreover, RBE reduced glucose uptake by downregulating glucose transporter 4 gene expression and enhanced lipolysis. RBE and its phytochemicals had no effect on intracellular calcium signaling in both preadipocytes and pancreatic β-cells. However, cyanidin-3-rutinoside (C3R) which synthesized from rutin presenting in RBE stimulated insulin secretion by promoting calcium influx via L-type voltage-dependent calcium channels (VDCCs) and activating the PLC-$IP_3$ pathway. Furthermore, C3R upregulated glucose-induced insulin secretion gene expression without cytotoxicity. These findings support the benefits of anthocyanins on the prevention of obesity, diabetes, and metabolic syndrome.



| | | |
|---|---|---|
| Field of Study: | Biomedical Sciences | Student's Signature ..... |
| Academic Year: | 2020 | Advisor's Signature ..... |
| | | Co-advisor's Signature ..... |
| | | Co-advisor's Signature ..... |

# ACKNOWLEDGEMENTS

Firstly, I really would like to thank my thesis advisors, Professor Dr. Sirichai Adisakwattana, Associate Professor Dr. Henrique Cheng and Dr. Tanyawan Suantawee for their meaningful guidance that motivate me into the right direction throughout my Ph.D. program. Moreover, I also would like to thank all committees: Assistant Professor Dr. Amornpun Sereemaspus, MD, Assistant Professor Dr. Sathaporn Ngamukote, Dr. Thititip Tippayamontri, and Dr. Thavaree Thilavech for all professional suggestions.

My sincerely thank goes to Dr. Thavaree Thilavech, Dr. Weerachat Sompong, and Dr. Tanyawan Suantawee for training me and provided very helpful advices. In addition, I would like to thank all colleagues in Phytochemical and Functional Food Research Unit for Clinical Nutrition for their support and good collaboration. Besides, I have to thank Dutsadi Phiphat scholarship and Department of Nutrition and Dietetics, Faculty of Allied Health Sciences, Chulalongkorn University.

Special thank goes to Dr. Cheng for supporting, taking good care of me, and providing many great experiences, along with my lab mates, Dhruthi Sing and Amit Sharma for encouraging me when I conducted the research at Department of Comparative Biomedical Sciences, School of Veterinary Medicine, Louisiana State University, Baton Rouge, LA, USA. While I stayed there, I got many good cares from Thai people in Baton Rouge that made me felt like home.

The last but not least, I totally appreciate my dearest family, my lovely friends, especially, Sasikarn Looprasertkul, Netima Deeswasmongkol, Napassorn Tiensermsub, Siriwan Chumroenvidhayakul, Pilailak Channuwong and Sakawrut Poosri and my beloved Chawarach Tanphongphiphatchai who always make me smile, stay by my side, hold my hand tight, give me warm hugs, and support everything I decided to do until I achieve the Ph.D. program.

Phutthida Kongthitilerd

# TABLE OF CONTENTS

Page

# List of tables

Page

# List of figures

Page

**Table 1** List of abbreviations

| Abbreviations | Full name |
|---|---|
| ACC | Acetyl CoA carboxylase |
| AdipoQ | Adiponectin |
| AdipoQ-R1, R2 | Adiponectin receptor-1,2 |
| Akt1 | Protein kinase B |
| 2-APB | 2-Aminoethoxydiphenyl borate |
| aP2/Fabp4 | Fatty acid binding protein 4 |
| ATGL | Adipose triglyceride lipase |
| β-actin | Beta-actin |
| C3G | Cyanidin-3-*O*-glucoside |
| C3R | Cyanidin-3-*O*-rutinoside |
| cAMP | Cyclic adenosine monophosphate |
| CA | *p*-Coumaric acid |
| $[Ca^{2+}]_i$ | Intracellular calcium concentration |
| $Cav_{1.2}$ | L-type calcium channel subunit |
| Cy | Cyanidin |
| CE | Catechin equivalent |
| C/EBPα,β,γ | CCAAT-enhancer binding protein-alpha,beta,gamma |
| DAG | Diacylglycerol |
| EGTA | Ethylene glycol-bis(2-aminoethylether)-N,N,N´,N´-tetraacetic acid |
| ER | Endoplasmic reticulum |
| FA | Ferulic acid |
| FAS/FasN | Fatty acid synthase |
| Fura-2AM | Fura-2 acetoxymethyl ester |
| GAE | Gallic acid equivalent |
| GK | Glucokinase |
| Glut2 | Glucose transporter 2 |
| Glut4 | Glucose transporter 4 |

| Abbreviations | Full name |
|---|---|
| GSIS | Glucose-stimulated insulin secretion |
| HPLC | High performance liquid chromatography |
| HSL | Hormone-sensitive lipase |
| IBMX | 3-isobutyl-1-methylxanthine |
| Ins | Insulin |
| InsR | Insulin receptor |
| $IP_3$ | Inositol triphosphate |
| $IP_3R$ | Inositol triphosphate receptor |
| $K_{ATP}$ | ATP-sensitive $K^+$ channel |
| $Kir_{6.2}$ | ATP-sensitive $K^+$ channel subunit |
| LPL | Lipoprotein lipase |
| MTT | 3-(4,5-dimethylthiazol-2-yl)-2,5-diphenyl tetrazolium bromide |
| 2-NBDG | 2-(*N*-(7-Nitrobenz-2-oxa-1,3-diazol-4-yl) amino)-2-Deoxyglucose |
| P3G | Peonidin-3-*O*-glucoside |
| PCA | Protocatechuic acid |
| $PIP_2$ | Phosphatidylinositol 4,5-bisphosphate |
| PKA | Protein kinase A |
| PLC | Phospholipase C |
| PPARγ | Peroxisome proliferator-activated receptor-gamma |
| RBE | Riceberry rice extract |
| SOCs | Store-operated calcium channels |
| TG | Thapsigargin |
| UHPLC-MS/MS | Ultra-high performance liquid chromatography mass spectrometry |
| VDCCs | Voltage-dependent calcium channels |
| WAT | White adipose tissue |

# Chapter I
# Introduction

## 1.1 Background of the study

Metabolic syndrome is a complex disorder of metabolism including dyslipidemia, hypertension, and hyperglycemia (Grundy *et al*. 2004, Kassi *et al*., 2011). Obesity, especially abdominal obesity, is mostly related to metabolic syndrome (Tchernof and Després, 2013). Obesity is defined as excess body fat accumulation due to the imbalance between energy intake and energy expenditure. Excess energy is stored as lipid accumulation in adipose tissue, which plays an important role in energy homeostasis and nutrient metabolism via glucose uptake, lipogenesis, adipokines secretion, and lipolysis (Engin and Engin, 2017). The expansion of white adipose tissue by increasing fat-cell size (hypertrophy) and fat-cell number (hyperplasia) is a typical characteristic of obesity (Rutkowski *et al*., 2015). White adipose tissue consists of adipocytes and preadipocytes. Hyperplasia or increasing fat-cell number is caused by proliferation of preadipocytes and differentiation to adipocytes or adipogenesis (Luo and Liu, 2016). The adipogenesis mechanism involves cascade of transcription factors. Initially, C/EBPβ is activated by IBMX and C/EBPδ by dexamethasone in the early phase of adipogenesis (Lowe *et al*., 2011). After that, C/EBPβ stimulates C/EBPα and PPARγ which are key regulators of adipogenesis (Lowe *et al*., 2011). Moreover, adipogenesis is induced and maintained by insulin which stimulates C/EBPα and PPARγ via the PI3K-Akt1 signaling pathway (Boucher *et al*., 2014). Consequently, C/EBPα and PPARγ activate the expression of adipogenic genes leading to preadipocyte differentiation, glucose uptake, fatty acid transportation, and lipogenesis (Lowe *et al*., 2011). In addition, intracellular calcium signaling is a mechanism underlying the control of adipocyte function (Tran *et al*., 2014, Tran *et al*., 2015). Furthermore, hypertrophy or an increase in fat-cell size results from excessive synthesis and accumulation of triglyceride in lipid droplets through the lipogenesis pathway (Luo and Liu, 2016). The hypertrophic

adipocytes express and secrete pro-inflammatory cytokines leading to insulin resistance and β-cells dysfunction, a cause of metabolic syndrome (Choe *et al*., 2016, Pepin *et al*., 2016). Therefore, inhibition of preadipocyte proliferation and differentiation or stimulation of lipolysis could prevent obesity and metabolic syndrome.

Studies show that β-cells dysfunction during obesity is associated with inflammatory cytokines secretion from hypertrophic adipocytes (Watanabe *et al*., 2013) and increase in ROS production and oxidative stress (Hasnain *et al*., 2016). Insulin from pancreatic β-cells is a major hormone controlling glucose homeostasis and metabolism (care, 2014). Normally, insulin secretion is stimulated by an increase in plasma glucose via the glucose-stimulated insulin secretion (GSIS) pathway. Glucose is transported through glucose transporter 2 (Glut2) and phosphorylated to glucose-6-phosphate using glucokinase enzyme (GK). After its metabolism, ATP/ADP ratio increases and induces ATP-sensitive potassium channels ($K_{ATP}$) closure. This is followed by cell membrane depolarization leading to voltage-dependent calcium channels (VDCCs) opening and calcium influx. The increase in intracellular calcium concentration stimulates insulin secretion (Mears, 2004). Consequently, stimulation of insulin secretion from pancreatic β-cells could also prevent metabolic syndrome.



General approaches to prevent metabolic syndrome are lifestyle modifications by caloric restriction and increasing physical activity. Moreover, medications are also prescribed but there are many adverse effects. Hence, anti-obesity and anti-diabetic compounds found in plants represent an alternative approach for the prevention of metabolic syndrome. Anthocyanins are water-soluble phenolic compounds found in purple, red, or blue plants. The six most common anthocyanins are cyanidin (Cy), delphinidin (Dp), malvidin (Mv), peonidin (Pn), pelargonidin (Pg), and petunidin (Pt) (Ghosh, 2005). There are many health benefits of anthocyanins such as antioxidant, prevention of cardiovascular disease, anti-cancer, neuroprotection effect, anti-obesity, and anti-diabetic effects (Khoo *et al*., 2017).

Studies revealed that the anti-obesity effect of anthocyanin is due to cell cycle arrest, decreased lipid accumulation via downregulation of transcription factors, and lipolysis (Rahman *et al*., 2016). In addition, anthocyanin extracts from fermented blueberry juice (Sánchez-Villavicencio *et al*., 2017), cranberry (Kowalska *et al*., 2014, Kowalska *et al*., 2015), blue pea flower (Chayaratanasin *et al*., 2019), and blueberry peel (Song *et al*., 2013) inhibits adipogenesis and lipogenesis in 3T3-L1 cells. Recently, source of anthocyanins was reported in Riceberry rice, a new variety of rice from Thailand. Riceberry rice is a dark-purple rice that originated from Khoa Dawk Mali 105 rice and Hom Nin rice at the Rice Science Center, Kasetsart University, Thailand. Previous studies show several health benefits of Riceberry rice such as anti-cancer on human cancer cell lines from colon cancer, breast cancer, and acute myeloid leukemia (Leardkamolkarn *et al*., 2011) and on a leukemic mouse model (Somintara *et al*., 2016). Moreover, Riceberry rice bran extract has antioxidant and cytoprotective effects from oxidative damage (Jittorntrum *et al*., 2009), prevents renal dysfunction (Arjinajarn *et al*., 2016), and hepatotoxicity in rats (Arjinajarn *et al*., 2017). Riceberry rice bran oil improves glycemic levels in diabetic rats by upregulating glucose transporter 4 (Glut4) expression in muscle (Ruethaithip and Surasiang, 2011, Kongkachuichai *et al*., 2013, Posuwan *et al*., 2013, Prangthip *et al*., 2013). It also inhibits key enzymes of carbohydrate and lipid digestion and absorption (Poosri *et al*., 2019). Interestingly, Riceberry rice bread consumption improves glycemia and antioxidation activity in heathy subjects (Thiranusornkij *et al*., 2019, Chusak *et al*., 2020). However, there is no study on the anti-obesity effects of Riceberry rice.



Hyperglycemia is one of the metabolic conditions associated with obesity (Watanabe *et al*., 2013). Improvement of pancreatic β-cell function could help control postprandial hyperglycemia. The anthocyanin rich Riceberry rice has anti-diabetic properties through several mechanisms. Additional studies show that anthocyanin from mulberry (Lee *et al*., 2015), chokeberry (Rugină *et al*., 2015), purple corn (Hong *et al*.,

2013), and Cornus fruits (Jayaprakasam *et al*., 2005) prevents β-cell death from oxidative stress while stimulating insulin secretion. In addition, anthocyanins and their derivatives such as cyanidin (Cy), cyanidin-3-glucoside (C3G), and cyanidin-3-rutinoside (C3R), are major anthocyanins in many plants and can improve pancreatic β-cells function. A study showed that Cy stimulates insulin secretion by activating calcium influx through L-type VDCCs and upregulating Glut2, $Kir_{6,2}$, and $Cav_{1.2}$ genes expression in INS-1 cells (Suantawee *et al*., 2017). Moreover, C3G isolated from *Lonicera caerulea* fruit increases insulin secretion by enhancing phosphorylation of the insulin receptor (InsR), insulin receptor substrate 1 (IRS-1), and phosphoinositide 3-kinase protein (PI3K) in INS-1 cells (Lee *et al*., 2016). C3G from mulberry protects against glucotoxicity-induced apoptosis and induces insulin secretion from pancreatic β-cells (Lee *et al*., 2015). In addition, C3R protects β-cells from glucotoxicity-induced apoptosis by decreasing oxidative stress and enhancing antioxidant enzyme activity in INS-1 cells (Choi *et al*., 2018). C3R also induces insulin secretion by upregulating GK expression and ATP production in MIN-6 cells (Zheng *et al*., 2016). However, the mechanism by which Riceberry rice extract and its phytochemicals, in particular anthocyanin derivatives induce insulin secretion through intracellular calcium signaling is unknown.



Based on the literature, there is a need to investigate the effect of Riceberry rice on obesity (e.g., preadipocyte proliferation and adipogenesis) and its regulation of insulin secretion from pancreatic β-cells.

### 1.2 Research questions

1. What are the phytochemical compounds and major anthocyanins in Riceberry rice extract?

2. How does Riceberry rice extract affect cell proliferation and adipogenesis in preadipocytes?

3. How does Riceberry rice extract and its phytochemicals induce insulin secretion from pancreatic β-cells?

### 1.3 Objectives of the study

1. To investigate the phytochemical compositions and major anthocyanins in Riceberry rice extract.

2. To investigate the effects of Riceberry rice extract on cell proliferation and adipogenesis in 3T3-L1 preadipocytes.

3. To investigate the mechanism of Riceberry rice extract and its phytochemicals on insulin secretion from pancreatic INS-1 cells.

### 1.4 Hypotheses of the study

1. Riceberry rice extract contain high amount of phenolic and flavonoid compounds with cyanidin-3-glucoside being the major anthocyanin.

2. Riceberry rice extract inhibits preadipocyte proliferation and adipogenesis by inducing cell cycle arrest and downregulating major transcription factors and adipogenic gene expression.

3. Riceberry rice extract and its phytochemical compounds stimulate insulin secretion from pancreatic INS-1 cells via an intracellular calcium-dependent mechanism.

1.5 Conceptual framework

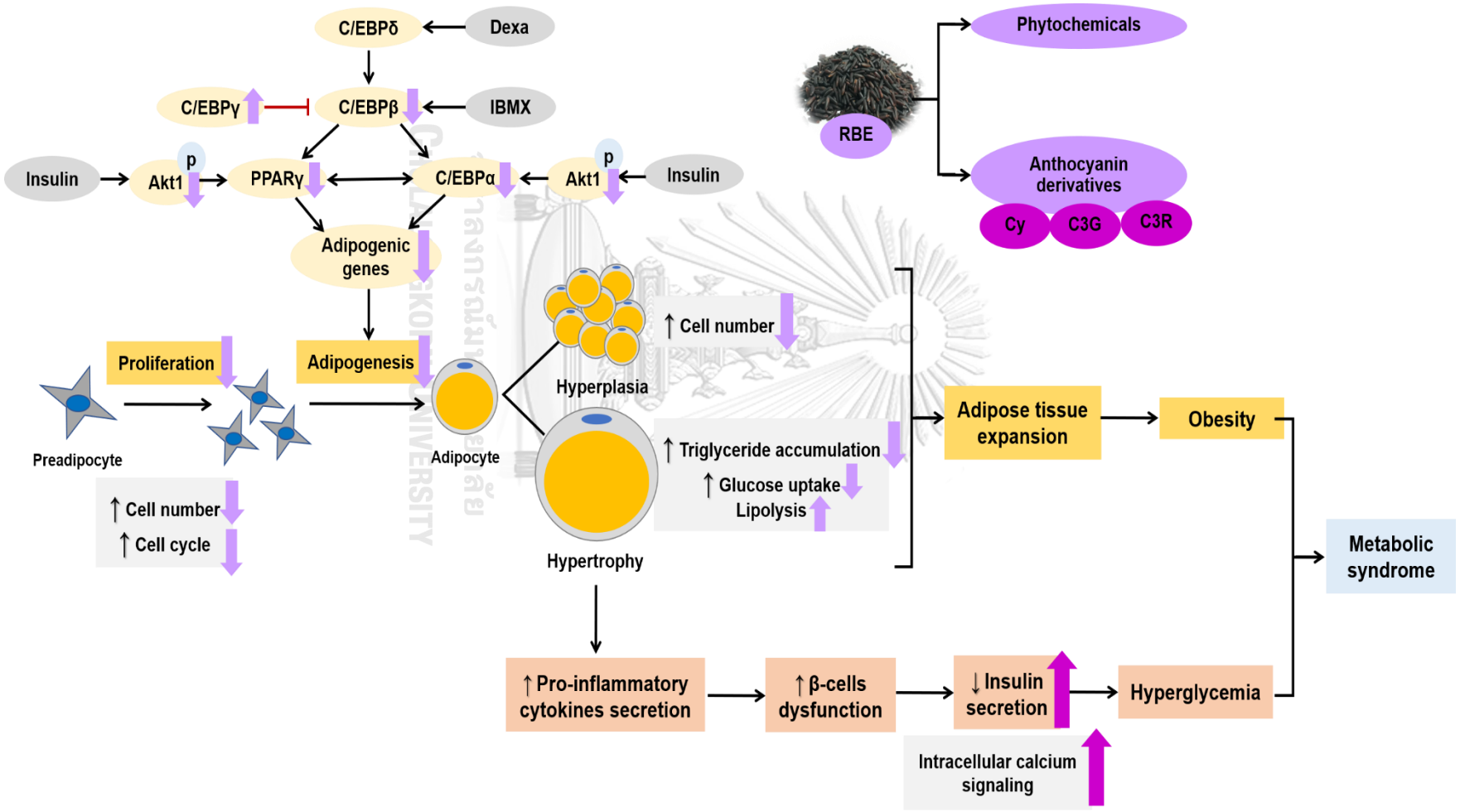

# Chapter II

# Literature review

## 2.1 Metabolic syndrome

Metabolic syndrome is a complex disorder that involves a multiplex risk factor for cardiovascular disease (CVD) (Kassi *et al*., 2011). The National Cholesterol Education Program Adult Treatment Panel III report (ATP III) includes abdominal obesity, dyslipidemia, high blood pressure, insulin resistance, proinflammatory and prothrombotic states as the main components of metabolic syndrome (Grundy *et al*., 2004).

There are several clinical criteria to define metabolic syndrome from the National Cholesterol Education Program (NCEP) Adult Treatment Panel III report (ATP III), World Health Organization (WHO), the International Diabetes Federation (IDF), and the American Association of Clinical Endocrinologists (AACE). The most practical are from the IDF as shown in Table 2, respectively (Saklayen, 2018).

**Table 2** IDF clinical criteria for metabolic syndrome (2006)

| Risk factor | Defining level |
|---|---|
| **Abdominal obesity** (waist circumference) | |
| Men | > 94 cm |
| Women | > 80 cm |
| **Triglycerides** | **≥** 150 mg/dL |
| **HDL cholesterol** | |
| Men | < 40 mg/dL |
| Women | < 50 mg/dL |
| **Blood pressure** | **≥** 130 / 85 mm Hg |
| **Fasting glucose** | **≥** 100 mg/dL |

**IDF = The International Diabetes Federation (Saklayen, 2018)

The incidence of metabolic syndrome is related with obesity and type 2 diabetes. High prevalence of metabolic syndrome is associated with abdominal obesity (Saklayen, 2018). A global survey of obesity in 195 countries, between 1980 and 2015 revealed that there are 604 million obese adults and 108 million children. Moreover, the global rate of death related to high BMI increased by 28.3%, between 1990 and 2015. Based on IDF diabetes atlas, global prevalence of diabetes in 2015 is 8.8% and is expected to increase to 10.4% in 2040 (Saklayen, 2018).

Some studies show the prevalence of metabolic syndrome among the Thai population. In 2003, the prevalence of metabolic syndrome among Thai adults (602 participants) in the Khon Kaen province was 15%. The prevalence increased from 9.5% among the 20-39 age group to 24.7% among the 50+ age group in men, and 7% to 29.5% in women, respectively (Pongchaiyakul *et al*., 2007). In 2011, Aekplakorn, *et al*. reanalyzed the InterASIA data, which is a national cross-sectional survey of cardiovascular risk factors, to determine the prevalence of metabolic syndrome among Thai population (5,305 adults randomly selected from four geographic regions of Thailand). The data indicated that overall prevalence was 24.0% based-on IDF criteria and 32.6% based-on ATP III criteria (Aekplakorn *et al*., 2011). In 2017, based-on ATP III criteria, the overall prevalence of metabolic syndrome among Thai adults (222 participants) in Pathum Thani province was 36.49%. The most significant risk factor related to the increase in metabolic syndrome were BMI ≥23 kg/$m^2$, age group 55-65 years, lack of exercise, and high waist to height ratio (Yuenyongchaiwat *et al*., 2017). Moreover, a study on metabolic syndrome among Thai children (348 participants) in Ongkhaluck province was performed. The overall prevalence in this population was 4.0% and metabolic syndrome was found in 0.7% of non-obese/overweight children and 17.6% of obese/overweight children (Rerksuppaphol *et al*., 2014).

**2.2 Obesity and adipose tissue expansion**

Obesity, especially abdominal obesity, is mostly related with metabolic syndrome (Tchernof and Després, 2013). Obesity is defined as excess body fat accumulation due to the imbalance between energy intake and energy expenditure. Excess energy is stored as lipid accumulation in adipose tissue, which plays an important role in energy homeostasis and nutrient metabolisms (Engin and Engin, 2017). According to Thai National Health Examination Survey (NHES) since 1991, the prevalence of obesity in Thailand has increased more than 2.5 folds over 23 years and will grow at the same rate (Teerawattananon and Luz, 2017). The severity of obesity is related to several diseases such as coronary heart disease by 97%, cancers by 61%, and type 2 diabetes mellitus by 21% (Engin and Engin, 2017). The international standard method to classified obesity in adults is body mass index (BMI) that calculated by following equation:

$$\text{BMI} = \frac{\text{Body weight } (\text{kg})}{\text{Height}^2\ (\text{m})}$$

**Table 3** Obesity classification by body mass index (BMI) in Asian adults

| Classification | BMI ($kg/m^2$) | Risk of metabolic syndrome |
|---|---|---|
| Underweight | < 18.5 | Low risk |
| Normal weight | 18.5 – 22.9 | Average |
| Overweight | 23.0 – 24.9 | Increased |
| Obese class I | 25.0 – 29.9 | Moderate |
| Obese class II | ≥ 30 | Severe |

(WHO, 2004)

Moreover, the body fat distribution is an important factor for health. There are two types of obesity including abdominal obesity or apple shape and peripheral obesity or pear shape as shown in Figure 1 (Karpe and Pinnick, 2015). Abdominal obesity or visceral obesity is the main factor related with metabolic syndrome (Tchernof and Després, 2013).

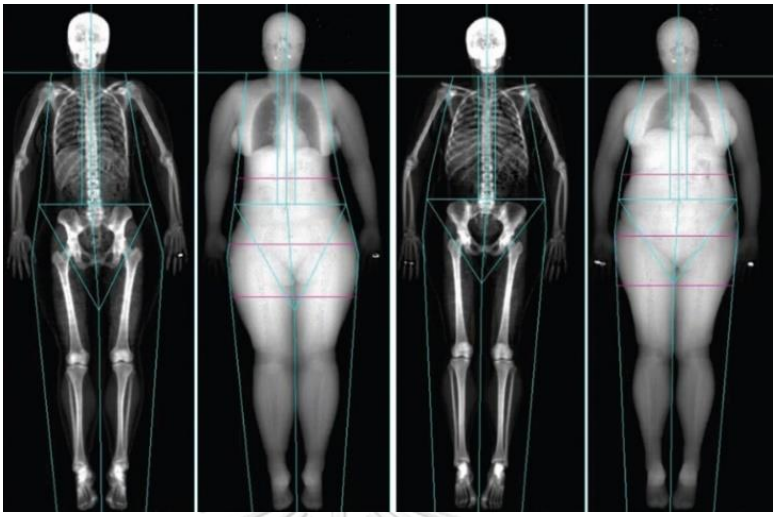

**Figure 1** Different shape of obesity.
Peripheral obesity or pear shape (left) and abdominal obesity or apple shape (right) by dual-energy X-ray absorptiometry (DEXA) for body composition analysis (Karpe and Pinnick, 2015).

There are three major types of adipose tissue with different character and function developed from different lineage including white adipose tissue (WAT), brown adipose tissue (Maki *et al*., 2017), and beige adipocyte as shown in Figure 2 (Gaggini *et al*., 2017).

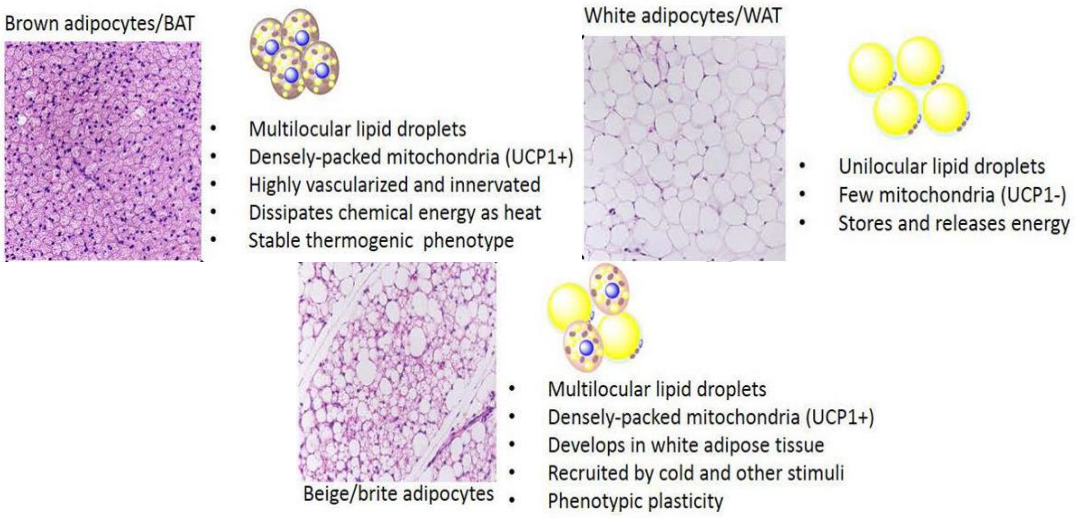


**Figure 2** Different characteristics of adipocytes.

There are three types of adipocytes including white adipocytes with large lipid droplet and few mitochondria that mainly stores energy, beige adipocytes with multilocular lipid droplets and many UCP1-expressing mitochondria develops in WAT, and brown adipocytes (Maki *et al*., 2017) with multilocular lipid droplets and many UCP1-containing mitochondria that can generate heat via thermogenesis (Wang and Seale, 2016).

The largest pool of adipose tissue in the body is WAT representing more than 50% of total body weight in obese adult. WAT is mainly located beneath the skin called 'subcutaneous fat' and surround intra-abdominal organ called 'visceral fat' which are related to abdominal obesity and metabolic syndrome (Choe *et al*., 2016). WAT consists of adipocytes, preadipocytes, endothelial cells, blood cells, fibroblasts, macrophages, and other immune cells (Sarjeant and Stephens, 2012). The expansion of white adipose tissue by increasing fat-cell size (hypertrophy) and fat-cell number (hyperplasia) is a characteristic of obesity as shown in Figure 3 (Rutkowski *et al*., 2015, Choe *et al*., 2016).

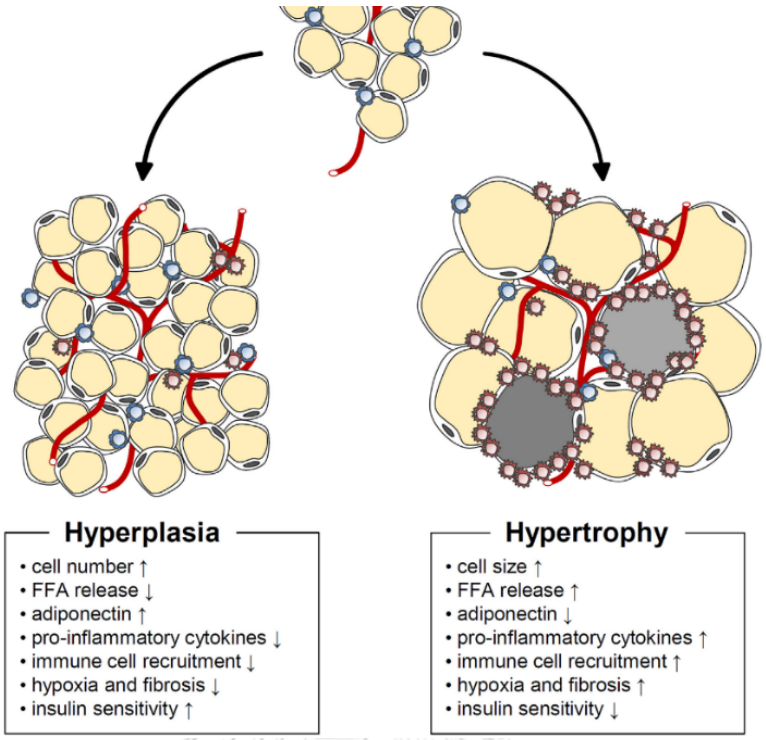


**Figure 3** White adipose tissue expansion.

White adipose tissue expands by increasing fat-cell number (hyperplasia) and increasing fat-cell size (hypertrophy) (Choe *et al*., 2016).

### 2.3 Adipogenesis and adipocyte life cycle

The major component of WAT are adipocytes and preadipocytes. The expansion of WAT depends on adipocyte life cycle including cell proliferation, cell differentiation or adipogenesis, glucose uptake and triglyceride accumulation via lipogenesis. Hyperplasia is caused by proliferation of preadipocytes and differentiation from preadipocytes to adipocytes or adipogenesis (Luo and Liu, 2016). Hypertrophy results from excessive triglyceride accumulation in lipid droplets of adipocytes through the lipogenesis pathway. The hypertrophic adipocytes have elevated expression and secretion of pro-inflammatory cytokines that lead to insulin resistance and metabolic syndrome (Choe *et al*., 2016).

- Cell proliferation

Preadipocytes, a fibroblast-like cells, are adipose precursor cells in adipose tissue (Hausman *et al*., 2001). Cell proliferation is a process of cell growth and division into two daughter cells that is regulated by growth factors through a cell cycle process, which includes G0 (resting state), G1 (first gap), S (DNA synthesis), G2 (second gap), and M (mitotic) phase (Berridge, 2014, Marquez *et al*., 2017). Therefore, inhibition of preadipocyte proliferation by inducing cell cycle arrest could be one mechanism to decrease fat-cell number in adipose tissue.

- Cell differentiation or adipogenesis

The adipose tissue expansion by hyperplasia also increases adipocyte number through the differentiation process. Adipogenesis is defined as the process of preadipocyte differentiation to adipocyte characterized by changes in morphology and function as shown in Figure 4 (Hausman *et al*., 2001). Adipogenesis results from a cascade of transcription factors, especially PPARγ and C/EBPs which are key regulators of adipogenesis (Camp *et al*., 2002, Sarjeant and Stephens, 2012). First, C/EBPβ and C/EBPδ, the key regulators in the early phase of adipogenesis bind to promoters of PPARγ and C/EBPα. Then, PPARγ and C/EBPα upregulate the expression of adipogenic genes involved in lipogenesis (aP2, ACC, FasN), glucose uptake (Glut4), adipokines secretion (adiponectin, leptin, resistin) and lipolysis (perilipin, HSL, ATGL) (Lowe *et al*., 2011). Consequently, downregulation of key adipogenic transcription factors could be one major mechanism to prevent obesity.

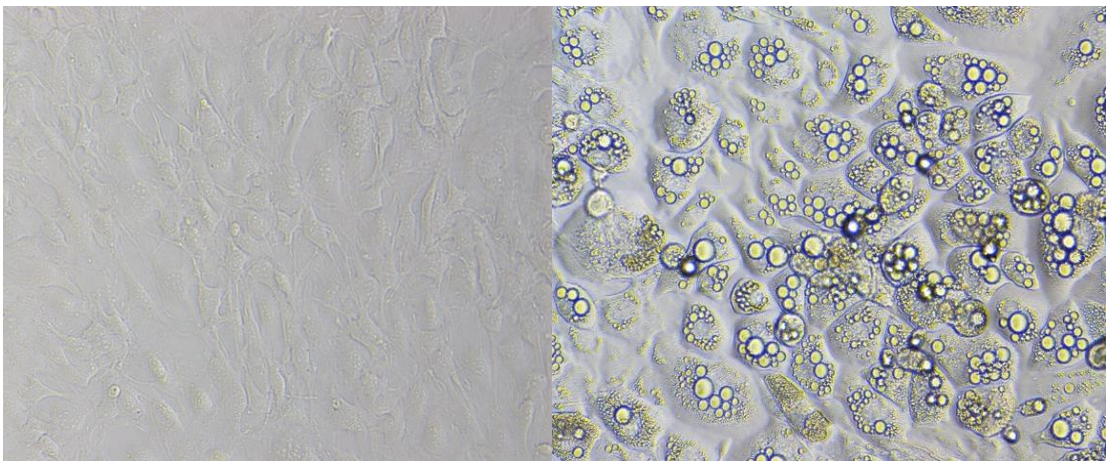

**Figure 4** Characteristics of preadipocytes and adipocytes.
(Left) Preadipocytes are fibroblast-like shape with no lipid droplets in their cytosol. (Right) Adipocytes are round shape with many lipid droplets in their cytoplasm (Hausman *et al*., 2001).

- Lipogenesis

Hypertrophy involves in adipose tissue expansion due to excess triglyceride accumulation in lipid droplets (Choe *et al*., 2016). The precursors of lipogenesis are fatty acids that are transported by passive diffusion into the cell and glucose transported via Glut4 (Guo *et al*., 2009). Glucose is metabolized to acetyl CoA in mitochondria then converted to malonyl CoA in the cytosol by ACC (Tang *et al*., 2007), which is one of the rate-limiting enzymes of lipogenesis (Luo and Liu, 2016). Next, fatty acids are produced by FasN (Fasshauer and Paschke, 2003), which is another rate-limiting enzyme. After that, fatty acid on fatty-acid binding protein (aP2) in the cytosol is converted to fatty acyl-CoA by acyl-CoA synthetase enzyme. Finally, triglycerides are synthesized in the ER through esterification of fatty acids by diacylglycerol acyltransferase (DGAT) enzyme, which is a critical step in triglycerides synthesis. Triglycerides are neutral lipids that are stored in core of lipid droplets in adipocyte as shown in Figure 5 (Luo and Liu, 2016). Therefore, the decrease in triglyceride

accumulation by inhibiting rate-limiting enzyme of lipogenesis could be another mechanism to prevent obesity.

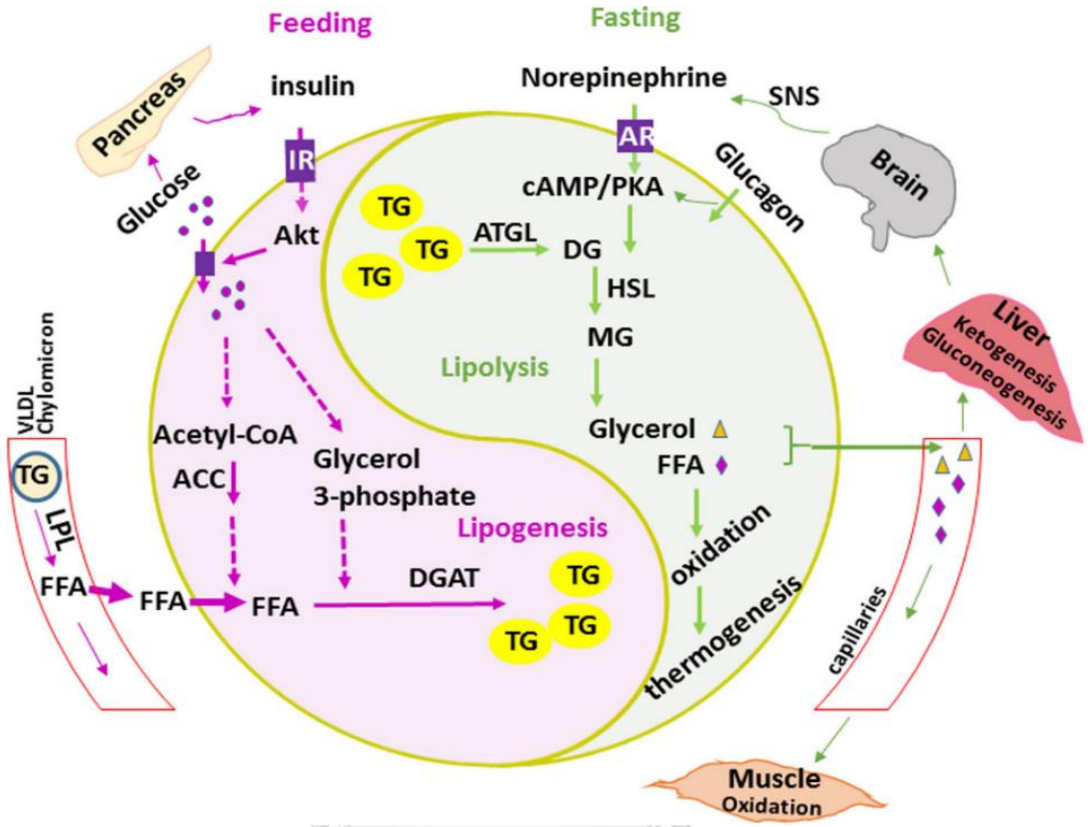


**Figure 5** Lipid metabolism in adipocyte.

Lipogenesis is a triglyceride accumulation process in adipocytes in response to insulin during a feeding state. Lipolysis is the triglyceride breakdown process during fasting state or exercising (Luo and Liu, 2016).

- Glucose uptake

Glucose is one of the substrates for lipogenesis, and its uptake by adipocytes is another important means to regulate glucose homeostasis and nutrient metabolism in response to insulin. Normally, Glut4 is expressed in insulin-sensitive cells including skeletal muscle, cardiac muscle, and adipocyte but not expressed in preadipocytes (Ducluzeau *et al.*, 2002, Brewer *et al.*, 2014). Insulin is a major regulator of glucose uptake by promoting Glut4

translocation via the PI3K-Akt signaling pathway. After stimulation by insulin, Glut4 in intracellular storage vesicles in cytosol are translocated, docked, and fused to the plasma membrane (James, 2005, Leney and Tavaré, 2009). A reduction in glucose uptake by inhibiting Glut4 expression and translocation could be one of mechanism to decrease triglyceride accumulation in adipocytes.

- Adipokine secretion

Adipose tissue acts as an endocrine organ by secreting adipocytokines or 'adipokines' that regulate nutrient metabolism and energy homeostasis. The most important adipokines related with metabolic syndrome are adiponectin, leptin, and resistin (Zhang *et al.*, 2015). Adiponectin (AdipoQ), an adipocyte complement-related-protein of 30 kDa (ACRP30) plays a role on glucose and lipid metabolisms in insulin-sensitive cells as an endogenous insulin-sensitizer. The structure of adiponectin consists of N-terminal collagen-like domain and C-terminal globular domain. The adiponectin receptors are G-protein-coupled including AdipoR1, which is expressed in skeletal muscle, and AdipoR2, expressed in liver and adipose tissue. Adiponectin reduces plasma glucose and fatty acids concentration by promoting fatty acid oxidation and glucose uptake in muscle and by reducing lipid synthesis and gluconeogenesis in liver. Plasma adiponectin levels are negative correlated with obesity, insulin resistance, type 2 diabetes, and metabolic syndrome. Adiponectin deficiency leads to insulin resistance, obesity, type 2 diabetes, and atherosclerosis. Type 2 diabetic patients have decreased blood adiponectin levels (Fasshauer and Paschke, 2003, Meier and Gressner, 2004, Rabe *et al.*, 2008, Zhang *et al.*, 2015). Resistin, 12.5 kDa cysteine-rich hydrophobic signal peptide cleaved before secretion, acts as an insulin antagonist. High serum resistin are associated with obesity, insulin resistance, and type 2 diabetes progression. In obese or insulin resistance models, resistin concentration is increased (Meier and Gressner,

2004, Zhang *et al*., 2015). Leptin, 16 kDa protein, plays a key role on body weight by suppressing appetite and promoting energy expenditure via the central nervous system, especially hypothalamus. Obese people express high serum leptin concentration. Leptin resistance and hyperleptinemia is important for the development of insulin resistance (Meier and Gressner, 2004, Zhang *et al*., 2015). The effects of adipokines on metabolic syndrome and the regulation of adipokine secretion from adipocytes could be important for metabolic syndrome prevention.

- Lipolysis

Another major function of adipocytes is to regulate lipid metabolism via triglyceride breakdown or lipolysis. In general, there are two processes of lipolysis including basal lipolysis and stimulated lipolysis as shown in Figure 6 (Bolsoni-Lopes *et al*., 2015). For stimulated lipolysis, β3-adrenergic receptor (G-protein-coupled receptor) is activated for lipolysis via the cAMP-PKA pathway. Protein kinase A (PKA) stimulates perilipin, HSL, and ATGL enzyme by direct phosphorylation (Duncan *et al*., 2007, Guo *et al*., 2009). The phosphorylated perilipin, which are membrane proteins on lipid droplet allows lipase enzymes to reach the neutral lipid core (Tansey *et al*., 2004). Subsequently, triglyceride is hydrolyzed to diacylglycerol (DAG) and free fatty acid (Graham *et al*., 2004) by p-ATGL. Then, DAG is hydrolyzed to monoacylglycerol (Bardy *et al*., 2013) and FFA by p-HSL. Finally, MAG is hydrolyzed to free glycerol and FFA by monoacylglycerol lipase (MGL). Free fatty acids are used as substrate to provide cellular ATP via the β-oxidation or to generate heat via thermogenesis in mitochondria (Bolsoni-Lopes *et al*., 2015). Activation of lipolysis could decrease adipose tissue expansion and be used to treat obesity.

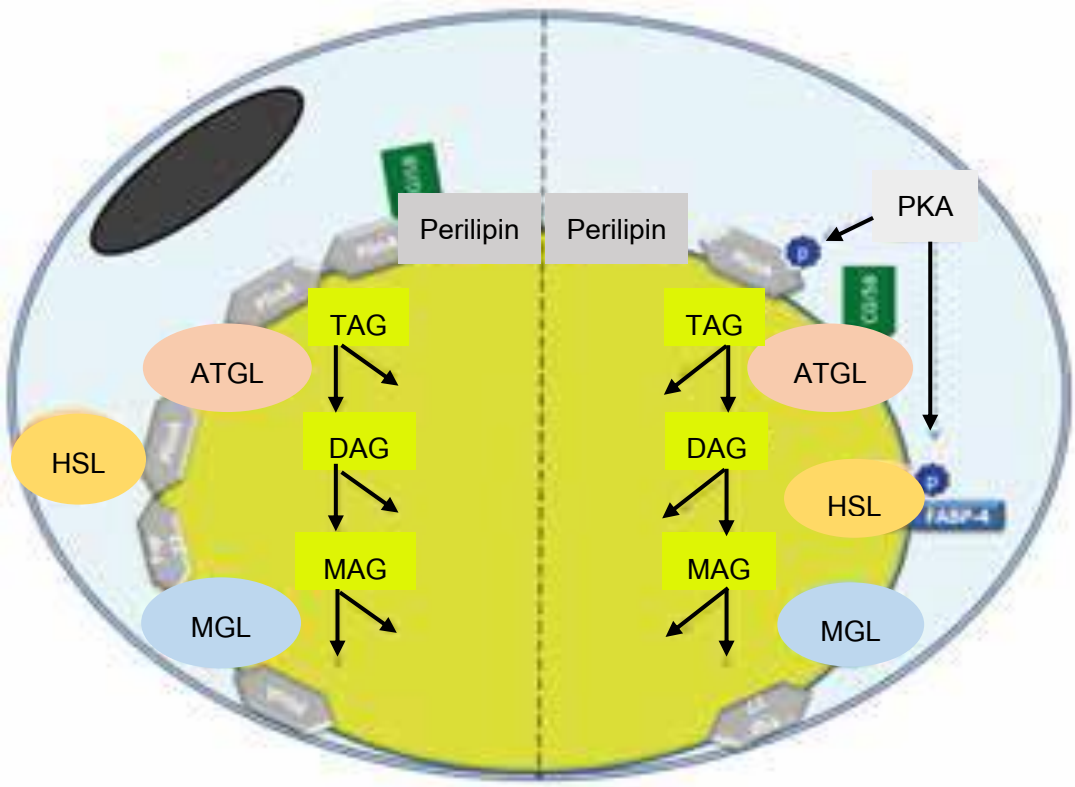


**Figure 6** Lipolysis pathways.

(Left) Basal lipolysis, (Right) stimulated-lipolysis via cAMP-PKA signaling pathway, and sequential hydrolysis of triglyceride in lipid droplet (Bolsoni-Lopes *et al.,* 2015).

### 2.4 Obesity and pancreatic β-cells dysfunction

The effects of white adipose tissue expansion during obesity, especially hypertrophic adipocytes, is inflammation associated with pancreatic β-cells dysfunction. In lean adipose tissue, adipocytes secrete anti-inflammatory cytokines including IL-4, IL-13, and IL-10 that suppress inflammation in adipose tissue. In obese adipose tissue, hypertrophic adipocytes promote inflammation by secreting pro-inflammatory cytokines including TNFα (tumor necrosis factor-α), MCP-1 (monocyte chemotactic protein-1), and IL-6 (interleukin-6) that recruit macrophages filtration into adipose tissue. Then, chronic inflammation in visceral adipose tissue induces macrophages accumulation in pancreatic islets that lead to β-cells apoptosis and decrease in islet mass. Studies show that cytokines secreted from macrophages including TNFα and IL-1β can inhibit insulin secretion from pancreatic β-cells as shown in Figure 7 (Watanabe *et al*., 2013).

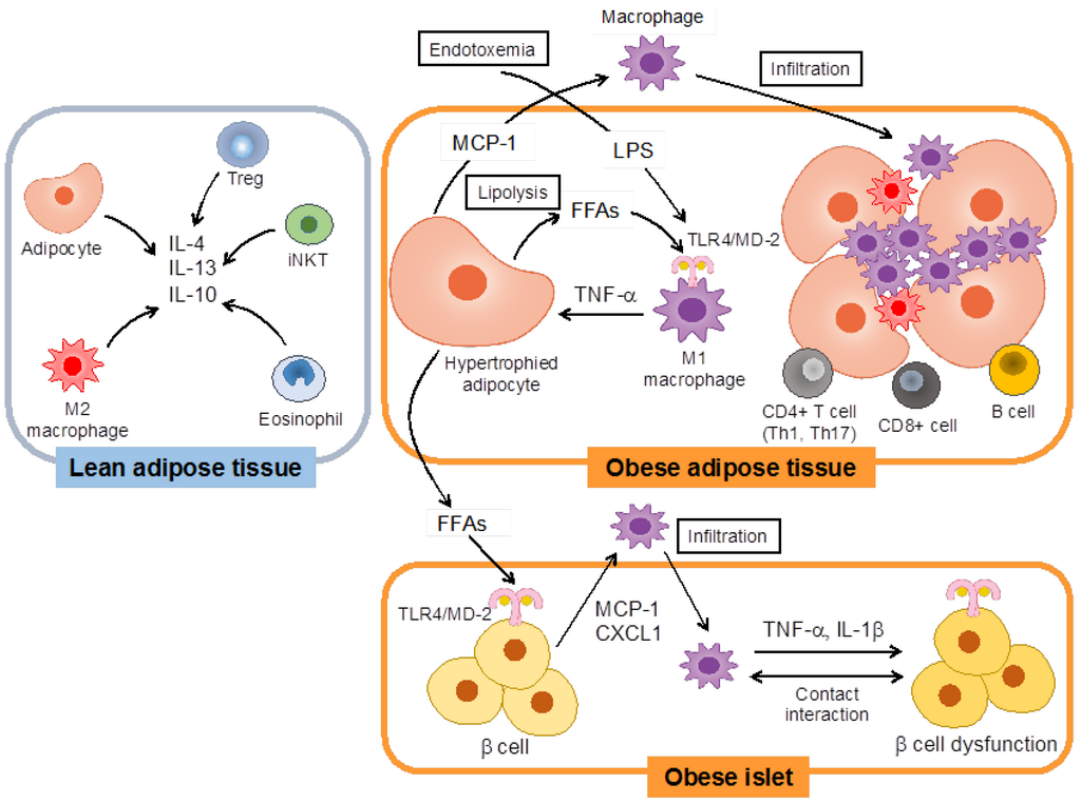


**Figure 7** Obesity induced β-cells dysfunction.

Obese adipose tissue secrete pro-inflammatory cytokines from hypertrophic adipocytes leading to inflammatory changes and pancreatic β-cells dysfunction (Watanabe *et al*., 2013).



Furthermore, another factor that induce pancreatic β-cells dysfunction is oxidative stress (Hasnain *et al*., 2016). Normally, reactive oxygen species (ROS) and free radicals such as superoxide ($O_2^{\cdot-}$), hydroxyl radical (OH·), hydrogen peroxide ($H_2O_2$), nitric oxide (NO·) are generated in mitochondria during nutrient metabolism. The high nutrient load can induce β-cells dysfunction and death via oxidative stress (Andrikopoulos, 2010). Therefore, the antioxidant enzymes such as catalase, superoxide dismutase (Matsukawa *et al*., 2016), and glutathione speroxidase are required for β-cell protection against ROS and oxidative stress (Tang *et al*., 2007). Consequently, the anti-

obesity and antioxidant effects of anthocyanins could improve pancreatic β-cell function by inducing insulin secretion.

### 2.5 Insulin secretion from pancreatic β-cells

Insulin secretion is a major function of pancreatic β-cells to regulate glucose homeostasis and metabolisms. Normally, insulin secretion is stimulated by raising plasma glucose via the GSIS pathway (Bensellam *et al*., 2012). Intracellular calcium signaling is required for insulin secretion. First, plasma glucose is transported into β-cells via Glut2 and metabolized by GK enzyme. After glucose metabolism, the ratio of ATP/ADP is increased, leading to the closure of $K_{ATP}$ and membrane depolarization. The depolarization opens VDCCs, leading to calcium influx and increase in intracellular calcium concentration ($[Ca^{2+}]i$). The increase in intracellular calcium stimulates insulin exocytosis as shown in Figure 8 (Mears, 2004, Bensellam *et al*., 2012).

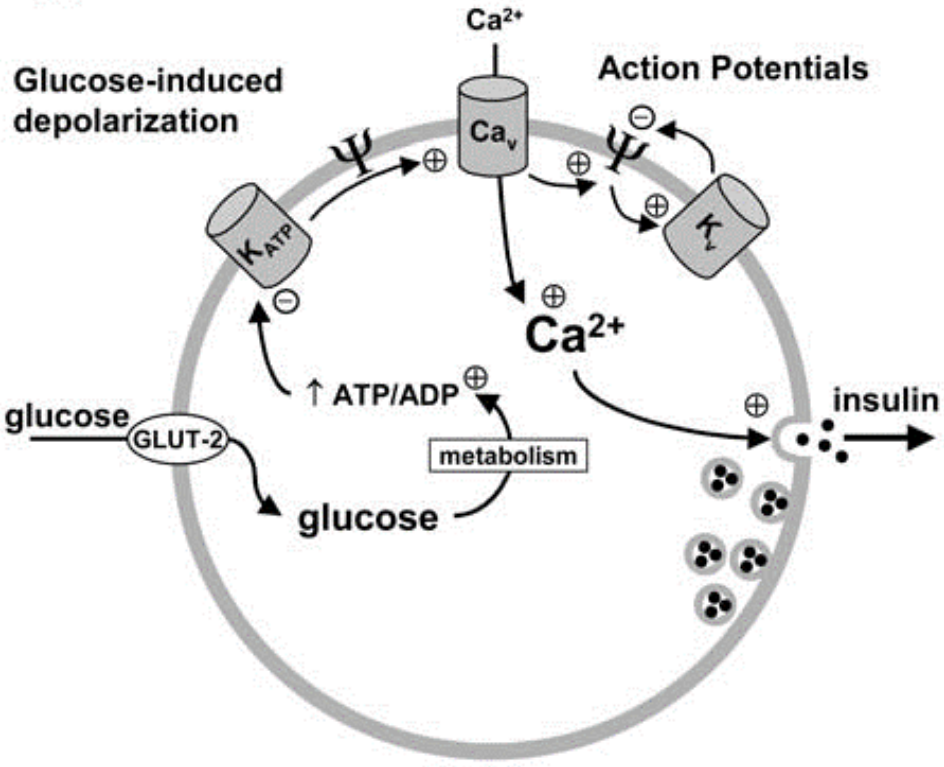


**Figure 8** Glucose-stimulated insulin secretion (GSIS).

Insulin secretion from pancreatic β-cells is stimulated by glucose (Mears, 2004).

## 2.6 Intracellular calcium signals

Calcium ion ($Ca^{2+}$) is an important second messenger that mediate many cellular processes such as gene transcription, cell apoptosis, cell proliferation, and cell differentiation (Clapham 1995). In the resting state, intracellular calcium concentration $[Ca^{2+}]i$ in cytosol ($10^{-7}$ M) is lower than extracellular concentration $[Ca^{2+}]e$ ($10^{-3}$) by 10,000 times. Normally, the low cytosol calcium concentration is maintained by calcium transporter on plasma membrane that extrude calcium to extracellular space. Moreover, there are pumps on the organelle membrane that uptake calcium including the ER, mitochondria, and Golgi apparatus (Bagur and Hajnóczky, 2017). Intracellular calcium signaling is due to increases in calcium concentration in the cytosol due to calcium influx from extracellular space and/or calcium release from intracellular stores (Nowycky and Thomas, 2002). Calcium signaling depends on channels, transporters, pumps, storage organelles, and calcium-sensing proteins as shown in Figure 9 (Krebs *et al*., 2015).

- Calcium influx

The process of calcium transport from the extracellular space into the cytosol increases intracellular calcium to generate calcium signals. There are two major types of calcium channels on the plasma membrane: voltage-dependent calcium channels (VDCCs) and store-operated calcium channels (SOCs). VDCCs are the main pathway for calcium influx in excitable cells and activate by changes of membrane potential. The VDCC consists of L-type and P/Q-type (high-voltage activated channels), T-type (low-voltage activated channels), R-type, and N-type (Mears, 2004, Islam, 2010). Other calcium channels are activated by ligand-binding such as store-operated calcium channels (SOCs). The SOCs, which respond to calcium store depletion in the ER, consist of two components: Orai channels (-1, -2, -3) on the plasma membrane and STIM (-1, -2) proteins on ER membrane that sense calcium the in the ER lumen (Bootman *et al*., 2001).

- Calcium release

Another mechanism that increases intracellular calcium concentration is release from intracellular stores such as the ER, mitochondria, and Golgi apparatus. The ER is an important storage organelle due to its relationship with STIM-1 and SOCs. The calcium release channels on the ER and Golgi apparatus consist of IP3-receptors ($IP_3R$) and ryanodine receptors (RyRs). The $IP_3R$ (-1, -2, -3) are ligand-gated ionotropic channels that are activated by $IP_3$ (Inositol 1,4,5-triphosphate) from phospholipase C enzyme (PLC) breakdown of $PIP_2$. The RyRs (-1, -2, -3) is stimulated by cyclic ADP ribose (cADPR) which is synthesized from β-$NAD^+$ by ADP-ribosyl cyclase enzyme (Bootman *et al.*, 2001). In mitochondria, there are $Na^+/Ca^{2+}$ exchangers (NCX) that release calcium to the cytosol and uptake sodium into mitochondrial matrix (Nowycky and Thomas, 2002).

- Calcium efflux

To maintain low intracellular calcium concentration, cells will transport the ion out of the cells via calcium pumps and into storage organelles. There are two types of calcium transporter on the plasma membrane: the calcium ATPase (PMCA) which pump calcium out using ATP and the $Na^+/Ca^{2+}$ exchanger (NCX) that utilizes sodium in exchange for calcium (Nowycky and Thomas, 2002). In storage organelles, the calcium transporter on the ER membrane is the sarco- and endoplasmic reticulum calcium ATPase (SERCA) that pump calcium into ER lumen. On the mitochondria membrane, the calcium uniporter (MCU) can uptake calcium into mitochondria matrix. Moreover, the P-type calcium transporter (PMR1/ATP2c1) transport calcium into the Golgi apparatus (Nowycky and Thomas, 2002).

- Calcium-sensing proteins

The mechanism by which calcium controls various cellular responses are dependent on effector proteins that sense calcium concentration in cytosol. After an increase in intracellular calcium, calmodulin (CaM) is activated and binds to free calcium ions with conformation changes and interaction with downstream targets like calcium/CaM-dependent protein kinase (CaMK) and calcineurin (CaN). CaMK is an important enzyme that phosphorylates downstream targets such as CaMKK, CaMKI, CaMKII, and CaMKIV. Calcineurin (CaN) is an important phosphatase that is regulated via direct binding to free calcium ions and CaM. CaN is involved in lymphocyte activation, and neuronal and muscle development. In addition, calpain, a protein protease is binds to calcium ions and mediates cell processes including integrin-mediated cell migration, cytoskeletal remodeling, cell differentiation, and apoptosis (Bagur and Hajnóczky, 2017).

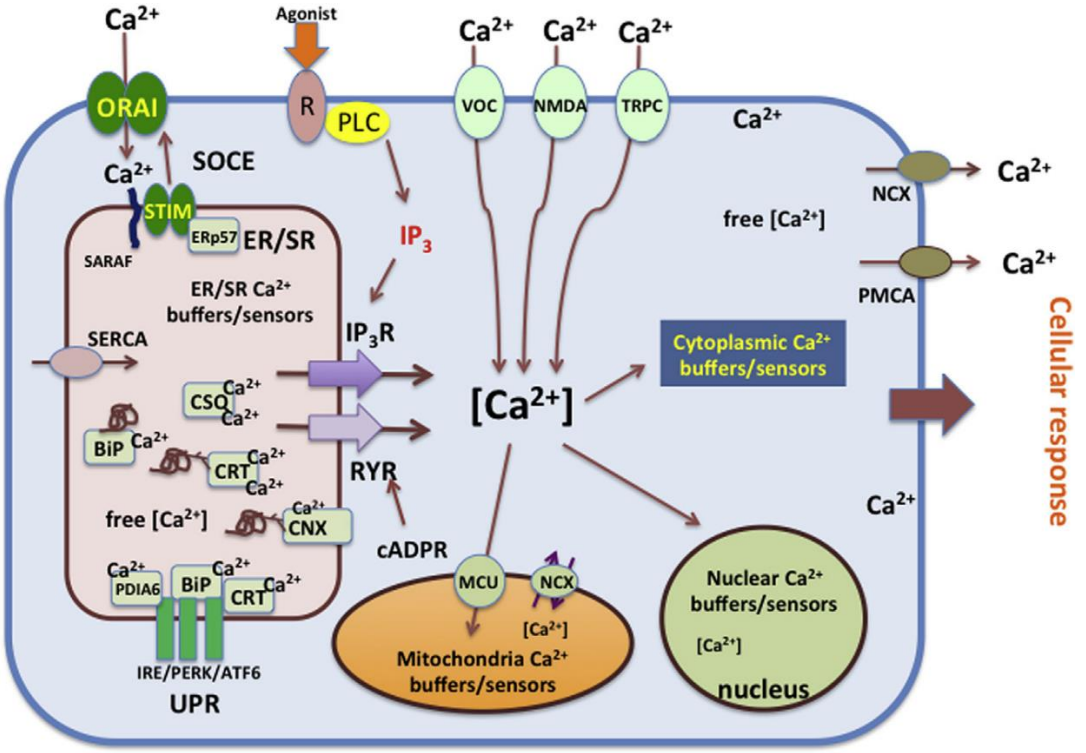


**Figure 9** Intracellular calcium signaling regulation.

The channels involved in calcium influx consist of VDCC, TRPC, NMDA, Orai and STIM in SOCE on the plasma membrane. The channels involved in calcium release consist of $IP_3R$ and RyR on the endoplasmic reticulum membrane and NCX on the mitochondria membrane. The channels involved in calcium efflux are PMCA and NCX, SERCA on the ER, and MCU on the mitochondria (Krebs *et al.*, 2015)



2.6.1 Calcium signaling in adipocytes

Previous studies show that intracellular calcium signaling can mediate adipocyte life cycle and function such as adipogenesis, lipogenesis, apoptosis, glucose uptake, and lipolysis (Hu *et al.*, 2009, Turovsky *et al.*, 2012).

In murine 3T3-L1 cells, calcineurin, calcium-dependent phosphatase enzyme, inhibit adipogenesis by downregulating PPARγ and C/EBPα, which are major transcription factors for adipogenesis (Neal and Clipstone, 2002). Interestingly, the inhibitory effects of capsaicin on adipogenesis are mediated by calcium influx via TRPV1 calcium channels that downregulate PPARγ expression (Zhang *et al.*, 2007). Moreover, prostaglandin 2α inhibit adipogenesis by

downregulating PPARγ and C/EBPα through the calcineurin pathway (Liu and Clipstone, 2007). Activation of calreticulin, a major calcium-binding protein in the ER lumen increases intracellular calcium and downregulate PPARγ with inhibition of adipogenesis (Meldolesi, 2008). In mouse adipocytes, angiotensin II induces lipogenesis and inhibits lipolysis by activating intracellular calcium signals (Dolgacheva *et al*., 2016).

In human adipocytes, calcium signaling also controls adipocyte differentiation and function. In the early phase of adipogenesis, calcium influx via L-type calcium channels inhibits adipogenesis and decreases triglyceride accumulation. On the other hand, the increases in intracellular calcium in the late phase of differentiation promotes lipogenesis by upregulating FasN gene expression and reducing lipolysis (Shi *et al*., 2000). In human adipose-derived stem cells (hASCs), arginine vasopressin inhibits adipogenesis by promoting calcium influx through SOC calcium channels and enhancing calcium release from ER via the $IP_3R$. After binding to the V1a receptor, AVP activates the PLC-$IP_3$ pathway to increase intracellular calcium and downregulate PPARγ, C/EBPα, C/EBPβ, C/EBPγ, aP2, and adiponectin expression (Tran *et al*., 2015). Histamine enhances adipogenesis and lipid accumulation in hASCs by stimulating calcium signals. Histamine activates H1 receptors and the PLC-$IP_3$ pathway to promote calcium release from ER and influx through L-type calcium channels under TRPM4 regulation (Tran *et al*., 2014).

For glucose uptake, calcium ions are one of the mediators for insulin signaling to promote Glut4 translocation and glucose uptake in adipocytes through the PI3K pathway (Turovsky *et al*., 2016). Depletion of calcium ions using calcium chelators can attenuate insulin signaling and inhibit Glut4 translocation and insulin-stimulated glucose uptake in 3T3-L1 cells (Worrall and Olefsky, 2002).

For cell apoptosis, calcium signaling is involved in 1,25-dihydroxy vitamin D3 (vit D3)-induced apoptosis in 3T3-L1 adipocytes. The increase in intracellular

calcium activates calpain, a calcium-dependent protease and caspase-12 which is calpain-dependent protein that induces cell apoptosis (Sergeev, 2009).

2.6.2 Calcium signaling in pancreatic β-cells

The most important effect of intracellular calcium in pancreatic β-cells is insulin secretion regulation. Pancreatic β-cells are electrically and depolarization activate VDCCs and calcium signals. Therefore, the main pathway of intracellular calcium regulation in β-cells is calcium influx through L-type VDCCs, but also SOCs are involved (Mears, 2004, Islam, 2010). Previous study shows that TRPM4 (transient receptor potential protein (TRP)) channels, a calcium-activated non-selective cation channel regulate calcium influx into β-cells by depolarization leading to VDCCs activation. The results indicate that TRPM4 is important for glucose-induced insulin secretion in pancreatic β-cells (Cheng *et al*., 2007). In HIT-T15 β-cells, somatostatin, which normally inhibits calcium influx via L-type VDCCs and insulin secretion can also activate calcium signals and induce insulin secretion in the presence of arginine vasopressin (Cheng *et al*., 2002). In addition, exposure to fluoroquinolones, which are broad spectrum antimicrobial drugs induces hypoglycemia and stimulate insulin secretion. Fluoroquinolones inhibits $K_{ATP}$ channels leading to cell depolarization and calcium influx through the L-type VDCCs. It also stimulates calcium release from the ER (Bito *et al*., 2013). Free fatty acids are important insulin regulators via the GPR40 receptor, a Gq-protein coupled receptor for medium- and long-chain FFA that activates calcium influx through L-type VDCCs in INS-1 cells (Schnell *et al*., 2007). Interestingly, PERK (protein kinase R-like endoplasmic reticulum kinase), a kinase enzyme on the ER membrane is essential for normal development and function of pancreatic β-cells. PERK is directly activated by calcium and interacts with CN that regulate TRP and SOC channels for glucose-stimulated insulin secretion. Hence, the interaction between PERK and calcineurin is important for calcium signaling and insulin secretion (Wang *et al*., 2013).

## 2.7 Prevention of metabolic syndrome

The first strategy to prevent metabolic syndrome is weight reduction since abdominal obesity is the main indicator of metabolic syndrome and other risk factors. Lifestyle modifications by caloric restriction and exercise are primary recommendations (Grundy, 2016). An American Heart Association / National Heart, Lung, and Blood Institute provided the therapeutic goals and recommendations for clinical management of metabolic syndrome in 2005. The first aim is reducing body weight for 7-10% in first year and then continue weight loss until a BMI < 25 kg/$m^2$ by decreasing caloric intake for 500-1000 calories/day with increasing physical activity. The recommendation for physical activity is regular to moderate-intensity exercise at least 30 min for 5 day/week. Moreover, food with decreased saturated fats, *trans* fats, cholesterol, and sodium, while using simple sugars with increasing fruits, vegetables, and whole grains (Grundy *et al*., 2005). A prospective cohort study in Spain from 1999 to 2017, showed the relationship between a healthy lifestyle and incidence of metabolic syndrome among populations (10,807 participants). The healthy lifestyle was determined using 9 habits of Healthy Lifestyle Score questionnaires including non-smoking, physical activity (>20 MET-h/week), Mediterranean diet pattern, moderate alcohol consumption (0.1-5.0 g/day for women, 0.1-10.0 g/day for men), low time spent watching television (<2 h/day), avoidance of binge drinking (≤5 alcoholic drinks), having a short afternoon nap (0.1-0.5 h/day), time with friends (>1 h/day), and time working (≥40 h/week). Based-on ATP III criteria, the data indicated that higher Healthy Lifestyle Scores significantly correlated with lower risk of metabolic syndrome (Garralda-Del-Villar *et al*., 2019). In addition to lifestyle modifications, anti-obesity and anti-hyperglycemia drugs are also used.



### 2.7.1 Therapeutic approach for obesity

Based on the severity of abdominal obesity and metabolic syndrome, there are many anti-obesity drugs that approved by Food and Drug Administration (FDA) as shown in Table 4 (Francisco Bonamichi *et al*., 2018).

**Table 4** FDA-approved drugs for obesity treatment

| Drug | Mechanism | Side effect |
|---|---|---|
| Oristat (Xenical®) | Triacylglycerol lipase inhibitor (decrease fat digestion and absorption, and increase fecal fat excretion) | Gastrointestinal symptoms (diarrhea, flatulence, abdominal pain, oily stool, and fecal urgency) and liver toxicity |
| Naltrexone/bupropion (Contrave®) | Opioid receptor antagonist/ Noradrenaline and dopamine reuptake inhibitor (suppress the mesolimbic-dopaminergic reward system that enhance food intake) | Tachycardia, insomnia, and nausea |
| Bupropion/zonisamide | Noradrenaline/dopamine reuptake inhibitor, mitochondrial carbonic anhydrase inhibitor, and acts as GABA receptors | Headache, nausea, and insomnia |
| Phentemine (Adipex®) | Noradrenergic sympathomimetic amine (enhance energy expenditure, decrease appetite and food intake) | Dry mouth, insomnia, elevate heart rate, rise blood pressure, adverse cardiac events |
| Phentermine/topiramide (Qsymia®) | Release of catecholamines and inhibits excitatory glutamate receptors and carbonic anhydrate | Paraesthesia, insomnia, dizziness, altered taste sensation, constipation, dry mouth |
| Liraglutide (Victoza®, Saxenda®) | GLP-1 receptor agonist (stimulate glucose- | Nausea, vomiting, diarrhea, constipation, hypoglycemia, |

| Drug | Mechanism | Side effect |
|---|---|---|
| | dependent insulin secretion) | and less common side effects (pancreatitis, cholecystitis, renal impairment, suicidal indeation) |

(Francisco Bonamichi *et al*., 2018)

There are some drugs used for obesity treatment such as empagliflozin (Jardiance®), which is a sodium-glucose cotransporter 2 (SGLT2) inhibitor that inhibits glucose uptake into the cells and cetilistat (Cetislim®), which is a pancreatic lipase inhibitor that decreases lipid digestion (Francisco Bonamichi *et al*., 2018).

In spite of the adverse effects of medications, anti-obesity agents from natural bioactive compounds could be used as an alternative form of treatment. Several studies show the anti-obesity effects of phytochemicals through inhibition of cell proliferation, adipogenesis, lipogenesis, or promotion of lipolysis. Baicalein, a flavonoid from *Scutellaria baicalensis* inhibits lipid accumulation in 3T3-L1 cells by inducing cell cycle arrest at the G0/G1 phase in early stage of adipogenesis (Seo *et al*., 2014). Coffee extract inhibits adipogenesis in 3T3-L1 cells. In early phase of adipogenesis, the extract decreases cell proliferation by inducing cell cycle arrest and downregulating early transcription factors, C/EBPβ. Moreover, the extract inhibits the key transcription factors of adipogenesis including PPARγ and C/EBPα (Maki *et al*., 2017). Garlic-derived compounds inhibit adipogenesis and lipid accumulation by downregulating gene expression involved in adipogenesis (C/EBPα and PPARγ), lipogenesis (ACC and FAS), fatty acid transport (FABP4, CD36, and LPL), and adipocytokines (leptin, resistin, MCP-1), while increasing gene expression of fatty acid oxidation and adiponectin in 3T3-L1 cells (Chang *et al*., 2015). Daidzein, a soybean isoflavones inhibits preadipocyte proliferation and

adipogenesis by downregulating PPARγ and C/EBPα and adipogenic genes expression including FAS and ACC (He *et al*., 2016). Sun ginseng inhibits proliferation and differentiation of 3T3-L1 cells and reduces lipid accumulation in *C. elegans* by downregulating PPARγ and C/EBPα. In addition, sun ginseng inhibits Glut4 and IRS-1 expression levels by inhibiting Akt phosphorylation in the early phase of adipogenesis (Lee *et al*., 2017). Açai polyphenols reduce lipid accumulation by downregulating PPARγ, C/EBPα, C/EBPβ, and adipogenic genes including FABP4, FAS, leptin, while increase adiponectin expression levels. It can also decrease ROS production and pro-inflammatory cytokines in 3T3-L1 cells (Martino *et al*., 2016). Andrographolide, a diterpenoid in *Andrographis paniculate*, a Chinese herbal medicine inhibits adipogenesis by downregulating PPARγ, C/EBPα, and C/EBPβ. Andrographolide reduces lipid accumulation by suppressing FAS and stearoyl-CoA desaturase expression. and induces cell cycle arrest at G0/G1 phase by suppressing cyclin A, cyclin E, and CDK2 expression in 3T3-L1 cells (Chen *et al*., 2016). Lucidone from Makino fruits suppresses adipogenesis by decreasing transcription of PPARγ, C/EBPα, LPL, FABP4, Glut4, and adiponectin in 3T3-L1 cells. In high-fat diet fed mice, lucidone reduces body weight, decreases adipose tissue, lowers plasma cholesterol, triglyceride, glucose, and insulin levels (Hsieh and Wang, 2013). The 6-gingerol inhibits adipogenesis, decreases lipid accumulation, and reduces lipid droplet size by downregulating PPARγ, C/EBPα, FAS, Fabp4 by suppressing insulin-stimulated Akt phosphorylation (Tzeng and Liu, 2013). Resveratrol inhibits lipogenesis in murine 3T3-L1 and human SGBS cells by downregulating ACC (Tang *et al*., 2007) and inhibiting the insulin signaling pathway (Li *et al*., 2016).

2.7.2 Therapeutic approach for hyperglycemia and β-cells dysfunction

Based on the severity of hyperglycemia and metabolic syndrome, the treatment focuses on the control of blood glucose. The medications used as shown in Table 5.

**Table 5** FDA-approved drugs for hyperglycemia treatment

| Drug | Mechanism | Side effect |
|---|---|---|
| Meglitinides (Repaglinide/Nateglinide) | Enhance insulin production and secretion from pancreatic β-cells | Hypoglycemia |
| Miglitol / Acarbose | Alpha-glucosidase inhibitors (decrease glucose digestion) | Stomach pain, diarrhea, gas, and abnormal liver tests |
| Thiazolidinediones (TZDs) (Pioglitazone / Rosiglitazone) | Promote glucose uptake and insulin sensitivity on muscle cell, adipocyte, and liver | Fluid retention, weight gain, heart failure, anemia, and upper respiratory tract infection |
| Sitagliptin / Alogliptin (Januvia®) | DPP-4 inhibitors (induce insulin secretion from pancreatic β-cells) | Upper respiratory infection and headache |
| Sulfonylureas (Glimepiride / Glyburide) | Enhance insulin production and secretion from pancreatic β-cells | Hypoglycemia, weight gain, headache, and dizziness |
| Biguanides (Metformin) | Inhibit gluconeogenesis of liver | Diarrhea, indigestion, nausea, vomiting, gas, feeling weak, and headache |
| Bromocriptine (Cycloset®) | Dopamine receptor agonists | Nausea, headache, feel very tried, feel dizzy, and vomiting |
| Colesevelam (Welchol®) | Bile acid sequestrants | Constipation, dyspepsia, and nausea |
| Dapagliflozin / Canagliflozin | SGLT2 (sodium-dependent glucose transporter 2) | Vaginal yeast infections, urinary tract infections, |

| Drug | Mechanism | Side effect |
|---|---|---|
| (Farxiga®) | inhibitors (increase glucose excretion to urine) | and changes in urination |

(FDA, 2015, FDA, 2018)

Previous studies show that caffeic acid, naringenin, and quercetin, are phenolic compounds that enhance glucose-stimulated insulin secretion, improve glucose sensitivity, and β-cell survival under glucotoxicity conditions (Bhattacharya *et al*., 2014). Ocimum sanctum Linns or holy basil leaf extracts possess anti-hyperglycemia effects by reducing fasting plasma glucose in diabetic rats after one month of feeding. It stimulates insulin secretion by increasing intracellular calcium from pancreatic β-cells (Hannan *et al*., 2006). The phytosterol glucoside extracted from Akebia quinata or Chocolate vine promotes glucose-stimulated insulin secretion by upregulating PDX-1, ERK1/2, IRS-2, PI3K, and Akt expression (Lee *et al*., 2020). Rhamnoside (2R, 3R taxifolin 3-o-rhamnoside), a flavonoid from Hydnocarpus alpine or torathi, has hypoglycemic effects in diabetic rats after 21 days of treatment. Rhamnoside decreases blood glucose by increasing liver glycogen contents via hepatic enzymes stimulation and insulin secretion (Balamurugan *et al*., 2015). Silibinin, a natural flavonone, protects pancreatic β-cells against glucotoxicity and induces insulin secretion by upregulating PDX-1, IRS-2, and insulin and regulating the Insig-1/SREBP-1c pathway (Chen *et al*., 2014). Flavonoid isolated from dried flower buds of Cleistocalyx operculatus protects pancreatic β-cells against glucotoxicity and induces glucose-stimulated insulin secretion by upregulating the GLP-1R, PDX-1, PRE-INS, and Glut2-GCK expression, and suppressing nitric oxide production and MCP-1 expression (Hu *et al*., 2014). Kaempferol, a flavonol in several plants such as tea, Gingko biloba, and grapefruit, protects pancreatic β-cells against glucotoxicity by increasing cell viability, suppressing cell apoptosis by decreasing caspase-3 activity and upregulating anti-apoptotic

protein, Bcl-2 expression. Moreover, kaempferol induces insulin secretion by increasing intracellular cAMP and ATP production in high glucose treated pancreatic β-cells (Zhang and Liu, 2011). Quercetin protects pancreatic β-cells against oxidative damage by $H_2O_2$ and enhances glucose-stimulated insulin secretion through the ERK1/2 pathway (Youl *et al*., 2010). Genistein, an isoflavones, induces glucose-stimulated insulin secretion (GSIS) via increasing intracellular cAMP and calcium signals and activating the PKA pathway. However, the genistein's effects is not mediated by the protein tyrosine kinase (PTK) pathway, KATP channels, glucose uptake, cellular ATP production, and estrogen receptor (Liu *et al*., 2006, Fu and Liu, 2009) Ginsenoside Rh2, an active compound of Panax ginseng or red ginseng, reduces blood glucose and increases insulin and plasma C-peptide levels in Wistar rats. Ginsenoside Rh2 stimulates acetylcholine (Ach) release to activate muscarinic M3 receptors on pancreatic β-cells (Lee *et al*., 2006).

### 2.8 Anthocyanins

Anthocyanins, water-soluble pigments belonging to phenolic and flavonoid groups are effective natural phytochemicals in purple, red, or blue plants. Anthocyanins are the derivatives of the flavylium (2-phenylbenzopyrylium) structure containing two benzoyl rings (A and B) with heterocyclic ring (C) as shown in Figure 10 (Ghosh, 2005). There are six common aglycone form of anthocyanins including cyanidin (Cy), delphinidin (Dp), malvidin (Mv), peonidin (Pn), pelargonidin (Pg), and petunidin (Pt) based on different number and position of hydroxyl groups and methylation degree of these hydroxyl groups (Fernandes *et al*., 2014).

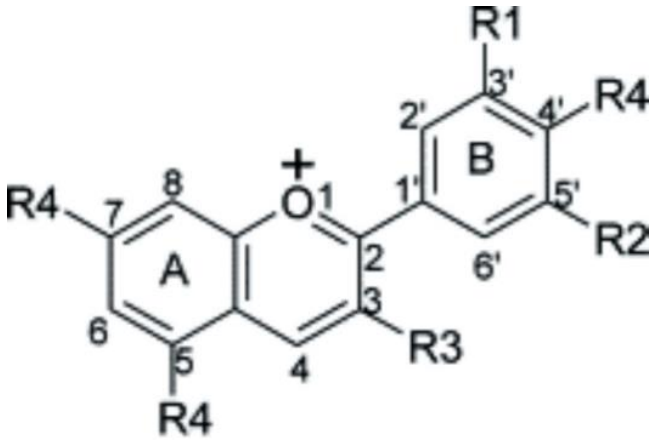


| Anthocyanin | R1 | R2 | R3 | R4 |
|---|---|---|---|---|
| Cyanidin | OH | H | OH, glycosyl | OH, glycosyl |
| Delphinidin | OH | OH | | |
| Malvidin | OCH3 | OCH3 | | |
| Peonidin | OCH3 | H | | |
| Pelargonidin | H | H | | |
| Petunidin | OCH3 | OH | | |

**Figure 10** Chemical structure of six common subtypes of anthocyanins

The color and stability of anthocyanin depends on the pH of solution. Normally, anthocyanin stable in acidic condition (pH 1-3) as flavylium cations with red color. At pH 4-5, carbinol pseudo base structure forms and is colorless. At pH 7-8, purple quinoidal base forms as blue color (Ghosh, 2005, Khoo *et al*., 2017). Glycosylation increases anthocyanin stability and improves water solubility such as C3G, pelargonidin-3-glucoside, peonidin-3-glucoside (P3G), and C3R (Ghosh, 2005).

The distribution of anthocyanin subtypes in fruits and vegetables is cyanidin (Cy) 50%, delphinidin (Dp) 12%, peonidin (Pn) 12%, pelargonidin (Pg) 12%, malvidin (Mv) 7%, and petunidin (Pt) 7%, respectively, while C3G is the most abundant in plants. Example of anthocyanin sources are shown in Figure 11 (Khoo *et al*., 2017).

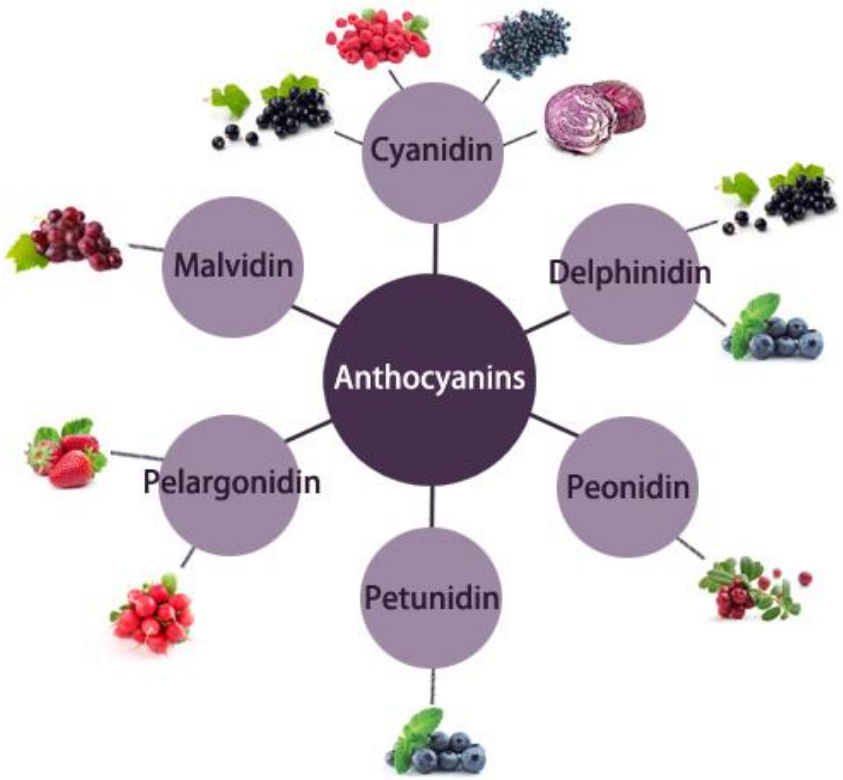


**Figure 11** Anthocyanin subtypes and sources.

Based on the anthocyanin properties, there are many health benefits such as antioxidant, anticancer, anti-inflammation, anti-diabetes, anti-obesity, anti-aging, and cardiovascular protective effects. The present study focuses on the anti-obesity and anti-diabetes effects of anthocyanins.



2.8.1 Anti-obesity effects of anthocyanins

Studies have demonstrated the anti-obesity effects of anthocyanins and anthocyanin-rich fruits. Delphinidin, an anthocyanin subtype, reduces lipid accumulation and promotes lipolysis in adipocytes. In the early phase of adipogenesis, delphinidin induces cell cycle arrest in G0/G1 phase and suppresses adipogenic transcription factors including C/EBPβ and C/EBPδ. It also downregulates PPARγ and C/EBPα, key transcription factors of adipogenesis (Rahman *et al.*, 2016). C3G increases adiponectin secretion and decreases the secretion of pro-inflammatory adipokines (TNFα and MCP-1) involved in

inflammation through infiltration of macrophages into adipose tissue (Matsukawa *et al*., 2016). Lyophilized cranberries reduce lipid accumulation by downregulating PPARγ, C/EBPα, SREBP1, Fabp4, FAS, LPL, and perilipin-1. Moreover, cranberries decrease leptin gene expression and increase adiponectin gene expression (Kowalska *et al*., 2015). Black soybean extract, which is rich in anthocyanins, inhibits lipogenesis genes including ACC (Tang *et al*., 2007) and C/EBPα, and stimulate lipolytic enzyme including LPL and HSL in mesenteric fat. The extract has anti-inflammatory effects by suppressing TNFα, IL-6, and IL-10 expression (Kim *et al*., 2015). Isolated anthocyanins from grape suppress adipocyte differentiation by decreasing expression levels of PPARγ, C/EBPα, FasN and ACC (Lee *et al*., 2014). Anthocyanins isolated from the fruit of *Vitis colgnetiae Pulliat* inhibit adipogenesis in 3T3-L1 cells by downregulating PPARγ, C/EBPα, C/EBPβ, aP2, leptin and FasN via the AMPK pathway (Han *et al*., 2018). Blueberry peel extract and juice extract exhibited anti-adipogenic effects in 3T3-L1 cells by downregulating PPARγ and C/EBPβ and decreasing Akt signaling and enhancing the AMPK pathway (Song *et al*., 2013, Sánchez-Villavicencio *et al*., 2017). In rat adipocytes, Cy and C3G improve adipocyte function by increasing adiponectin and leptin secretion and enhancing lipolysis by upregulating HSL (Khoo *et al*., 2017).

In animal models, anthocyanins supplementation or anthocyanin-rich fruits can reduce body weight and decrease body fat mass such as C3G from purple corn, Cornelian cherries, blueberry juice (Khoo *et al*., 2017), black raspberry, mulberry water extract, tart cherry powder, and chokeberry (Tsuda, 2012). In obese mice, treatment with C3G from purple corn for 12 weeks and Cornelian cherries (containing delphinidin, cyanidin, and pelargonidin-3-galactosides) for 8 weeks decrease weight gain and lipid accumulation in liver (Khoo *et al*., 2017). Blueberry juice, mulberry juice, and Chinese mulberry (containing C3G, C3R, and pelargonidin-3-glucoside) inhibit weight gain, decrease serum cholesterol, lipid accumulation, leptin secretion, and improve insulin resistance (Azzini *et al*., 2017).

Blackcurrant supplementation in mice for 12 weeks decrease adipocyte size of epididymal fat and upregulate gene expression involve in mitochondria biogenesis in skeletal muscle. Mulberry ethanol extract induces fatty acid oxidation and decrease fatty acid and cholesterol biosynthesis (Azzini *et al*., 2017).

In obese mice model, Goka fruit, Cornelian cherries, and sweet orange improve glucose tolerance and insulin sensitivity, reduce plasma insulin and lipid accumulation in liver. Black elderberry can decrease serum triglyceride, inflammatory markers levels, and improve insulin resistance (Azzini *et al*., 2017).

In Zucker fatty rats, tart cherry powder supplementation reduces body weight gain, retroperitoneal fat mass, and proinflammatory cytokines (IL-6 and TNF-α) expression (Tsuda, 2012). Supplementation with 8% wild blueberry powder for 8 weeks increases serum adiponectin level and reduces inflammatory markers in white adipose tissue and improve dyslipidemia (Azzini *et al*., 2017). Aronia fruits suppress visceral fat accumulation and hyperglycemia by inhibiting pancreatic lipase activity leading to a decrease in lipid absorption in rats after 4 weeks of supplementation (Azzini *et al*., 2017).

In clinical trials, blueberry beverage (containing 50 g of freeze-dried blueberries) supplementation for 8 weeks improves blood pressure, plasma oxidized LDL, and serum MDA related to metabolic syndrome and CVD risk factors. Moreover, blueberry smoothie (containing 45 g of blueberry powder) consumption twice daily for 6 weeks improves insulin sensitivity in healthy participants. In overweight participants, red orange juice consumption for 12 weeks has anti-obesity effects by reducing body mass index compared to placebo group. In addition, bilberry supplementation decreases weight and waist circumference in obese women (Azzini *et al*., 2017).

2.8.2 Anti-diabetic effects of anthocyanins

In pancreatic β-cells, C3G from mulberry protects against glucotoxicity-induced apoptosis by decreasing oxidative stress, increasing antioxidant defense

system, and regulating intrinsic apoptotic pathway (cytochrome c and caspase-3) and increases insulin secretion (Lee *et al*., 2015). Chokeberry extract protects β-cells against oxidative stress via activating antioxidant enzymes including catalase, superoxide dismutase (Matsukawa, Villareal et al.), glutathione peroxidase, and increasing GSH (glutathione) levels (Rugină *et al*., 2015). The C3G isolated from *Lonicera caerulea* fruit improves insulin secretion by enhancing phosphorylation of insulin receptor, insulin receptor substrate 1 (IRS-1), phosphoinositide 3-kinase protein (PI3K) in INS1 cells (Lee *et al*., 2016). Chinese bayberry C3G protects pancreatic β-cells from oxidative stress-induced injury, prevents cell death, increase cell viability, decrease ROS production in mitochondria, and inhibits cell necrosis. Moreover, C3G increases insulin-like growth factor II (IGF-II) expression and insulin protein level in INS-1 cells and reduces blood glucose and improve glucose tolerance in diabetic mice (Sun *et al*., 2012). Purple corn anthocyanins protect pancreatic β-cells from high glucose-induced cell death and stimulated insulin secretion in HIT-T15 cells and db/db mice (Hong *et al*., 2013). Moreover, it enhanced glucose-stimulated insulin secretion via activation of free fatty acid-receptor 1 (FFAR1) and GK enzymes in INS-1E cells (Luna-Vital, 2018). The compounds from Cornus fruits that enhance insulin secretion are delphinidin-3-glucoside, C3G, and pelargonidin-3-galactoside, respectively (Jayaprakasam *et al*., 2005). Cyanidin stimulates insulin secretion by activating calcium influx through L-type VDCC calcium channels and upregulate Glut2, $Kir_{6,2}$, and $Cav_{1.2}$ genes expression in INS-1 cells (Suantawee *et al*., 2017).

In diabetic mice, bilberry anthocyanin improves hyperglycemia and insulin sensitivity by promoting Glut4 expression in skeletal muscle and white adipose tissue and inhibiting glucose production in liver (Khoo *et al*., 2017). C3G increases serum adiponectin concentration and improves endothelial function leading to the decrease in CVD risk in diabetic mice (Różańska and Regulska-Ilow, 2018). Moreover, blueberry powder supplementation decreases inflammatory markers

expression TNF-α, IL-6, MCP-1, and iNOS and improves oxidative stress in high-fat diet fed mice (Różańska and Regulska-Ilow, 2018). In streptozotocin-induced diabetic rats, black soybean seed coat extract (containing 72% of C3G) supplementation reduces blood glucose level by increasing Glut4 expression and translocation, promoting insulin receptor phosphorylation, and preventing apoptosis of pancreatic β-cells (Różańska and Regulska-Ilow, 2018). Cornelian cherry prevents β-cells dysfunction and increases insulin levels in high-fat fed mice (Gowd *et al*., 2017).

In clinical trials, according to Nurses' Health Study I and II and Health Professionals Follow-Up Study, the results indicate that higher anthocyanin content in diet is associated with lower risk of type 2 diabetes (Różańska and Regulska-Ilow, 2018). In healthy adults, berries significantly lower postprandial plasma glucose level compared to placebo group (Różańska and Regulska-Ilow, 2018). In obese adults, blueberries consumption for 6 weeks increases insulin sensitivity. In addition, strawberries improve inflammation by reducing C-reactive protein and IL-6 levels in overweight and obese individuals (Różańska and Regulska-Ilow, 2018). In diabetic patients with 160 mg of anthocyanins extracted from bilberry and blackcurrant supplementation twice daily, the results indicate that the treatment group had significant lower fasting plasma glucose level and insulin resistance index with higher serum adiponectin concentration compared to the placebo group (Khoo *et al*., 2017).

### 2.9 Cyanidin-3-rutinoside (C3R)

Cyanidin-3-rutinoside (C3R) is a glycoside form of cyanidin backbone which attached to a rutinose sugar moiety at 3-OH position on the C-ring as shown in Figure 12. The molecular formula is C27H31ClO15 and molecular weight is 631 g/mol.

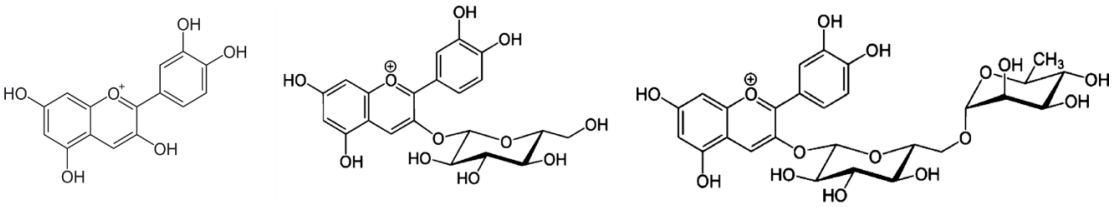


**Figure 12** Chemical structure of cyanidin, cyanidin-3-glucoside, and cyanidin-3-rutinoside.

C3R was first identified in Antirrhinum majus flower and found in the skin of red-purple fruits such as sweet cherry (Gonçalves *et al.*, 2018), cornelian cherry (Dumitraşcu *et al.*, 2019), mulberry (Zheng *et al.*, 2016), black currant (Castro-Acosta *et al.*, 2016), and lychee (Sarni-Manchado *et al.*, 2000) as shown in Figure 13.

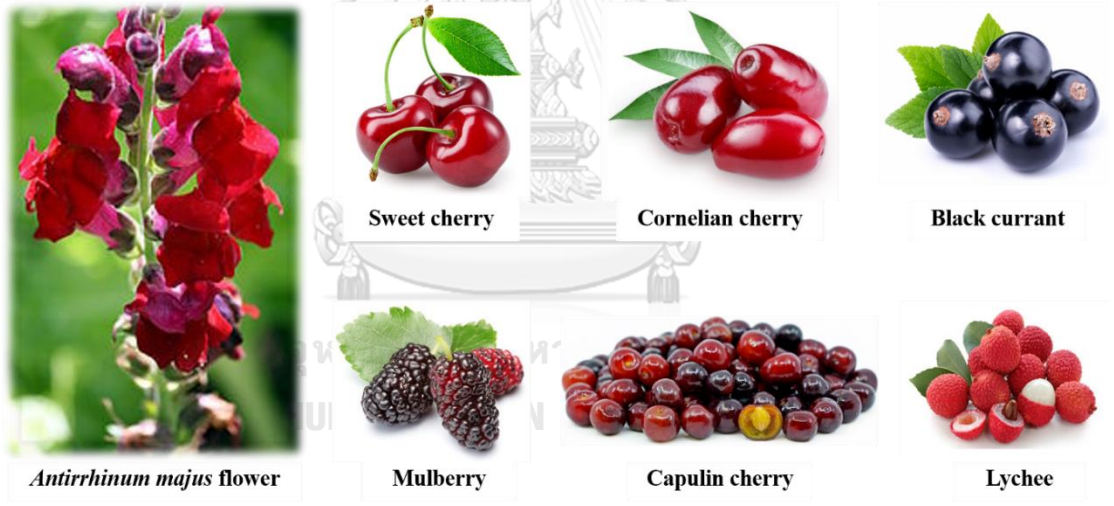


**Figure 13** Natural sources of cyanidin-3-rutinoside (C3R).

2.9.1 Bioavailability of cyanidin-3-rutinoside (C3R)

Previous studies show that C3R is absorbed, distributed, and excreted in intact form in both rats and humans. After oral administration with C3R 800 μmol/kg of body weight, C3R concentration rapidly increases in plasma in unchanged form, reaches maximum within 30 min, and gradually decreases 2 h post-administration in rats (Matsumoto *et al.*, 2001). In addition, rats with oral

intake of anthocyanin-rich extract from wild mulberry show maximum concentration of C3R in plasma and kidneys 15 min post-intake (Hassimotto *et al*., 2008). In GI tract, peak C3R concentration is detected in stomach and small intestine 15 min post-intake and at 30 min post-intake in large intestine. However, after 8 h of administration, C3R is undetectable in plasma, kidney, stomach, and small intestine, and only a small amount is detected in large intestine (Hassimotto *et al*., 2008). Experiments using the everted sac model indicated that C3R is absorbed through the intestinal mucosa due to its hydrophilic property and transported by enterocyte via the sodium-dependent glucose transporter (SGLT1) (Hassimotto *et al*., 2008) and is metabolized within 10 h. Cyanidin aglycone and protocatechuic acid (PCA) are metabolites of C3R and can be found after 4 h in feces (Hassimotto *et al*., 2008). C3R is metabolized more slowly C3G because C3R cannot be deglycosylated by endogenous β-glycosidase (lactase phloridzin hydrolase) in small intestine (Hassimotto *et al*., 2008). In humans, plasma C3R concentration reaches a peak within 2 h after black currant consumption. After that, C3R is excreted in human urine between 2 and 4 h post-intake (Matsumoto *et al*., 2001).

2.9.2 Anti-diabetic effects of cyanidin-3-rutinoside (C3R)

As with other anthocyanins, C3R express several anti-hyperglycemic activities. C3R reduces postprandial hyperglycemia by delaying carbohydrate digestion. Studies show that C3R inhibits yeast α-glucosidase enzyme in a non-competitive manner (Adisakwattana *et al*., 2004). C3R has synergistic effects with acarbose to inhibit mammalian intestinal α-glucosidase enzyme including maltase and sucrase (Adisakwattana *et al*., 2011) In addition, C3R inhibits pancreatic α-amylase enzyme in a non-competitive manner with additive effects with acarbose (Akkarachiyasit *et al*., 2011). In animal models, supplementation with C3R at 100 and 300 mg/kg reduces postprandial plasma glucose after 30-90 min of loading with maltose and sucrose in normal rats (Adisakwattana *et al*., 2011). Moreover,

rats treated with 30 mg/kg C3R and acarbose express lower postprandial plasma glucose than acarbose treated group (Adisakwattana *et al*., 2011). C3R prevents diabetic complications due to its anti-glycating properties against monosaccharides- and methylglyoxal-induced protein glycation and prevents oxidative DNA damage (Thilavech *et al*., 2015, Thilavech *et al*., 2016).

In regards to pancreatic β-cells, C3R protects cells from glucotoxicity-induced apoptosis by reducing reactive oxygen species (ROS), lipid peroxidation, and nitric oxide levels, increasing antioxidant enzymes activity, decreasing pro-apoptotic proteins expression, and inducing anti-apoptotic protein expression (Choi *et al*., 2018). Furthermore, C3R induces insulin secretion from pancreatic β-cells under $H_2O_2$-induced oxidative stress by upregulating GK expression leading to intracellular ATP production, inhibiting ROS production, and decreasing $H_2O_2$-induced apoptosis rate (Zheng *et al*., 2016).

## 2.10 Riceberry rice (*Oryza sativa* L.)


**Figure 14** Riceberry rice (*Oryza sativa* L.) whole-grain and spike.

Riceberry rice is a new variety of rice from Thailand that is dark-purple and originated from Khoa Dawk Mali 105 rice and Hom Nin rice at the Rice Science Center, Kasetsart University, Thailand in 2002. Riceberry rice contains phytonutrients in its rice bran both water soluble, mainly anthocyanins, and lipid soluble such as carotenoid,

gamma oryzanol, and vitamin E as shown in Table 6. In clinical studies at Faculty of Medicine, Ramathibodi Hospital, Mahidol University, the results indicated that Riceberry whole-grain rice has a 'medium' glycemic index (GI=62). Previous studies show that the main anthocyanins in Riceberry rice extracts (RBE) are C3G and P3G (Jittorntrum *et al*., 2009, Leardkamolkarn *et al*., 2011, Posuwan *et al*., 2013, Prangthip *et al*., 2013, Arjinajarn *et al*., 2017).

**Table 6** Nutrient compositions of Riceberry whole-grain rice

| Composition | Amount |
|---|---|
| Fe | 13 – 18 mg/kg |
| Cu | 31.9 mg/kg |
| Omega-3 | 25.51 mg/100g |
| Vitamin E | 678 μg/100g |
| Folate | 48.1 μg/100g |
| Beta-carotene | 63 μg/100g |
| Polyphenol | 113.5 mg/100g |
| Tannin | 89.33 mg/100g |
| Gamma-oryzanol | 462 μg/g |
| Water-soluble antioxidant | 47.5 mg ascorbic acid equivalent/100g |
| Lipid-soluble antioxidant | 33.4 mg trolox equivalent/100g |



2.10.1 Biological properties of Riceberry rice

Based on the phytochemical and nutrient composition of Riceberry rice bran, studies have shown its health benefits such as antioxidants, anti-cancer, anti-inflammatory, and anti-diabetic effects.

- Antioxidant effect

In 2009, Jittorntrum *et al.* studied the cytoprotective effect of Riceberry rice bran extract (RBE) in human intestinal Caco-2 cells and demonstrated its high antioxidant activity including FRAP, ORAC, and DPPH (Jittorntrum *et al*.,

2009). In 2016, this was confirmed in a gentamicin-induced nephrotoxicity rat model, where it inhibits oxidative stress, inflammation, and apoptosis via the PKC/Nrf2 pathway (Arjinajarn *et al*., 2016). In 2017, RBE also protects the liver with its anti-oxidative stress, anti-inflammatory and anti-apoptotic activity (Arjinajarn *et al*., 2017).

- Anti-cancer effect

Leardkamolkarn *et al*. studied the anti-cancer activity of RBE in human cancer cell lines colonic carcinoma (Caco-2), breast adenocarcinoma (MCF-7), and acute myeloid leukemia (HL-60) cells. The results indicate that RBE has anti-proliferation activity by inhibiting DNA synthesis and inducing cell cycle arrest. Moreover, RBE induces apoptosis by promoting DNA fragmentation, increasing p53 protein expression, and decreasing caspase-3 protein expression (Leardkamolkarn *et al*., 2011). Furthermore, studies with gramisterol in acute myelogenous leukemia cell line (WEHI-3 cells) and leukemic mouse model show that it can induce cell cycle arrest and apoptosis via suppression of p-STAT3 signaling. In a leukemic mouse model, gramisterol prevents immune system dysfunction by increasing IFN-r production and enhancing p-STAT1 transcription signaling in hematopoietic cells (Somintara *et al*., 2016).

- Anti-diabetic effects

RBE protects against metabolic syndrome by improving hyperglycemia and metabolic markers in diabetic rats. Feeding Riceberry rice bran (RB) and Riceberry rice bran oil (RBBO) to steptozotocin-induced diabetic rats improves blood glucose, HbA1c, lipid profile, Glut4 expression level in skeletal muscle, serum insulin concentration and insulin sensitivity (Ruethaithip and Surasiang, 2011, Kongkachuichai *et al*., 2013, Posuwan *et al*., 2013, Prangthip *et al*., 2013). RB and RBBO improves antioxidant enzyme activity (superoxide dismutase, catalase, glutathione peroxidase), oxidative stress (TBARS), coenzyme Q10 and ORAC levels. In addition, it improves tissue regeneration in pancreas, kidneys, heart, liver, and spleen (Posuwan *et al*., 2013, Prangthip *et al*., 2013). Other

functions for RBE are inhibition of carbohydrate and lipid digestion and absorption and downregulation of glucose transporter mRNA expression in Caco-2 cells (Poosri *et al*., 2019). In healthy adults, consumption of Riceberry rice bread (Chusak *et al*., 2020) and Riceberry rice yogurt (Anuyahong *et al*., 2020) reduces postprandial glycemia and increases plasma insulin.

# Chapter III
# Materials and methods

## 3.1 Materials

| Chemicals | Company |
|---|---|
| Rutin (97%+) | ACROS organics (Thermo Fisher, Geel Belgium) |
| Cyanidin-3-glucoside (C3G) | Cayman Chemical Co. (Ann Arbor, MI, USA) |
| Peonidin-3-glucoside (P3G) | Cayman Chemical Co. (Ann Arbor, MI, USA) |
| p-Coumaric acid (CA) | Cayman Chemical Co. (Ann Arbor, MI, USA) |
| Ferulic acid (FA) | Cayman Chemical Co. (Ann Arbor, MI, USA) |
| Protocatechuic acid (PCA) | Frontier Scientific, Inc. (Logan, UT, USA) |
| Gallic acid | Fluka™ (Seelze, Germany) |
| Catechin | Sigma-Aldrich Co. (St. Louis, MO, USA) |
| Folin-Ciocalteau reagent | Sigma-Aldrich Co. (St. Louis, MO, USA) |
| Aluminium chloride ($AlCl_3$) | Ajex Finechem (Taren Point, Australia) |
| Acetonitrile | Merck (Darmstadt, Germany) |
| Calcium chloride ($CaCl_2$) | Ajex Finechem (Taren Point, Australia) |
| Sodium chloride (NaCl) | Thermo Fisher (Waltham, MA, USA) |
| Sodium bicarbonate ($NaHCO_3$) | Thermo Fisher (Waltham, MA, USA) |
| Sodium nitrite ($NaNO_2$) | Qrec chemical Co, Ltd. (New Zealand) |
| Sodium hydroxide (NaOH) | Emsure, Sigma-Aldrich Co. (St. Louis, MO, USA) |
| Sodium acetate ($CH_3COONa$) | Kemaus, Elago Enterprises Pty Ltd. (Cherrybrook, Australia) |
| Potassium chloride (KCl) | Thermo Fisher (Waltham, MA, USA) |
| Magnesium sulfate ($MgSO_4$) | Thermo Fisher (Waltham, MA, USA) |
| Hydrochloric acid (HCl) | Merck (Darmstadt, Germany) |
| Potassium phosphate ($KH_2PO_4$) | Thermo Fisher (Waltham, MA, USA) |

| Chemicals | Company |
|---|---|
| EGTA | Thermo Fisher (Waltham, MA, USA) |
| Formic acid | Thermo Fisher (Waltham, MA, USA) |
| Ethanol | Merck (Darmstadt, Germany) |
| Methanol (analytical grade) | Merck (Darmstadt, Germany) |
| Isopropanol | Sigma-Aldrich Co. (St. Louis, MO, USA) |
| Chloroform | Sigma-Aldrich Co. (St. Louis, MO, USA) |
| HEPES | Merck (Darmstadt, Germany) |
| Glucose | Thermo Fisher (Waltham, MA, USA) |
| Ionomycin | MP Biomedicals™ (Solon, OH, USA) |
| Isoproterenol | Invitrogen™ (Thermo Fisher, Waltham, MA, USA) |
| Zinc powder | Ajex Finechem (Taren Point, Australia) |
| Thapsigargin | Sigma-Aldrich Co. (St. Louis, MO, USA) |
| U73122 | Tocris Bioscience™ (Bristol, UK) |
| U73343 | Tocris Bioscience™ (Bristol, UK) |
| 2-APB | Tocris Bioscience™ (Bristol, UK) |
| Nimodipine | Sigma-Aldrich Co. (St. Louis, MO, USA) |
| DMEM/high glucose | Hyclone Laboratories Inc. (Logan, UT, USA) |
| RPMI | Corning, Mediatech, Inc. (Manassas, VA, USA) |
| Fetal bovine serum (FBS) | Sigma-Aldrich Co. (St. Louis, MO, USA) |
| L-glutamine | ACROS organics (Thermo Fisher, Geel Belgium) |
| Sodium pyruvate | Gibco, Thermo Fisher (Waltham, MA, USA) |
| 2-mercaptoethanol | Sigma-Aldrich Co. (St. Louis, MO, USA) |
| Trypsin | Gibco, Thermo Fisher (Waltham, MA, USA) |
| Phosphate buffer saline (PBS) | Gibco, Thermo Fisher (Waltham, MA, USA) |
| Bovine serum albumin (BSA) | Sigma-Aldrich Co. (St. Louis, MO, USA) |

| Chemicals | Company |
|---|---|
| 3-Isobutyl-1-methylxanthine (IBMX) | Sigma-Aldrich Co. (St. Louis, MO, USA) |
| Dexamethasone | Sigma-Aldrich Co. (St. Louis, MO, USA) |
| Insulin | Sigma-Aldrich Co. (St. Louis, MO, USA) |
| MTT | MP Biomedicals™ (Solon, OH, USA) |
| Dimethyl sulfoxide (DMSO) | Sigma-Aldrich Co. (St. Louis, MO, USA) |
| Oil Red O | Sigma-Aldrich Co. (St. Louis, MO, USA) |
| 2-NBDG | Invitrogen™ (Thermo Fisher, Waltham, MA, USA) |
| Fura-2 acetoxymethyl ester (Fura-2AM) | Cayman Chemical Co. (Ann Arbor, MI, USA) |
| TRIzol™ | Invitrogen™ (Thermo Fisher, Waltham, MA, USA) |

| Equipment | Company |
|---|---|
| Spectrophotometer | Biotek (Winooski, VT, USA) |
| Spectrofluorometer | Perkin Elmer (Waltham, MA, USA) |
| Centrifuge | Hettich zentrifugen (Tuttlingen, Germany) |
| Rotary evaporator | Buchi (Switzerland) |
| Water bath | Memmert GmbH+ Co. KG (Schwabach, Germany) |
| Hot plate | IKA-Works (Staufen im Breisgau,Germany) |
| Vortex mixer | Gemmy industrial corp. (Taipei, Taiwan) |
| pH meter | Thermo Fisher (Waltham, MA, USA) |
| Biosafety cabinet (class II) | Esco Micro Pte. Ltd (Singapore) |
| $CO_2$ incubator | Skadi Europe B.V. (Netherland) |
| Inverted microscope | Nikon (Minato, Tokyo, Japan) |
| High-performance liquid chromatography (HPLC) | Shimadzu corp. (Kyoto, Japan) |
| HPLC C18 column | Vertical Chromatography Co., Ltd. |

| Equipment | Company |
|---|---|
| | (Nonthaburi, Thailand) |
| Ultimate 3000 UHPLC system | Thermo Fisher (Waltham, MA, USA) |
| Electrospray ionization-Quadrupole-Time of Flight Mass Spectrometer (ESI-Q-TOF-MS/MS) | Bruker Daltonik GmbH (Bremen, Germany) |
| MUSE™ Cell Analyzer | Millipore (Darmstadt, Germany) |
| Luminex® system | EMD Millipore (Darmstadt, Germany) |
| Real-time calcium imaging | TILL-Photonics Grafelfingen (Gräfelfing, Germany) |
| NanoDrop 1000 Spectrophotometer | Thermo Fisher (Waltham, MA, USA) |
| CFX384 Touch™ Real-time PCR detection system | Bio-Rad Laboratories (Hercules, CA, USA) |
| GeneAmp 9600 PCR system | Perkin Elmer (Waltham, MA, USA) |
| 7300 Real-time PCR system | Applied Biosystems (Waltham, MA, USA) |

| Miscellaneous | Company |
|---|---|
| 3T3-L1 cells (CL-173™) | American Type Culture Collection (Manassas, VA, USA) |
| RQ1 DNase kit | Promega (Madison, WI, USA) |
| Reverse Transcriptase system | Promega (Madison, WI, USA) |
| iTaq™ Universal SYBR® Green Supermix | Bio-Rad Laboratories (Hercules, CA, USA) |
| Direct-zol™ RNA MicroPrep | Zymo Research Co. (Irvine, CA, USA) |
| TURBO DNA-free™ kit | Ambion, Thermo Fisher (Waltham, MA, USA) |
| M-MLV Reverse Transcriptase | Invitrogen™ (Thermo Fisher, Waltham, MA, USA) |
| IDT™ Primers | Integrated DNA Technologies, Inc. (Coralville, IA, USA) |
| MUSE™ Cell Count and Viability kit | Millipore (Darmstadt, Germany) |

| Miscellaneous | Company |
|---|---|
| MUSE™ Cell Cycle kit | Millipore (Darmstadt, Germany A) |
| MILLIPLEX® MAP Phospho/Total Akt1 2-plex Magnetic Bead Panel kit | EMD Millipore (Darmstadt, Germany) |
| Triglyceride liquicolor GPO-POD kit | Human (Wiesbaden, Germany) |
| Free glycerol reagent | Sigma-Aldrich Co. (St. Louis, MO, USA) |
| Pierce™ BCA Protein Assay kit | Thermo Fisher (Waltham, MA, USA) |
| Ultrasensitive rat insulin ELISA kit | Mercodia (Uppsala, Sweden) |

### 3.2 Experiment 1: Phytochemical compositions of Riceberry rice extract (RBE)

To investigate the phytochemical composition and compounds in RBE.

#### 3.2.1 Extraction of Riceberry rice

Riceberry rice was harvested in the Roi Et Province, Thailand and obtained by random sampling in a local market. The extraction protocols followed a previous report (Anuyahong *et al*., 2020). A Riceberry rice (2 kg) in 5 L of water was warmed and stirred at 45°C for 40 min, then filtered through Whatman No.1 filter paper and frozen at -18°C for 48 h. After that, the aqueous extraction was lyophilized using a freeze dryer machine GFD-30S (GRT., Grisrianthong. Co., Ltd, Thailand) and dried under pressure of 0.15 mbar at -30°C for 27.5 h. The percentage of extraction ratio (% yield) was calculated by the following equation:

$$\% \text{ Yield} = \frac{\text{Extract powder weight (g)} \times 100}{\text{Riceberry rice dry weight (g)}}$$

#### 3.2.2 Determination of total phenolic content in RBE

To determine the total phenolic content in RBE, the Folin-Ciocalteau method was used according to a previous study with modifications (Kamboj *et al*., 2015). An aliquot of RBE 2 mg/mL in water (50 µL) was mixed with 50 µL of Folin-Ciocalteau reagent. After incubation at room temperature for 5 min in dark, 50 µL of 10% (w/v) sodium carbonate was added, then incubated at room temperature for 30 min in dark. The absorbance was measured at 760 nm using a micro-plate reader. Total phenolic content was calculated using a calibration curve of Gallic acid (0 - 0.125 mg/mL) and the results were presented as mg of gallic acid equivalents per g of extract (mg GAE/g extract).

3.2.3 Determination of total flavonoid content in RBE

To determine the total flavonoid content in RBE, the aluminium chloride ($AlCl_3$) with sodium nitrite ($NaNO_2$) method was used as previously reported (Pękal and Pyrzynska, 2014). RBE 2 mg/mL in water (100 µL) was mixed with 30 µL of 5% (w/v) sodium nitrite ($NaNO_2$) and added to 400 µL water. After incubation at room temperature for 5 min in dark, 30 µL of 10% (w/v) aluminium chloride ($AlCl_3$), 200 µL of 1 M sodium hydroxide (NaOH), and 240 µL of water were added. After mixing, the absorbance was measured at 510 nm using a spectrophotometer. Total flavonoid content was calculated using a calibration curve of catechin (0 - 1 mg/mL) and the results presented as mg of catechin equivalents per g of extract (mg CE/g extract).

3.2.4 Determination of total anthocyanin content in RBE

Total anthocyanin content in RBE was measured using the pH differential method with a spectrophotometer as described (Lee *et al*., 2005). An aliquot of RBE (500 µL) was mixed with 500 µL of 0.025 M KCl buffer (pH 1.0) or 500 µL of 0.4 M sodium acetate ($CH_3COONa$) buffer (pH 4.5). Both of solutions were incubated at room temperature for 15 min in dark, then the absorbance measured at 520 and 700 nm. According to the Beer-Lambert's Law, total anthocyanin content was calculated by the following equation:



$$\text{Total anthocyanin} = \frac{A \times MV \times DF \times 10^3}{\varepsilon \times L}$$

| | | |
|---|---|---|
| A | = | $(A520 - A700)_{pH1.0} - (A520 - A700)_{pH4.5}$ |
| MW | = | Molecular weight of C3G (449.38 g/mol) |
| DF | = | Dilution factor |
| $10^3$ | = | Converting factor from g to mg |
| L | = | Path length of cuvette (cm) = 1 cm |
| $\varepsilon$ | = | Molar extinction coefficient of C3G (26,900 L/mol.cm) |

The results were presented as mg of cyanidin-3-glucoside per g of extract (mg C3G/g extract).

3.2.5 Determination of anthocyanins in RBE

To measure the amount of anthocyanins in RBE, high-performance liquid chromatography (HPLC) was performed according to a previous study with minor modifications (Zhang *et al.*, 2004). RBE 1 mg/mL was dissolved in methanol with 2% HCl (v/v) and filtered through 0.45 µm nylon syringe filter before injection into HPLC system. A standard mixture of C3G with P3G and the RBE solution were injected at 20 µL of each sample. The sample was separated by using C18 column (250 x 4.6 mm, 5 µm, Varian®), which is a stationary phase of the system. After that, the analyte was eluted by mobile phase A solution (water: formic acid, 90:10, v/v) and mobile phase B solution (water: methanol: formic acid: acetonitrile, 40:22.5:10:22.5, v/v/v/v) at a flow rate of 0.6 mL/min by using an L-6200 intelligent pump. Chromatographic conditions were performed as shown in Table 7.

**Table 7** Chromatographic conditions of the HPLC system

| Time (min) | Pump A (%) | Pump B (%) |
|---|---|---|
| 0.01 | 85 | 15 |
| 5 | 80 | 20 |
| 35 | 73 | 27 |
| 45 | 35 | 65 |
| 50 | 0 | 100 |
| 53 | 85 | 15 |
| 60 | 85 | 15 |



Then, components of the extract were detected using an L-4250 UV visible variable wavelength detector at 515 nm. The major anthocyanins were calculated by comparing the peak area of each sample to the calibration curve of C3G and P3G at the same retention time. The results were presented as µg of C3G or P3G per mg of extract.

3.2.6 Identification of phytochemical contents in RBE

To identify the phytochemical compounds in RBE, liquid chromatography and tandem mass spectrometry (LC-MS/MS) was performed using an Ultimate 3000 UHPLC system (Thermo Scientific, Dionex, Sunnyvale, CA, USA) with an Electrospray ionization Quadrupole-Time of Flight Mass Spectrometer (ESI-Q-TOF-MS/MS; Model Impact II, Bruker Daltonik GmbH, Bremen, Germany). RBE 10 mg/mL was dissolved in 0.1% formic acid solution and filtered through 0.22 µm nylon syringe filter before injecting at a flow rate of 0.3 mL/min into the system for 20 min. The sample was separated using a Titan C18 reverse phase column (50 x 21 mm, 1.9 µm) at 30ºC. The HPLC gradients were run by 0–9 min: 5–30% B; 12–17 min:95% B; 17.5 min: 5% B and held for 2 min using an eluent A solution (0.1% v/v formic acid in water) and eluent B solution (0.1% v/v/ formic acid in acetonitrile) at the injection volume of 5 and 10 µL for positive and negative ionization mode, respectively.

The ESI inlet condition for mass spectra recording were: scanning mass-to-charge (m/z) range of 50 to 1000, capillary voltage of 3800 V for positive mode and 2500 V for negative mode, drying gas temperature at 200ºC with a flow rate of 8.0 L/min, and the nebulizer pressure of 2.0 bar. The collision energy values 20-50 eV was adjusted by automatic MS/MS experiments depending on m/z. Nitrogen was used as collision gas. For auto internal mass calibration, sodium formate solution was used as a calibrant.



The MS data were analyzed using Data Analysis 4.3 software (Bruker Daltonics, Bermen, Germany). The MS-DIAL software (RIKEN, version 4.18) was used to identify the detected compounds by matching with the Respect and GNPS mass spectral libraries based on weighted similarity score of accurate mass and MS/MS spectra at a cut off value of 80%.

### 3.3 Experiment 2: Inhibitory effects of Riceberry rice extract (RBE) on cell proliferation and adipogenesis in preadipocytes

To investigate the effects of RBE on cell proliferation and adipogenesis in 3T3-L1 preadipocytes.

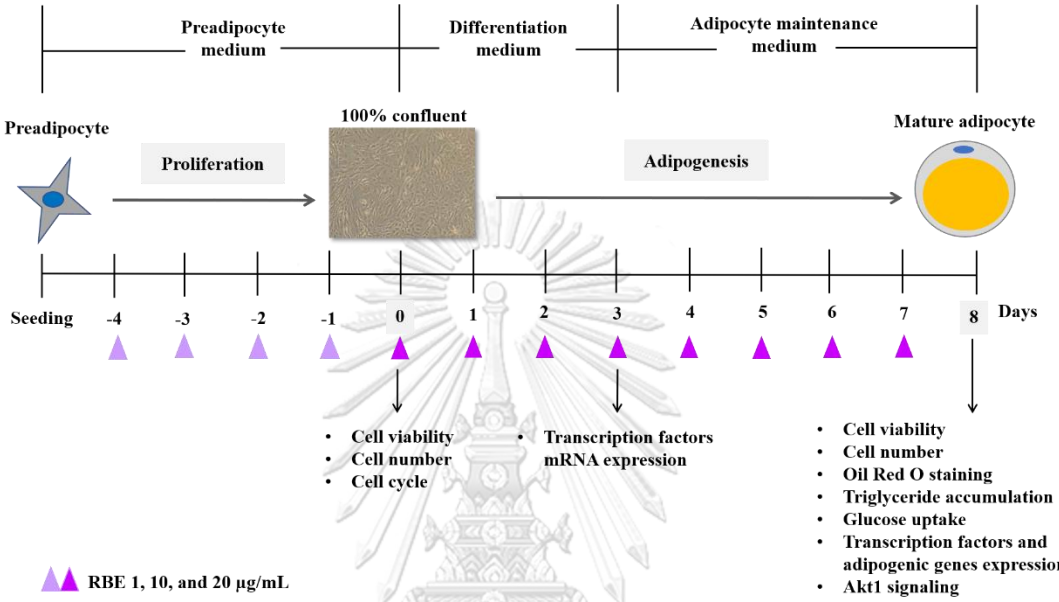


**Figure 15** Experimental design for Riceberry rice extract (RBE) treatment of 3T3-L1 cells

Preadipocytes (Cell proliferation)

3.3.1 Cell culture of 3T3-L1 preadipocytes

Mouse preadipocyte, 3T3-L1 cells from ATCC® (CL-173™) were cultured in Dulbecco's Modified Eagle's Medium (DMEM) containing 10% of heat-inactivated fetal bovine serum (FBS), 100 IU/mL penicillin, and 100 µg/mL streptomycin. Cells were maintained in the humidified atmosphere with 5% $CO_2$ at 37°C. Cells were grown in T25 and T75 culture flask until achieve 80-90% confluence, and then subcultured into new passages or seeded for experiments. All experiments were performed on cells from passages 4-16.

3.3.2 Determination of cell number and viability after 4 days of treatment

To investigate the effects of RBE on cell number and viability, the MUSE™ Cell Count and Viability kit (Millipore, Germany) was performed using the MUSE™ Cell Analyzer (Millipore). Preadipocytes were seeded on 12-well plate (10,000 cells/mL) and cultured for 24 h, then treated with RBE at 1, 10, and 20 µg/mL for 4 days. According to the manufacturer's instructions (Merck Millipore), cells were trypsinized, centrifuged, and re-suspended with DMEM. The suspended cells 20 µL were mixed with 380 µL of MUSE™ Cell Count and Viability reagent and incubated at room temperature for 5 min in dark. Finally, the mixture was loaded into the MUSE™ Cell Analyzer with at least 10,000 cells for each sample.

The MUSE™ Cell Count and Viability kit contained two DNA-intercalating fluorescent dyes including membrane-permeant DNA staining dye that can separate nucleated cells from debris and DNA-binding dye that can separate viable cells from dead cells. The results were presented as percentage of viability (% of control) and total cell number (cells/mL).

3.3.3 Determination of cell cycle

To investigate the effects of RBE on cell cycle, the MUSE™ Cell Cycle kit (Millipore, Germany) was performed using the MUSE™ Cell Analyzer (Millipore). Preadipocytes were seeded on 6-well plate (10,000 cells/mL) and cultured for 24 h, then treated with RBE at 1, 10, and 20 µg/mL for 4 days. According to the manufacturer's instructions (Merck Millipore), cells were trypsinized, centrifuged, re-suspended with 1 mL of PBS (pH 7.4), and fixed in 3 mL of 70% cooled-ethanol at -20°C overnight. Next, fixed cells were washed and re-suspended in PBS twice. Then, the cell pellets were re-suspended with 200 µL MUSE™ Cell Cycle kit reagent and incubated at room temperature for 30 min in dark. Finally, the mixture was loaded into the MUSE™ Cell Analyzer with at least 10,000 cells for each sample.

The MUSE™ Cell Cycle kit contains propidium iodine (PI), which is a nuclear DNA staining dye that can discriminate cells at different stages of cell cycle with

different in DNA content. The results were presented as percentage of cells in G0/G1, S, G2/M phase.

Adipogenesis (Cell differentiation)

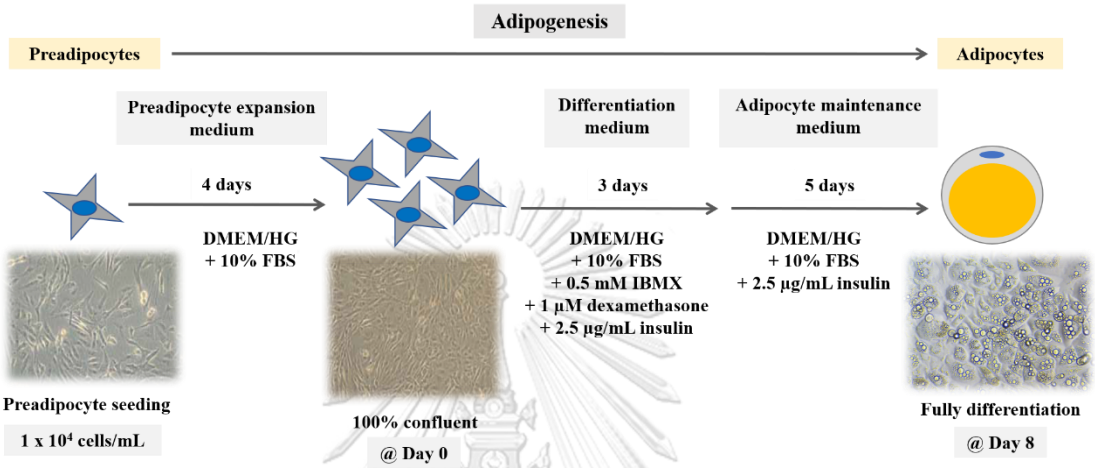


**Figure 16** Differentiation protocol for 3T3-L1 cells.

3.3.4 Cell differentiation of 3T3-L1 preadipocytes

Based on the recommendation by ATCC®, 3T3-L1 preadipocytes (ATCC®, CL-173™) were cultured in Dulbecco's Modified Eagle's Medium (DMEM) containing 10% of heat-inactivated FBS, 100 IU/mL penicillin, and 100 µg/mL streptomycin. Cells were maintained in the humidified atmosphere with 5% $CO_2$ at 37°C and grown in T75 culture flask until 80-90% confluent, then seeded on 12-well or 6-well plate (10,000 cell/mL) and cultured for 4 days. After reaching 100% confluence, cells were incubated with DMEM supplemented with 10% FBS, 0.5 mM IBMX, 1 µM dexamethasone, and 2.5 µg/mL insulin for differentiation. After 3 days of induction, cells were maintained in DMEM with 2.5 µg/mL insulin until fully differentiated on day 8 as shown in Figure 16. All experiments were performed with cells from passages 4-10.

3.3.5 Determination of cell number and viability

To investigate the effects of RBE on cell number and viability, preadipocytes were seeded on 12-well plate (10,000 cells/mL) and cultured for 4 days until 100% confluent, then treated with RBE at 1, 10, and 20 µg/mL for 8 days. After that, cells were trypsinized and resuspended in DMEM 1 mL/well. The suspension was mixed with trypan blue in 1:1 ratio and cells were counted using a hemocytometer. The results were presented as percentage of cell viability (% of control) and total cell number (cells/mL).

3.3.6 Determination of adipogenesis

To investigate the effects of RBE on adipogenesis, Oil Red O staining was performed after 8 days of treatment. According to the manufacturer's instructions (Sigma Aldrich®, Germany), the adipocytes were washed twice with PBS 1 mL/well, fixed in 1 mL/well of 10% formalin at room temperature overnight, and washed with water. Next, cells were incubated with 60% isopropanol 1 mL/well at room temperature for 5 min and stained with 200 µL/well Oil Red O working solution at room temperature for 20 min. Finally, the excess dye was washed five times with water. An inverted microscope was used to capture the stained adipocytes and the adipocyte number quantified using ImageJ software. The results were presented as total adipocyte count (cells/frame).



3.3.7 Determination of triglyceride accumulation

To investigate the effects of RBE on triglyceride accumulation, a liquicolor GPO-POD kit (Human, Germany) was used after 8 days of treatment. According to previously described method (Kang *et al*., 2013), the adipocytes were washed with PBS 1 mL/well and lysed with buffer 200 µL/well under sonication for 5 min. After centrifugation at 12,000 g at room temperature for 10 min, 5 µL of supernatant was incubated with 250 µL of triglyceride reagent at room temperature for 10 min in the dark. The absorbance was measured at 500 nm using a micro-plate reader. The triglyceride concentration was calculated by comparing to calibration curve of triglyceride standard (0 – 200 mg/mL) and the results presented as mg of triglyceride per mL (mg/mL).

3.3.8 Determination of transcription factors and adipogenic genes mRNA expression

To investigate the effects of RBE on transcription factors and adipogenic gene expression, real-time qPCR was performed after 3 days and 8 days of treatment. Total RNA of adipocytes was extracted, treated with DNase enzyme, reverse transcribed to cDNA followed by real-time qPCR as following:

- RNA extraction

  Total RNA extraction was performed using TRIzol™ reagent (Invitrogen™, Thermo Fisher, USA). According to the manufacturer's instructions (Invitrogen™), adipocytes were washed with cooled-PBS 1 mL/well, incubated with TRIzol™ reagent 1 mL/well at room temperature for 5 min, and mixed with 200 µL of chloroform. After incubation at room temperature for 3 min, the mixture was centrifuged at 12,000 g 4°C for 15 min. Then, the supernatant was collected, incubated with isopropanol at room temperature for 10 min, and centrifuged at 12,000 g 4°C for 10 min. Next, the pellets were washed with 75% ethanol 1 mL and centrifuged at 7,500 g 4°C for 5 min. Finally, RNA pellets were dried before re-suspension in water at 55°C for 15 min. The RNA concentration was measured using NanoDrop 1000 spectrophotometer (ng/µL).

- DNase treatment

  The DNase treatment was performed using RQ1 DNase treatment kit (Promega®, USA). According to the manufacturer's instructions (Promega), the RNA in each sample was diluted into 200 ng/µL, treated with RQ1 DNase enzyme at 37°C for 30 min, and stopped by adding 1 µL of RQ1 DNase stop solution at 65°C for 10 min.

- Reverse transcription

  To convert RNA to cDNA, reverse transcription was performed using the Reverse transcription system (Promega®, USA). According to the manufacturer's instructions (Promega), 5 µL of DNase-treated RNA was incubated with 2.5 µL of Oligo(dT) primer at 70°C for 5 min, cooled on ice for 5 min. After that, the RNA

template was mixed with reverse transcriptase master mix and incubated as shown in Table 8 and Table 9.

**Table 8** The reaction setup of cDNA synthesis

| Component | Volume (μL) |
|---|---|
| RNA template (RNA with Oligo(dT) primer) | 7.5 |
| Reverse transcriptase enzyme (RT) | 1 |
| RT 5x buffer | 4 |
| $MgCl_2$ (25 mM) | 2.4 |
| dNTP mixture (10 mM) | 1 |
| Molecular water | 4.1 |
| **Total volume** | **20** |

**Table 9** The protocol of cDNA synthesis reaction

| Step | Temperature and Time |
|---|---|
| Priming | 25°C for 5 min |
| Reverse transcription | 42°C for 1 h |
| RT inactivation | 70°C for 15 min |



- Real-time PCR

To determine mRNA expression levels, real-time qPCR was performed using iTaq™ Universal SYBR® Green Supermix (Bio-Rad, CA, USA). According to the manufacturer's instructions (Bio-Rad), the cDNA template in each sample was diluted into 25 ng/μL and mixed with the reaction setup component (Table 10) and incubated using a CFX384 Touch™ Real-Time PCR Detection system (Bio-Rad, CA, USA) as shown in Table 11. The primer sequences are listed in Table 12. The mRNA expression of target genes was normalized with β-actin as an internal reference gene. The results were presented as relative differences of

threshold cycle number (ΔCt) between each sample using $2^{-\Delta\Delta Ct}$ method as shown in following equation:

$$\Delta\Delta Ct = (Ct,target - Ct,\beta\text{-actin})_{sample} - (Ct,target - Ct,reference)_{control}$$

**Table 10** The reaction setup of real-time PCR

| Component | Volume (μL) |
|---|---|
| cDNA template | 2 |
| iTaq™ Universal SYBR® Green Supermix | 5 |
| Forward primer | 0.5 |
| Reverse primer | 0.5 |
| Molecular water | 2 |
| **Total volume per reaction** | **10** |

**Table 11** The thermal cycling protocol of real-time PCR

| Step | Temperature and Time |
|---|---|
| Polymerase activation | 95°C for 2 min |
| Denature | 95°C for 5 sec |
| Annealing | 60°C for 30 sec |
| Repeat 40 cycles | |
| Extension | 65°C for 5 sec |
| Melt-curve analysis | 65°C - 95°C (0.5°C increment/step) |

**Table 12** Primer sequences (mouse) used for real-time PCR

| Gene | Forward sequence (5' – 3') | Reverse sequence (5' – 3') |
|---|---|---|
| PPARγ | ACGTGCAGCTACTGCATGTGA | AGAAGGAACACGTTGTCAGCG |
| C/EBPα | GGAACTTGAAGCACAATCGATC | TGGTTTAGCATAGACGTGCACA |
| C/EBPβ | TGAGCGACGAGTACAAGATGC | GACAGCTGCTCCACCTTCTTCT |
| C/EBPγ | ATCGACTTCAGCGCCTACAT | GCTTTGTGGTTGCTGTTGAA |
| InsR | CAGAAGCACAATCAGAGTGAGTATGAC | ACCACGTTGTGCAGGTAATCC |
| AdipoQ | GCACTGGCAAGTTCTACTGCAA | GTAGGTGAAGAGAACGGCCTTGT |
| AdipoQ-R1 | CCCCCTTACCCCCGTCCTTAC | GGCGTGGCTTTGTTTGTCCTA |
| AdipoQ-R2 | TGCGCACACGTTTCAGTCTCCT | TTCTATGATCCCCAAAAGTGTGC |
| Leptin | GAGACCCCTGTGTCGGTTC | CTGCGTGTGTGAAATGTCATTG |
| Resistin | TGCCAGTGTGCAAGGATAGACT | CGCTCACTTCCCCGACAT |
| Fabp4 | AAGGTGAAGAGCATCATAACCCT | TCACGCCTTTCATAACACATTCC |
| FasN | AGGTGGTGATAGCCGGTATGT | TGGGTAATCCATAGAGCCCAG |
| ACC | CGGACCTTTGAAGATTTTGT | GCTTTATTCTGCTGGGTGAA |
| Glut4 | CAACTGGACCTGTAACTTCATTGT | ACGGCAAATAGAAGGAAGACGTA |
| β-actin | TGTCCACCTTCCAGCAGATGT | AGCTCAGTAACAGTCCGCCTAGA |



3.3.9 Determination of Akt1 signaling

To investigate the effects of RBE on Akt1 signaling in adipocytes, cells were cultured and differentiated in 6-well plate. After 8 days of RBE treatment, cells were washed with cold PBS and lysed with 200 µL/well of ice-cold 1X MILLIPLEX® MAP lysis buffer (EMD Millipore, Merck, Germany). Cell lysates were gently rocked for 15 min at 4ºC and centrifuged at 14,000 g under 4ºC for 15 min. Supernatants were collected and stored at -80ºC. The phosphorylation levels of Akt1 (Ser473) were determined using the MILLIPLEX® MAP Phospho/Total Akt1 2-plex Magnetic Bead Panel kit (EMD Millipore, Merck, Germany) according to the manufacturer's instruction. The fluorescence intensity of the beads was measured and analyzed using the Luminex® system (EMD Millipore, Merck, Germany). Data were normalized to the total protein concentration from the BCA

kit (Thermo Fisher, USA) using bovine serum albumin as a standard. The results were presented as the Median Fluorescence Intensity (MFI) per mg protein (MFI/mg protein).

3.3.10 Determination of glucose uptake

To investigate the effects of RBE on glucose uptake in adipocytes, 2-[N-(7-nitrobenz-2-oxa-1,3-diazol-4-yl) amino]-2-deoxy-D-glucose (2-NBDG) was performed as previously described with minor modifications (Manaharan *et al*., 2013). After 8 days, adipocytes were treated with RBE at 1, 10, and 20 µg/mL in PBS at 37°C for 2 h. Then, cells were incubated with 80 µM of fluorescent glucose analogue (2-NBDG) and 100 nM insulin in PBS at 37°C for 60 min. After that, excess 2-NBDG was washed three times with ice-cold PBS. The fluorescence intensity of 2-NBDG was determined at excitation wavelength of 485 nm and emission wavelength of 535 nm using fluorescence micro-plate reader. The fluorescence intensity reflected the amount of glucose uptake by adipocytes in each sample. Data were normalized to the total protein concentration from the BCA kit (Thermo Fisher, USA) using bovine serum albumin as a standard. The results were presented as percentage of glucose uptake (% of control).

3.3.11 Determination of lipolysis

To investigate the effects of RBE on lipolysis, glycerol release was measured using free glycerol reagent (Sigma Aldrich, Germany) as described in previous study with minor modifications (Pruszyńska-Oszmałek *et al*., 2017). After differentiation, adipocytes were starved in serum-free DMEM at 37°C overnight. For basal lipolysis, adipocytes were treated with RBE at 1, 10, and 20 µg/mL for 3 h with or without 100 nM isoproterenol, synthetic catecholamine for stimulated lipolysis. The medium from each sample was collected and mixed with free glycerol reagent (Sigma Aldrich, Germany) and reactions incubated at 37°C for 5 min and the absorbance measured at 540 nm. Glycerol content was expressed lipolysis rates for each sample after activation of hormone-sensitive lipase hydrolysis of triglycerides to glycerol and free fatty acids. The level of glycerol was calculated using a calibration curve of glycerol standard (0 – 260

μg/mL). Data were normalized to the total protein concentration from the BCA kit (Thermo Fisher, USA) using bovine serum albumin as a standard. The results were presented as mM of glycerol per mg protein (mM/mg protein).

3.3.12 Determination of intracellular calcium signaling in preadipocytes

To investigate whether the intracellular calcium signaling is required for RBE's effects in preadipocytes, the real-time calcium imaging was performed according to a previous study (Suantawee *et al*., 2017). Cells were grown on round glass coverslips (25 mm) in petri dish for 48 h until reaching 80-90% confluent. Then, cells were loaded with 2 μM Fura-2AM fluorescence dye at 37°C for 30 min. All experiments were performed in a calcium imaging buffer containing 136 mM NaCl, 4.8 mM KCl, 1.2 mM $CaCl_2$, 1.2 mM $MgSO_4$, 10 mM HEPES, 4 mM glucose, and 0.1% BSA (pH 7.4), except the experiments under extracellular calcium free conditions. The $CaCl_2$ was removed from the buffer and 0.1 mM EGTA added.

- To investigate the effects of RBE on intracellular calcium signals, cells were stimulated with RBE at 1, 10, and 20 μg/mL and 1 μM ionomycin as a positive control.
- To investigate the effects of other phytochemical compounds on intracellular calcium signals, cells were stimulated with 100 μM of coumaric acid (CA), ferulic acid (FA), protocatechuic acid (PCA), C3G, Cy, and C3R and 1 μM ionomycin as a positive control.
- To investigate the calcium sources for Cy and C3R responses, cells were stimulated with 100 μM Cy or C3R under extracellular calcium free condition or after depletion of the calcium stores in the ER with 1 μM Thapsigargin (TG).

The real-time intracellular calcium signals were recorded using a dual excitation fluorometric imaging system (TILL-Photonics Grafelfingen, Germany) controlled by TILLvisION software. Fura-2AM fluorescence in the cells was excited at 340 and 380 nm, and fluorescence emission collected at 510 nm, sampled at 1 Hz and computed as

F340/380 ratio. The results were presented as average calcium traces from all cells or peak calcium signals from three separate experiments.

### 3.4 Experiment 3: Stimulatory effects of cyanidin-3-rutinoside (C3R) on insulin secretion from pancreatic β-cells

To investigate the effects of C3R on insulin secretion from pancreatic INS-1 cells.

#### 3.4.1 Synthesis of C3R

C3R was synthesized from quercetin-3-O-rutinoside or rutin, one of the phytochemical compounds in RBE. According to published method (Elhabiri *et al*., 1995), rutin was dissolved in 3% methanol-HCl and mixed with zinc amalgum to generate C3R. Then, C3R was purified using column chromatography and evaporated using a rotary evaporator.

#### 3.4.2 INS-1 cell culture

Rat pancreatic β-cells, INS-1 cells were cultured in RPMI 1640 medium containing 11 mM glucose, 10% of heat-inactivated FBS, 2 mM L-glutamine, 10 mM HEPES, 1 mM sodium pyruvate, and 50 μM 2-mercaptoethanol. Cells were maintained in the humidified atmosphere with 5% $CO_2$ at 37°C and grown in T25 and T75 culture flask until 70-80% confluent, and then subculture into new passages or seeded for experiments. All experiments were performed with cells from passages 70-89.



#### 3.4.3 Determination of cell viability

To investigate the effects of C3R on cell viability, MTT assay was performed according to a previous method with minor modifications (Shi *et al*., 2011). Cells were seeded on 96-well plate (50,000 cells/mL) in 100 μL/well of culture medium and grown for 48 h, then treated with C3R (1-300 μM). After 24 h of treatment, cells were incubated with medium containing 0.5 mg/mL MTT (3-(4,5-dimethylthiazol-2-yl)-2,5-diphenyltetrazolium bromide) at 37°C for 3 h. Finally, purple formazan crystals in the living cells were dissolved by 100% DMSO and the absorbance was measured at 550

nm using a micro-plate reader. The quantity of formazan reflected the amount of viable cells in each sample. The results were presented as percentage of cell viability (% of control).

3.4.4 Determination of intracellular calcium signaling in pancreatic β-cells

To investigate whether intracellular calcium signaling is required for C3R induced insulin secretion, real-time calcium imaging was performed. INS-1 cells were grown on glass coverslips (25 mm) in petri dish for 48 h until reaching 80-90% confluent. Then, cells were loaded with 2 μM Fura-2AM fluorescence dye at 37°C for 30 min. All experiments were performed in a calcium imaging buffer containing 136 mM NaCl, 4.8 mM KCl, 1.2 mM $CaCl_2$, 1.2 mM $MgSO_4$, 10 mM HEPES, 4 mM glucose, and 0.1% BSA (pH 7.4), except the experiments performed under extracellular calcium free conditions. The $CaCl_2$ was removed and 0.1 mM EGTA added.

- To investigate the effects of RBE and other phytochemical compounds on intracellular calcium signals, cells were stimulated with RBE 100 μg/mL, 100 μM of CA, FA, PCA, C3G, and C3R and 1 μM ionomycin as a positive control.
- To investigate the effect of C3R on intracellular calcium signals, cells were stimulated with C3R at 1, 3, 10, 30, 60, 100, and 300 μM and 1 μM ionomycin as a positive control.
- To investigate the calcium sources for C3R responses, cells were stimulated with 100 μM C3R under extracellular calcium free condition or after depletion of calcium stores in the ER with 1 μM Thapsigargin (TG).
- To investigate whether C3R induces calcium influx through an L-type VDCCs, nimodipine (a VDCCs blocker) at 1-150 μM was used.
- To investigate whether the PLC-$IP_3$ pathway was involved in C3R's effect on intracellular calcium signals, cells were pretreated with 1-10 μM U73122 (the PLC inhibitor), 10 μM U73343 (an inactive analog of U73122), or 1-300 μM 2-APB (a selective $IP_3$ receptor blocker).

The real-time intracellular calcium signals were recorded using a dual excitation fluorometric imaging system (TILL-Photonics Grafelfingen, Germany) controlled by TILLvisION software. Fura-2AM fluorescence in the cells was excited at 340 and 380 nm, and fluorescence emissions collected at 510 nm, sampled at 1 Hz and computed as F340/380 ratio. The results were presented as average calcium traces from all cells or peak calcium signals from three separate experiments.

3.4.5 Determination of insulin secretion

Cells were seeded on 24-well plate (100,000 cells/well) and cultured for 3 days until reaching 80-90% confluence. Then, cells were incubated with Krebs-Ringer bicarbonate buffer (KRB) containing 136 mM NaCl, 4.8 mM KCl, 2.5 mM $CaCl_2$, 1.2 mM $KH_2PO_4$, 1.2 mM $MgSO_4$, 5 mM $NaHCO_3$, 10 mM HEPES, 4 mM glucose, and 0.1% BSA (pH 7.4) for 30 min. After that, cells were treated with C3R (1-300 μM) or 20 mM KCl (positive control) in KRB buffer. After incubation at 37°C for 30 min, the supernatant was collected for insulin determination using an ultrasensitive rat insulin ELISA (Mercodia AB, Uppsala, Sweden) and 25 μL of supernatant or calibrators were incubated with 100 μL of enzyme conjugate 1X solution at room temperature on a plate shaker 700-900 rpm. After incubation for 2 h, the plate was washed five times with 350 μL of wash buffer 1X solution. Then, 200 μL of substrate TMB was added and incubated at room temperature for 15 min. Finally, 50 μL of stop solution was added. After mixing the plate, the absorbance was measured at 450 nm. Insulin concentrations were calculated using a calibration curve of insulin calibrator (0-0.963 ng/mL) and normalized to the number of cells per well. The results were presented as ng per mL of insulin per $5x10^5$ cells.

3.4.6 Determination of insulin secretion-related genes expression

To investigate the effects of C3R on insulin secretion-related genes expression, real-time qPCR was performed. Cells were seeded on 6-well plate (200,000 cells/well) and cultured for 3 days until reaching 80-90% confluence, then treated with 100 μM C3R

for 6 h. Total RNA was extracted, treated with DNase enzyme, reverse transcribed to cDNA, and real-time qPCR performed as follow:

- RNA extraction

Total RNA extraction was performed using Direct-zol™ RNA MicroPrep (ZymoResearch Co., Irvine, CA, USA). According to the manufacturer's instructions (ZymoResearch), cells were extracted with TRIzol™ reagent 1 mL/well. To remove cell debris, cell lysate was centrifuged at 3,000 rpm 4°C for 5 min and mixed with 1 mL of 100% ethanol. The mixture was loaded into the column and centrifuged at 13,000 rpm 4°C for 30 sec. After complete loading the mixture, columns were loaded twice with prewash buffer 400 µL/column and centrifuged at 13,000 rpm 4°C for 30 sec. Then, the columns were loaded with wash buffer 700 µL/column and centrifuged at 13,000 rpm 4°C for 30 sec. To remove excess ethanol, the columns were centrifuged at 13,000 rpm 4°C for 2 min. Finally, the columns were soaked in water 15 µL/column for 3 min and centrifuged at 13,000 rpm 4°C for 3 min to dissolve RNA sample. The concentration of RNA was measured using NanoDrop 1000 spectrophotometer (ng/µL).

- DNase treatment

The DNase treatment was performed using TURBO DNA-free™ kit (Ambion, Thermo Fisher, Waltham, MA, USA). According to the manufacturer's instructions, RNA was incubated with DNase enzyme 1 µL/sample and buffer 1.2 µL/sample at 37°C for 30 min in water bath. After that, 1.42 µL/sample of stop solution was added and incubated at room temperature for 5 min. Finally, the mixture was centrifuged at 13,000 rpm 4°C for 3 min and supernatant was collected.

- Reverse transcription

To convert RNA to cDNA, reverse transcription was performed using M-MLV Reverse Transcriptase (Invitrogen™, Thermo Fisher, Waltham, MA, USA). According to the manufacturer's instructions, the reaction setup of cDNA synthesis was performed as shown in Table 13 at the final volume of 10 µL/reaction. Then, the reactions were incubated at 65°C for 5 min in the RT system and put on ice for 3 min. After that, the reactions were mixed with 5X first-strand buffer (4 µL/reaction), 0.1 M DTT (2 µL/reaction), RNase inhibitor (1 µL/reaction), and M-MLV reverse transcriptase enzyme (1 µL/reaction), then incubated by following protocol as shown in Table 14 using GeneAmp 9600 PCR system (Perkin Elmer, Waltham, MA, USA).

**Table 13** The reaction setup of cDNA synthesis for INS-1 cells

| Component | Volume (µL) |
|---|---|
| RNA template (1 µg) | Variable |
| Random primers | 1 |
| dNTP mixture | 1 |
| Molecular water | Variable |
| **Total volume** | **10** |



**Table 14** The protocol of cDNA synthesis reaction for INS-1 cells

| Step | Temperature and Time |
|---|---|
| Priming | 25°C for 10 min |
| Reverse transcription | 37°C for 50 min |
| RT inactivation | 70°C for 15 min |

- Real-time PCR

To determine the mRNA expression levels, real-time qPCR was performed using iTaq™ Universal SYBR® Green Supermix (Bio-Rad, Hercules, CA, USA). According to the manufacturer's instructions, the cDNA template was mixed with the reaction setup component as shown in Table 15 and incubated by following protocol as shown in Table 16 using a 7300 Real-time PCR system (Applied Biosystems, Waltham, MA, USA). The sequences of primer are shown in Table 17. The mRNA expression of target genes was normalized with β-actin as an internal reference gene. The results were presented as relative differences of threshold cycle number (ΔCt) between each sample using $2^{-\Delta\Delta Ct}$ method as shown in following equation:

$$\Delta\Delta Ct = (Ct,target - Ct,\beta\text{-actin})_{sample} - (Ct,target - Ct,reference)_{control}$$

**Table 15** The reaction setup of real-time PCR for INS-1 cells

| Component | Volume (μL) |
|---|---|
| cDNA template | 1 |
| 2X SsoAdvanced Universal SYBR® Green supermix | 11 |
| Forward primer | 1 |
| Reverse primer | 1 |
| Molecular water | 6 |
| **Total volume per reaction** | **20** |

**Table 16** The thermal cycling protocol of real-time PCR for INS-1 cells

| Step | Temperature and Time |
|---|---|
| Polymerase activation | 95°C for 10 min |
| Denaturation | 95°C for 15 sec |
| Annealing | 60°C for 1 min |
| Repeat 40 cycles | |
| Melt-curve analysis | 65°C - 95°C (0.5°C increment/step) |

**Table 17** Primer sequence (rat) used for real-time PCR

| Gene | Forward sequence (5' – 3') | Reverse sequence (5' – 3') |
|---|---|---|
| Ins | CACCCAAGTCCCGTCGTGAAGT | GATCCACAATGCCACGCTTCTG |
| GK | AAGGGAACAACATCGTAGGA | CATTGGCGGTCTTCATAGTA |
| Glut2 | TAAGGGGCACTGAGGACATC | TGCCAGCTGTCTGAAAAATG |
| $Cav_{1,2}$ | GAAATTCAAGAAGCGAAAAG | CCTGCTGTCACTCTGGTAG |
| $Kir_{6,2}$ | TCCACCAGGTAGACATCCC | TAGGAGCCAGGTCGTAGAG |
| β-actin | GCGTGACATCAAAGAGAAG | ACTGTGTTGGCATAGAGG |

### 3.5 Statistical analysis

Results are presented as mean ± SEM from three independent experiments. One-way analysis of variance (ANOVA) with Duncan's post hoc test and unpaired Student's *t*-test were used to analyze the statistical significance using SPSS version 22.0 (SPSS Inc., Chicago, IL, USA). Statistical significance was established at $P < 0.05$. All graphs were generated using Sigma Plot version 12.5 (Systat software, USA).

# Chapter IV
# Results

## 4.1 Phytochemical composition of Riceberry rice extract (RBE)

After extraction with water, the percentage extraction ratio (% yield) was 1.53%. RBE contained a total of 63.33 ± 2.40 mg GAE/g extract of phenolic compounds. Total flavonoid content and anthocyanin were 18.00 ± 0.00 mg CE/g extract and 10.13 ± 0.14 mg C3G/g extract, respectively. The anthocyanins detected in RBE were C3G (2.05 ± 0.04 µg C3G/mg extract) and P3G (0.78 ± 0.01 µg P3G/g extract) (Figure 17).

According to the chromatograms from UHPLC-MS/MS (Figure 18), there were seven compounds including C3G, P3G, petunidin-3-glucoside, caffeic acid, taxifolin, quercetin-3-rutinoside or rutin, and ferulic acid (Table 19 and 20). Their chemical structures are shown in Figure 19.

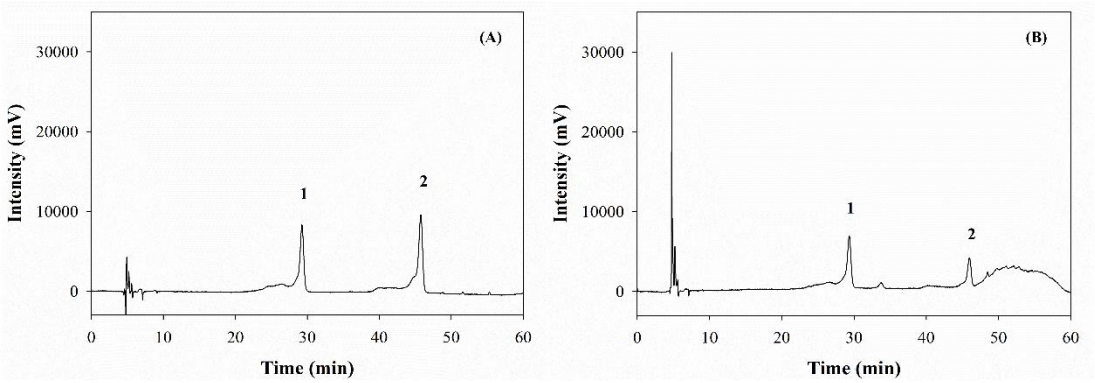


**Figure 17** HPLC chromatogram for (A) cyanidin-3-glucoside (1) and peonidin-3-glucoside (2) and (B) Riceberry rice extract.

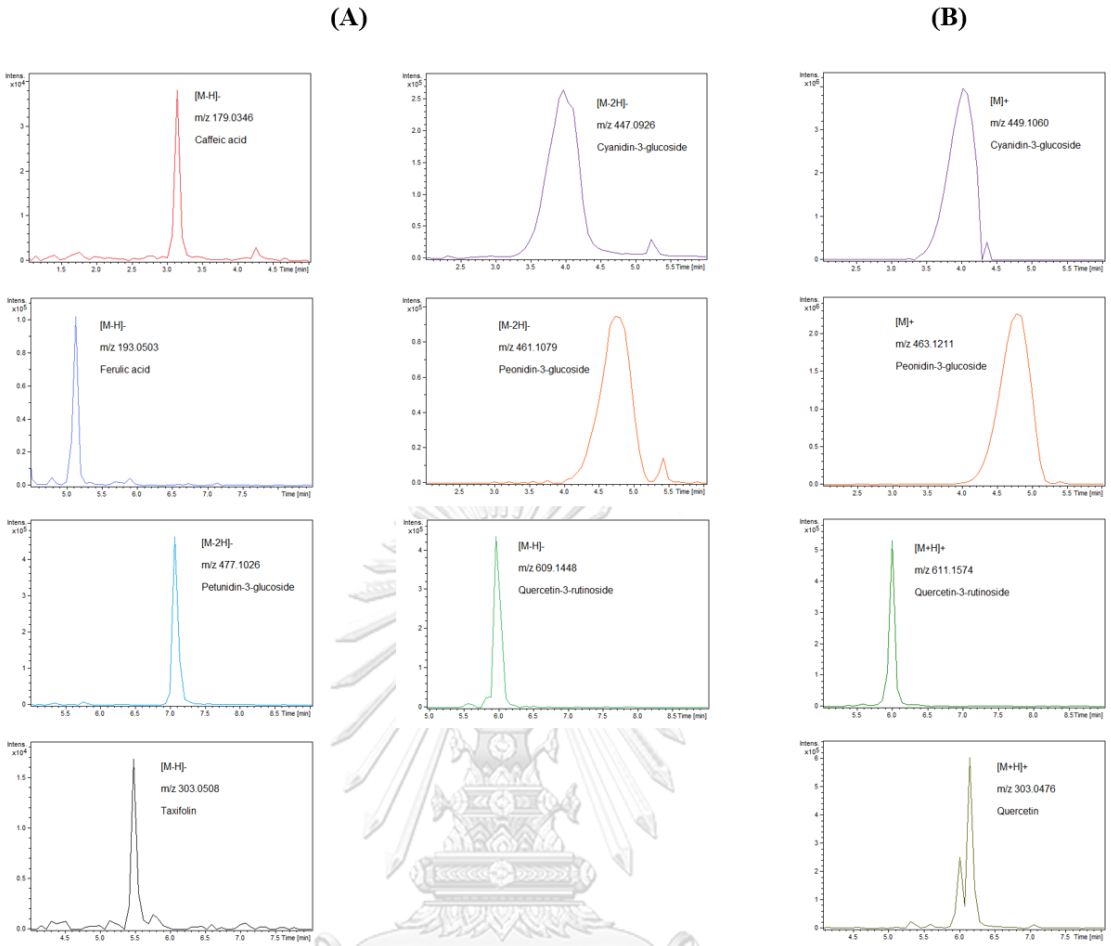


**Figure 18** Ion chromatogram of phytochemical compounds in Riceberry rice extract (RBE) using UHPLC-MS/MS in negative (A) and positive (B) ion mode.

**Table 18** MS and MS/MS data of phytochemical compounds in Riceberry rice extract (RBE) using UHPLC-MS/MS in negative mode.

| No | RT (min) | Compounds | Molecular Formula | Adduct type | Patent ion (m/z) | MS/MS fragments (m/z) |
|---|---|---|---|---|---|---|
| 1 | 3.14917 | Caffeic acid | $C_9H_8O_4$ | [M-H]- | 179.0346 | 135.0448, 134.0369, 136.0483, 179.0337, 107.0504, 117.0351, 137.0489, 151.0035, 133.0268, 107.0143 |
| 2 | 3.97533 | Cyanidin-3-glucoside | $C_{21}H_{21}O_{11}$ | [M-2H]- | 447.0926 | 284.032, 285.0389, 286.0423, 447.0923, 299.0554, 125.024, 448.0953, 287.0462, 283.0253, 147.0081 |
| 3 | 4.73268 | Peonidin-3-glucoside | $C_{22}H_{23}O_{11}$ | [M-2H]- | 461.1079 | 299.0551, 298.0477, 300.0587, 283.0241, 284.0319, 285.0382, 327.1456, 301.0648, 257.0455, 459.1878 |
| 4 | 5.14577 | Ferulic acid | $C_{10}H_{10}O_4$ | [M-H]- | 193.0503 | 134.0372, 178.0269, 133.0295, 135.0406, 179.0302, 149.0598, 193.0505, 137.0236, 106.0424, 136.0426 |
| 5 | 5.49005 | Taxifolin | $C_{15}H_{12}O_7$ | [M-H]- | 303.0508 | 125.0241, 217.0495, 175.0407, 285.0401, 178.9985, 151.0038, 153.0186, 151.0403, 177.0199, 181.0141 |
| 6 | 5.97192 | Quercetin-3-rutinoside | $C_{27}H_{30}O_{16}$ | [M-H]- | 609.1448 | 609.145, 300.0271, 301.0342, 610.1486, 611.1507, 302.0377, 178.9983, 343.045, 151.0031, 612.153 |
| 7 | 7.07342 | Petunidin-3-glucoside | $C_{22}H_{23}O_{12}$ | [M-2H]- | 477.1026 | 477.1026, 314.0424, 478.1059, 315.0475, 479.1081, 357.0608, 286.0472, 271.0239, 285.0405, 316.0499 |

**Table 19** MS and MS/MS data of phytochemical compounds in Riceberry rice extract (RBE) using UHPLC-MS/MS in positive mode.

| No | RT (min) | Compounds | Molecular Formula | Adduct type | Patent ion (m/z) | MS/MS fragments (m/z) |
|---|---|---|---|---|---|---|
| 1 | 4.02072 | Cyanidin-3-glucoside | $C_{21}H_{21}O_{11}$ | [M]+ | 449.1060 | 287.0533, 288.0568, 289.059, 290.0618 |
| 2 | 4.77668 | Peonidin-3-glucoside | $C_{22}H_{23}O_{11}$ | [M]+ | 463.1211 | 301.0687, 302.0722, 286.0453, 303.0744, 287.0491, 258.0507, 304.0767, 259.0563 |
| 3 | 6.01357 | Quercetin-3-rutinoside | $C_{27}H_{30}O_{16}$ | [M+H]+ | 611.1574 | 303.0473, 304.0509, 85.0275, 129.053, 305.0525, 145.048, 127.0374, 97.027, 147.0636, 151.0375 |
| 4 | 6.15097 | Quercetin | C15H10O7 | [M+H]+ | 303.0476 | 303.0475, 229.0477, 304.051, 153.0166, 257.0422, 137.0218, 165.0166, 285.0374, 201.053, 247.0578 |

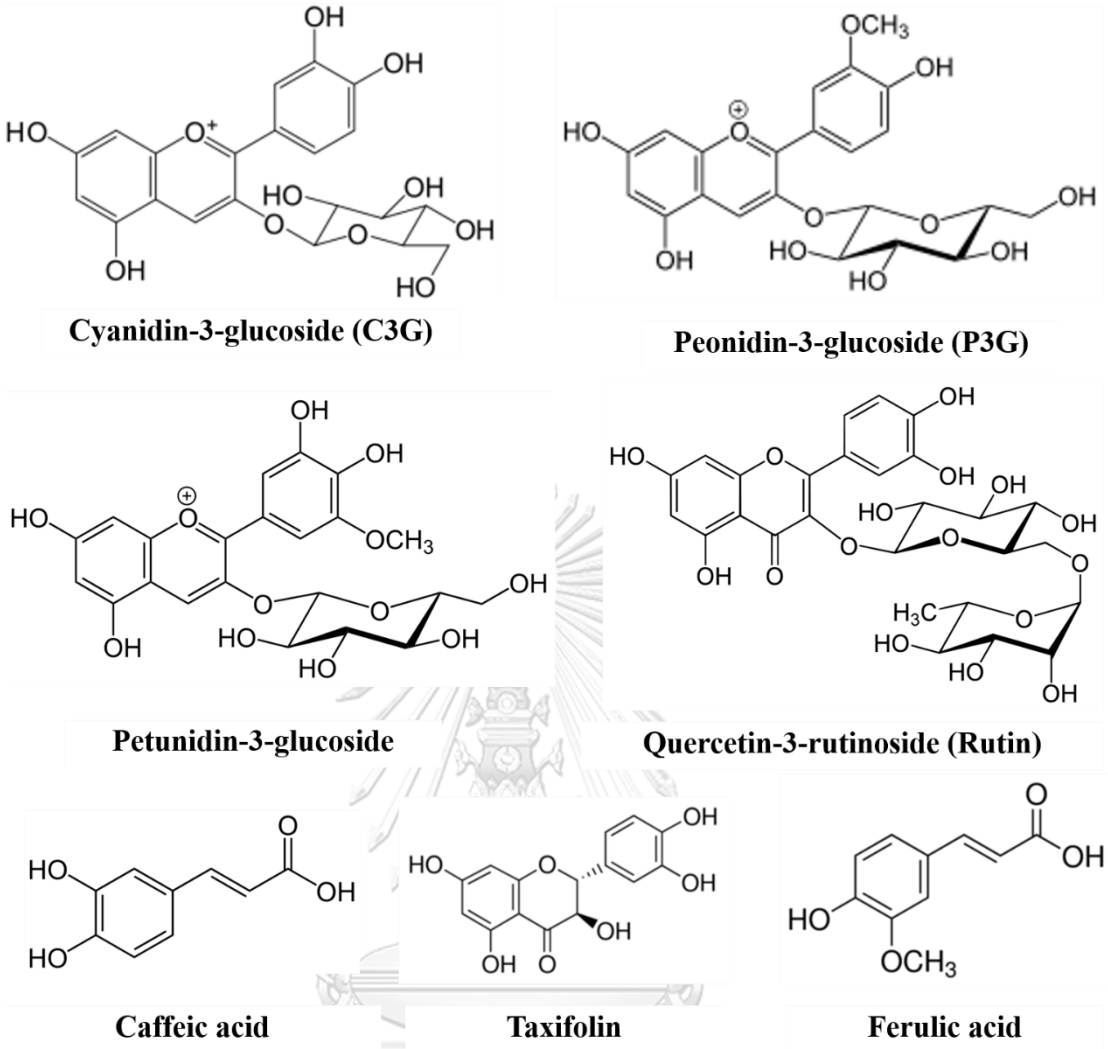




Figure 19 Chemical structures of phytochemical compounds in Riceberry rice extract.

**4.2 Riceberry rice extract inhibited adipogenesis in 3T3-L1 cells**

4.2.1 RBE inhibited preadipocytes proliferation.

After 4 days of treatment, there was no effect of RBE on cell viability as shown in Figure 20. RBE at 1, 10, and 20 μg/mL reduced the total cell number of preadipocytes by 13%, 24%, and 49%, respectively. A significant reduction was observed 20 μg/mL (Figure 21). Moreover, RBE at 10, and 20 μg/mL induced cell cycle arrest at the G0/G1 phase (Figure 22).

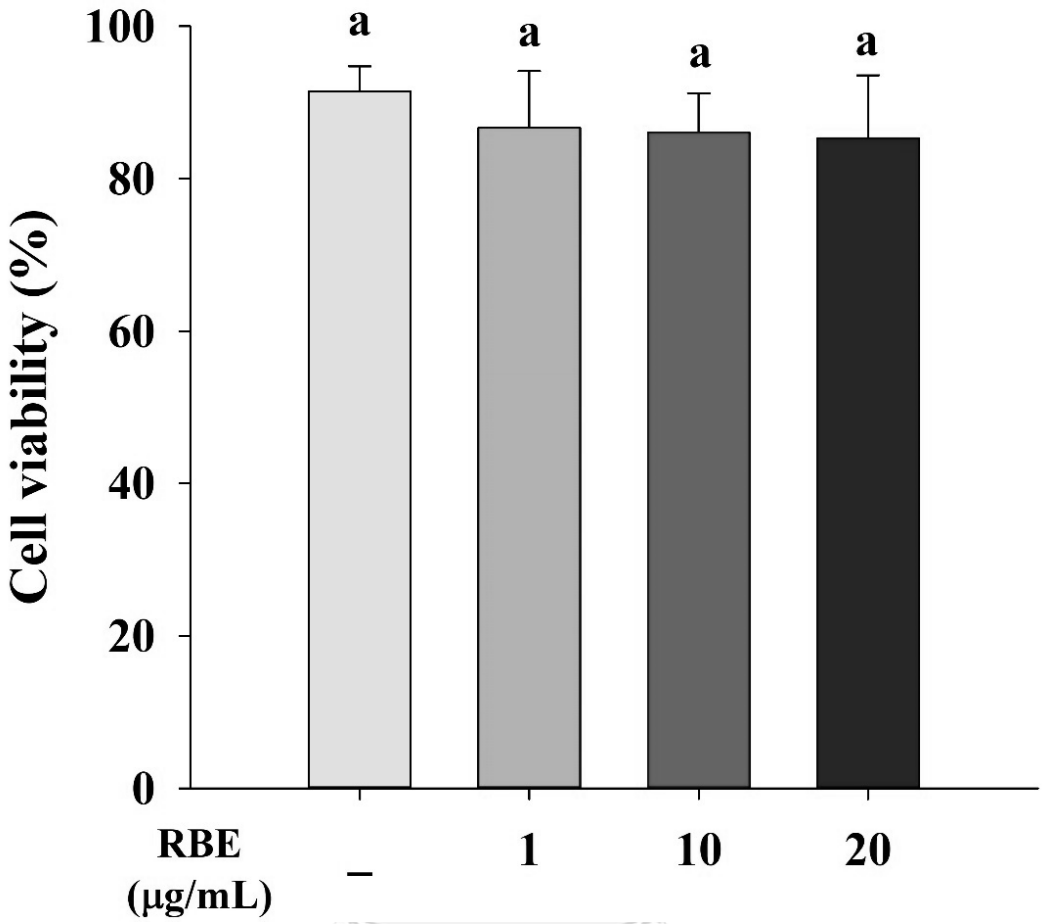




**Figure 20** The effects of Riceberry rice extract (RBE) on cell viability after 4 days of treatment.

Data obtained from the MUSE™ Cell Analyzer using MUSE™ Cell Count and Viability kit. Results are presented as mean ± SEM from the three independent experiments. Groups with different letters are significantly different ($P < 0.05$).

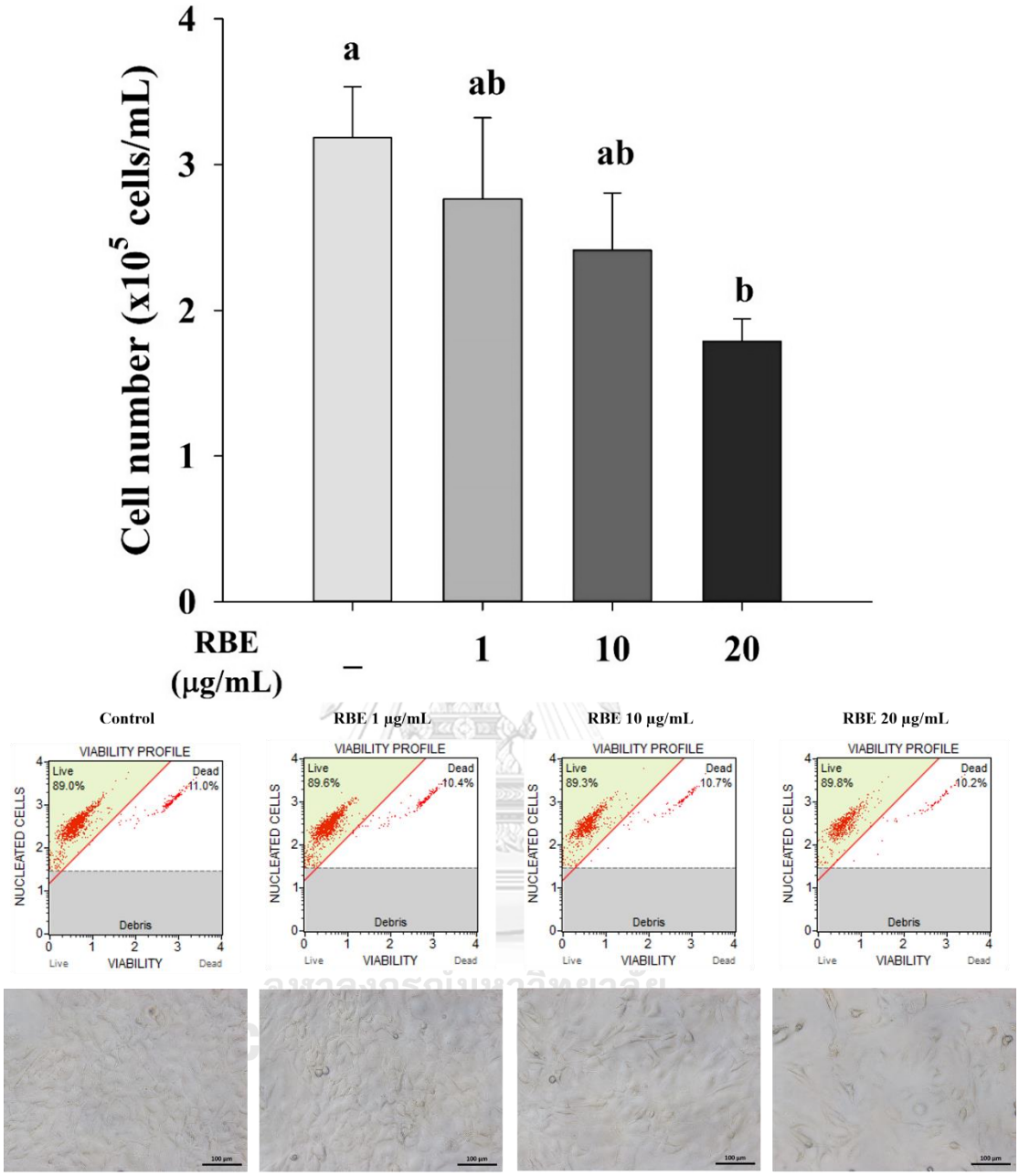


**Figure 21** The effects of Riceberry rice extract (RBE) on cell proliferation after 4 days of treatment.

Data obtained from the MUSE™ Cell Analyzer using MUSE™ Cell Count and Viability kit. Results are presented as mean ± SEM from the three independent experiments. Groups with different letters are significantly different ($P < 0.05$). Bright-field images (20X magnification). Scale bars are 100 µm.

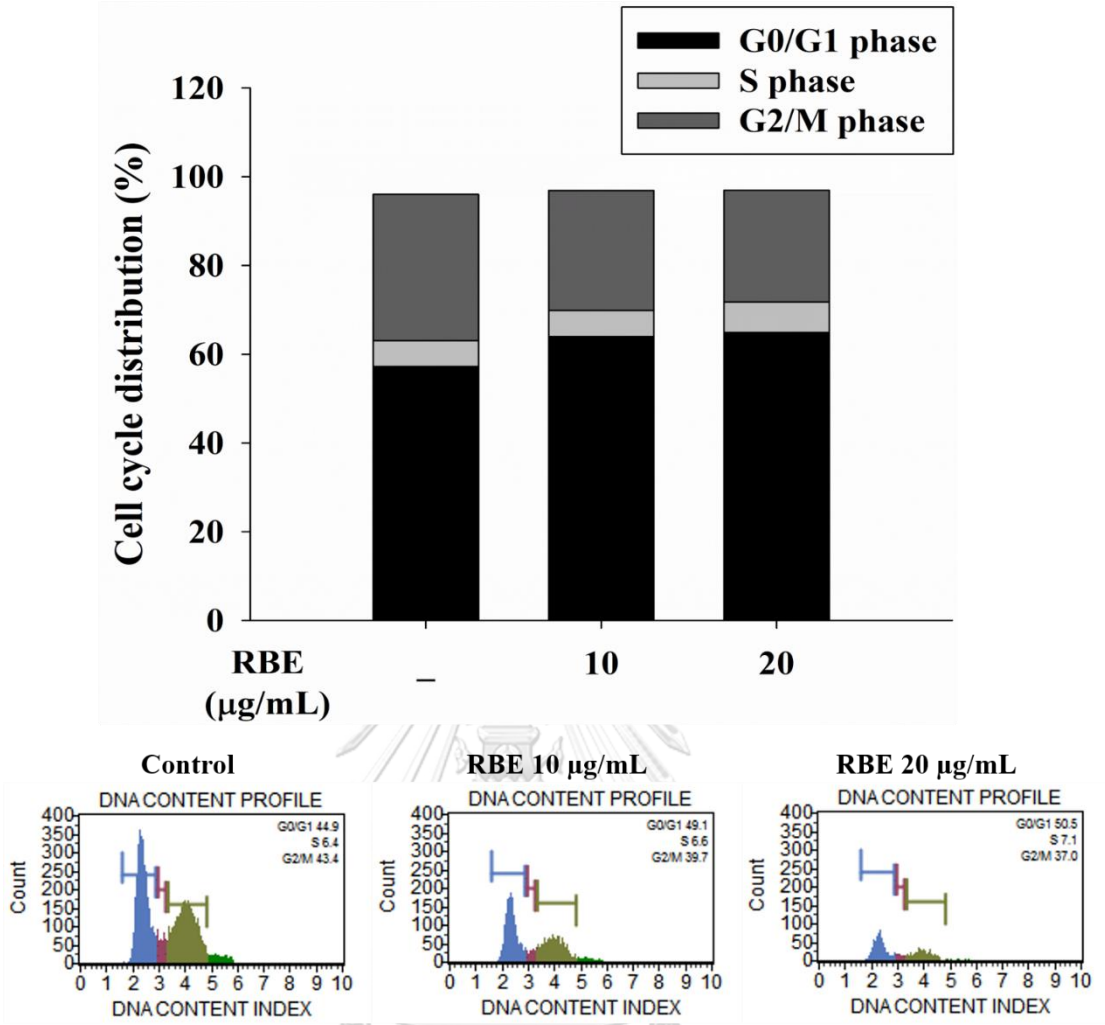


**Figure 22** The effects of Riceberry rice extract (RBE) on cell cycle after 4 days of treatment.

Data obtained from the MUSE™ Cell Analyzer using MUSE™ Cell Cycle kit and represented the G0/G1, S, and G2/M phase by blue, red, and green color, respectively. Results are presented as mean from the three independent experiments.

4.2.2 RBE inhibited adipogenesis.

After 8 days of continuous stimulation, RBE did not affect cell viability (Figure 23). However, RBE at 20 μg/mL significantly reduced the total cell number by 23% (Figure 24). After adipogenic induction, 3T3-L1 cells expressed the morphologicaly changes typical for adipocytes (round-shape and lipid droplets) compared to undifferentiated cells (Figure 25). ImageJ analysis showed a significantly decrease in the number of adipocytes by RBE in a concentration-dependent manner (Figure 25). In addition, triglyceride accumulation was significantly lowered by RBE at 1, 10, and 20 μg/mL (39%, 46%, and 50%) compared to control (Figure 26).

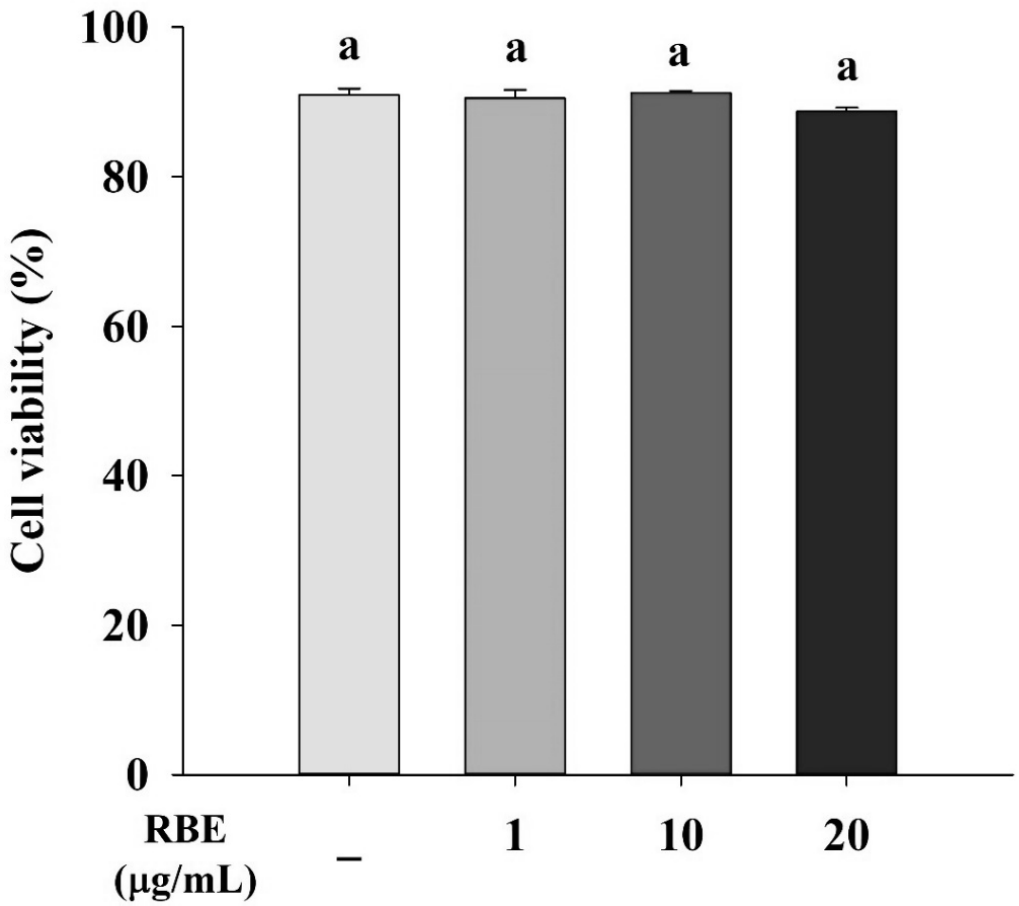


**Figure 23** The effects of Riceberry rice extract (RBE) on cell viability after 8 days of treatment.

Results are presented as mean ± SEM from the three independent experiments. Groups with different letters are significantly different ($P < 0.05$).

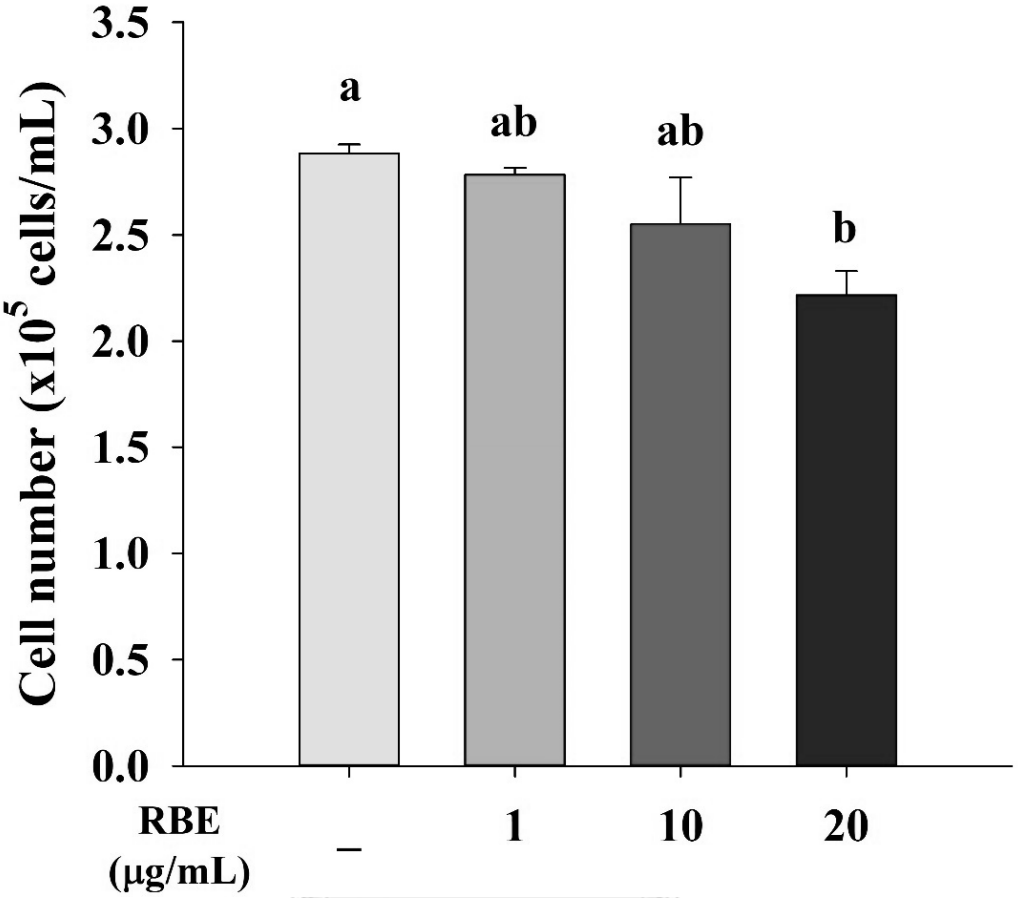


**Figure 24** The effects of Riceberry rice extract (RBE) on total cell number after 8 days of treatment.

Results are presented as mean ± SEM from the three independent experiments. Groups with different letters are significantly different ($P < 0.05$).

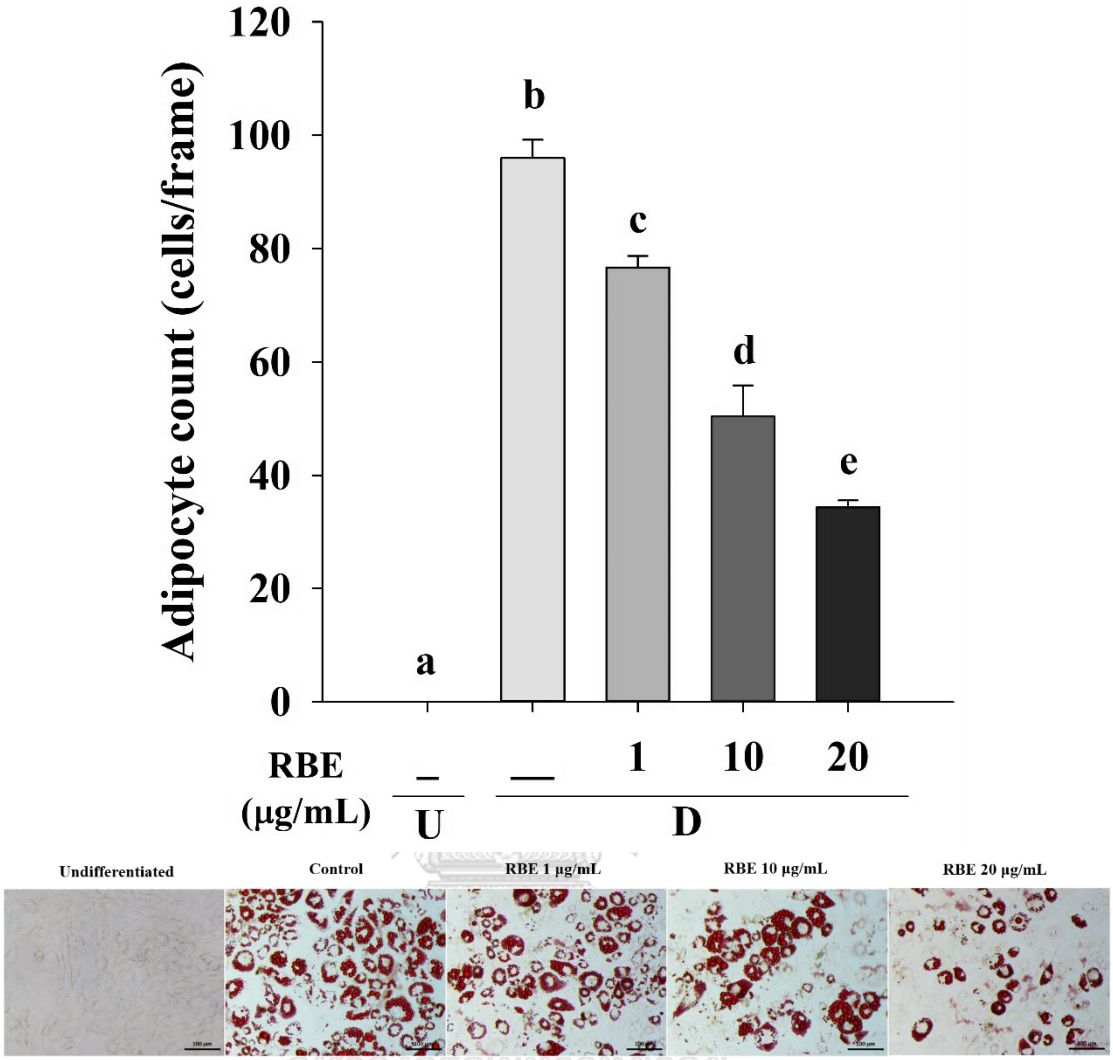




**Figure 25** The effects of Riceberry rice extract (RBE) on adipogenesis.

Images obtained from Oil Red O staining (20X magnification). Data were quantified using ImageJ software. Results are presented as mean ± SEM from the three independent experiments. Groups with different letters are significantly different ($P < 0.05$). U = undifferentiated cells. D = differentiated cells.

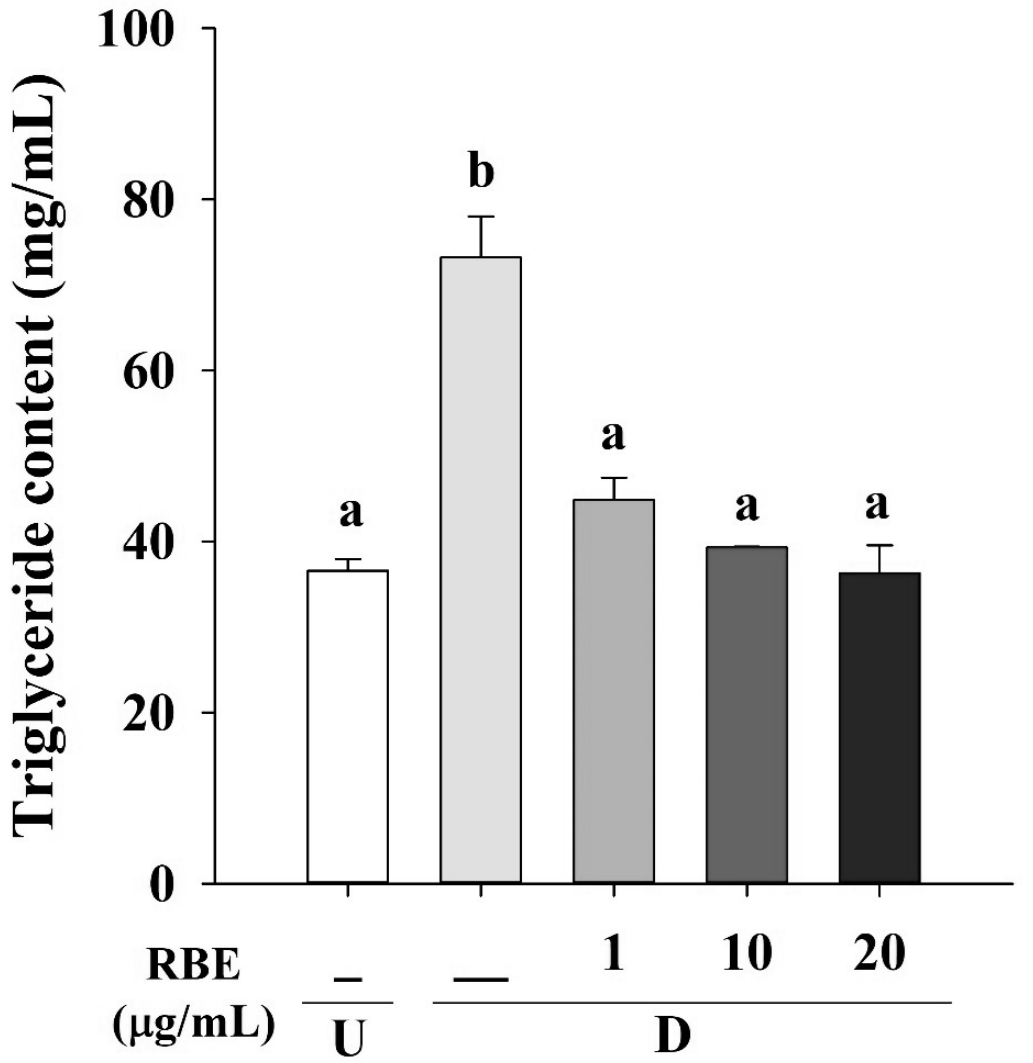




**Figure 26** The effects of Riceberry rice extract (RBE) on triglyceride accumulation in adipocytes.

Results are presented as mean ± SEM from the three independent experiments. Groups with different letters are significantly different ($P < 0.05$). U = undifferentiated cells. D = differentiated cells.

4.2.3 RBE downregulated adipogenic transcription factors

After adipogenic differentiation, the mRNA expression levels of PPARγ, C/EBPα, and C/EBPβ increased, while C/EBPγ levels decreased in differentiated cells compared to undifferentiated cells (Figure 27 and 28). In the early phase of adipogenesis, treatment of cells with RBE (20 μg/mL) for 3 days downregulated PPARγ and C/EBPα mRNA expression by 0.2-fold (Figure 27). In late phase of adipogenesis, RBE (20 μg/mL) downregulated PPARγ, C/EBPα, and C/EBPβ mRNA expression by 0.4-fold, 0.3-fold, and 0.1-fold, respectively (Figure 28). RBE (20 μg/mL) also upregulated C/EBPγ mRNA expression compared to differentiated control cells in both early phase and late phase of adipogenesis (Figure 27 and 28).

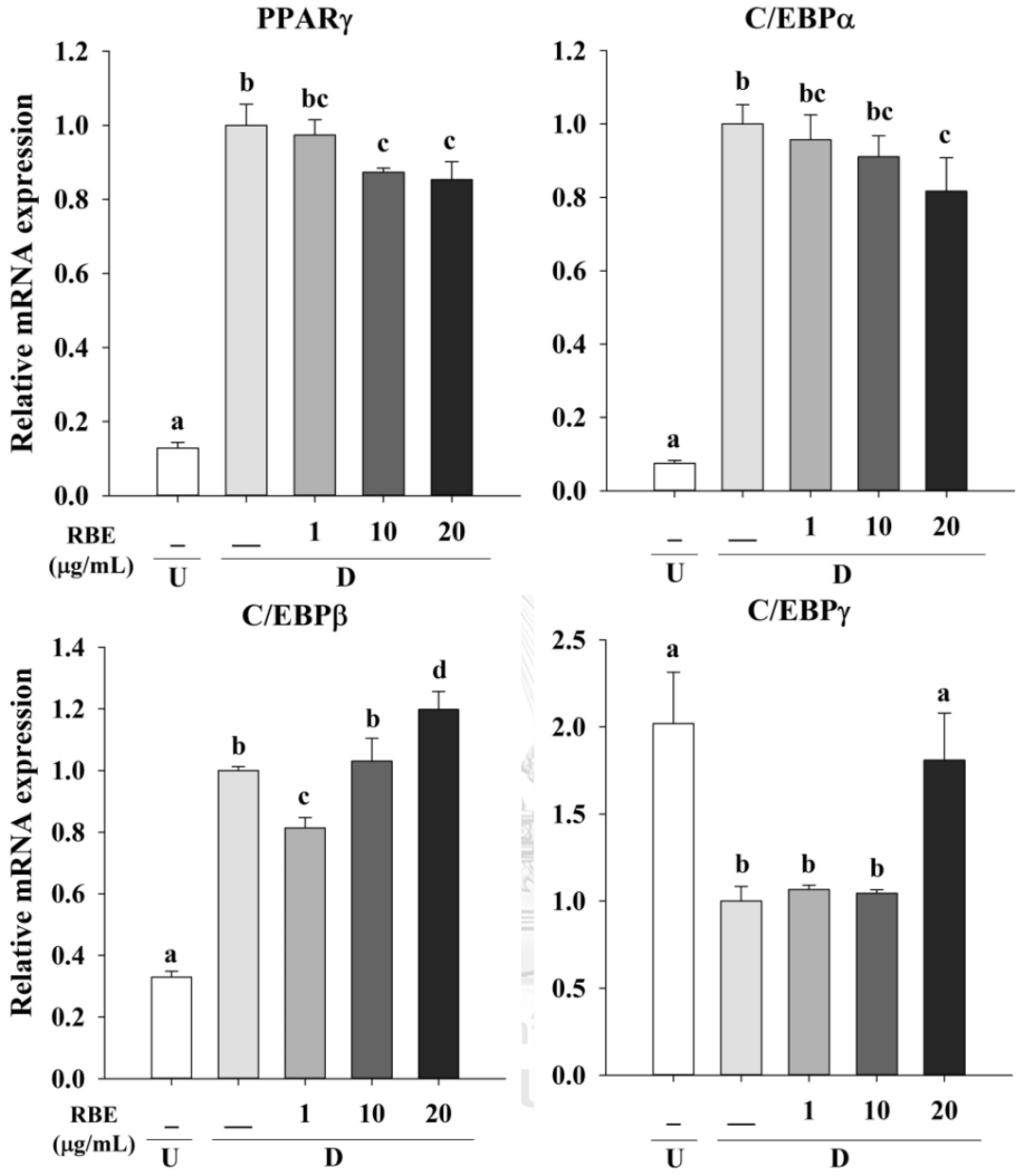


**Figure 27** The effect of Riceberry rice extract (RBE) on adipogenic transcription factor expression in early phase of adipogenesis (Day 3).

Results are presented as mean ± SEM from the three independent experiments. Groups with different letters are significantly different ($P < 0.05$). Data was normalized with β-actin. U = undifferentiated cells. D = differentiated cells.

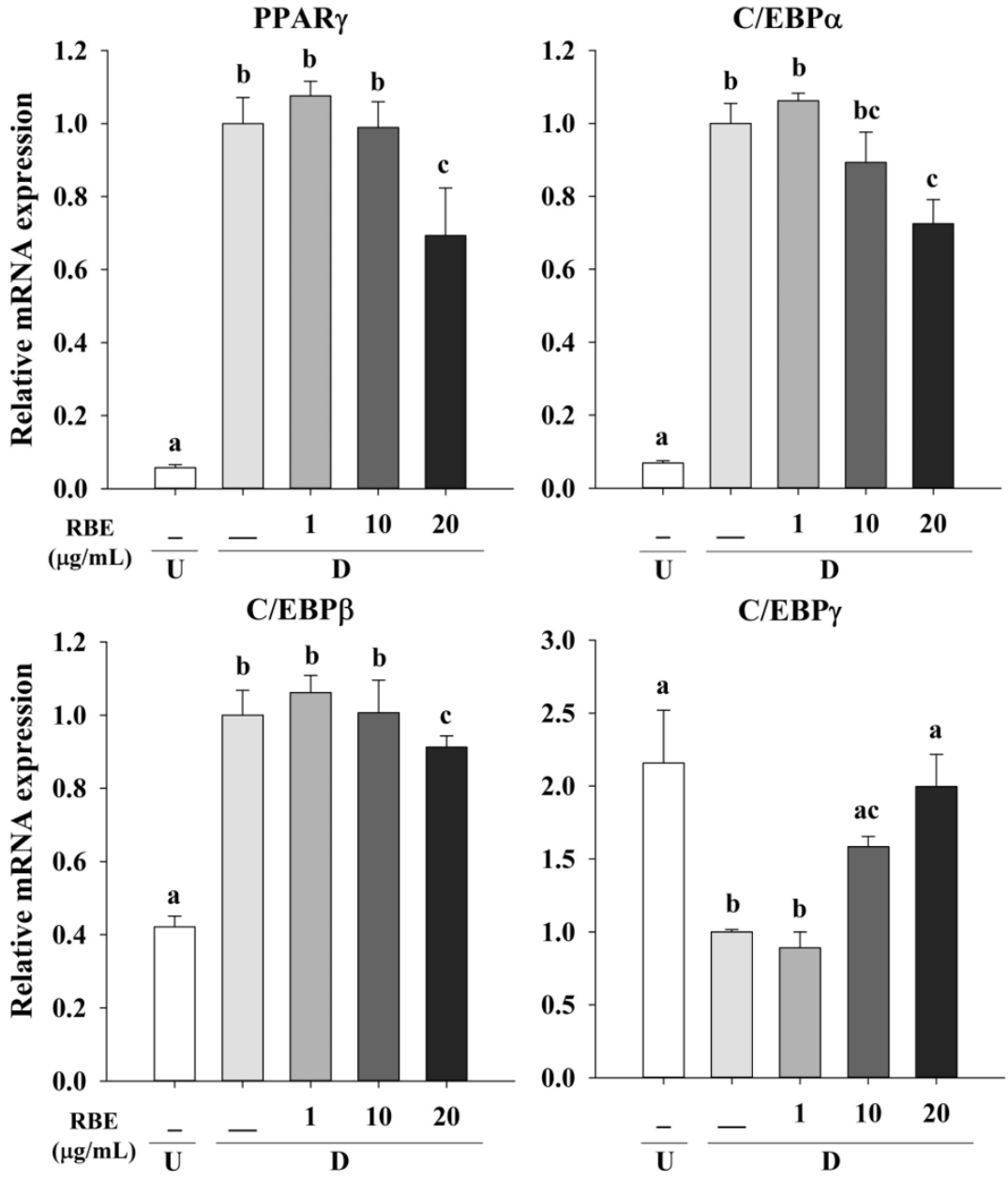


**Figure 28** The effects of Riceberry rice extract (RBE) on adipogenic transcription factors mRNA expression in late phase of adipogenesis (Day 8).

Results are presented as mean ± SEM from the three independent experiments. Groups with different letters are significantly different ($P < 0.05$). Data was normalized with β-actin. U = undifferentiated cells. D = differentiated cells.

4.2.4 RBE inhibited Akt1 signaling.

Akt1 signaling mediates adipogenic differentiation. Hence, we investigated whether RBE utilized this mechanism in 3T3-L1 cells. The p-Akt1 (Ser473)/total-Akt1 ratio increased in differentiated cells compared to undifferentiated cells. RBE treatment decreased this ratio (Figure 29).

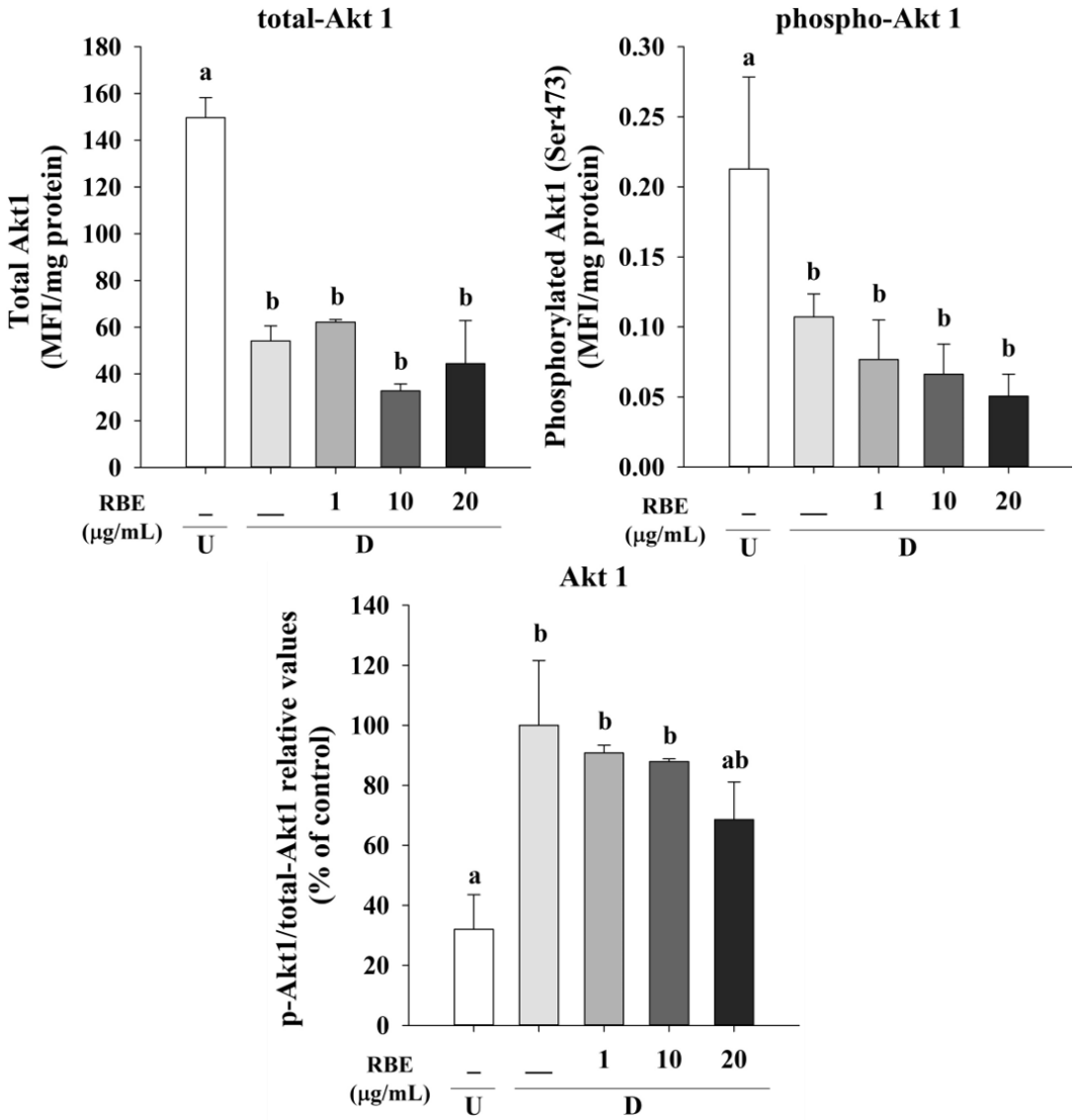




**Figure 29** The effects of Riceberry rice extract (RBE) on Akt1 signaling.

Results are presented as mean ± SEM from the three independent experiments. Groups with different letters are significantly different ($P < 0.05$). U = undifferentiated cells. D = differentiated cells.

4.2.5 RBE downregulated adipogenic gene expression.

Based on the effects of RBE on transcription factors, the mRNA expression of adipogenic genes were examined. After 8 days of adipogenic induction, all adipogenic genes were upregulated in differentiated compared to undifferentiated cells (Figure 30). RBE (20 μg/mL) downregulated the expression of ACC, aP2, AdipoQ, leptin, resistin, perilipin, HSL, LPL, ATGL, and adiponectin receptors R1 and R2 compared to differentiated control cells (Figure 30).

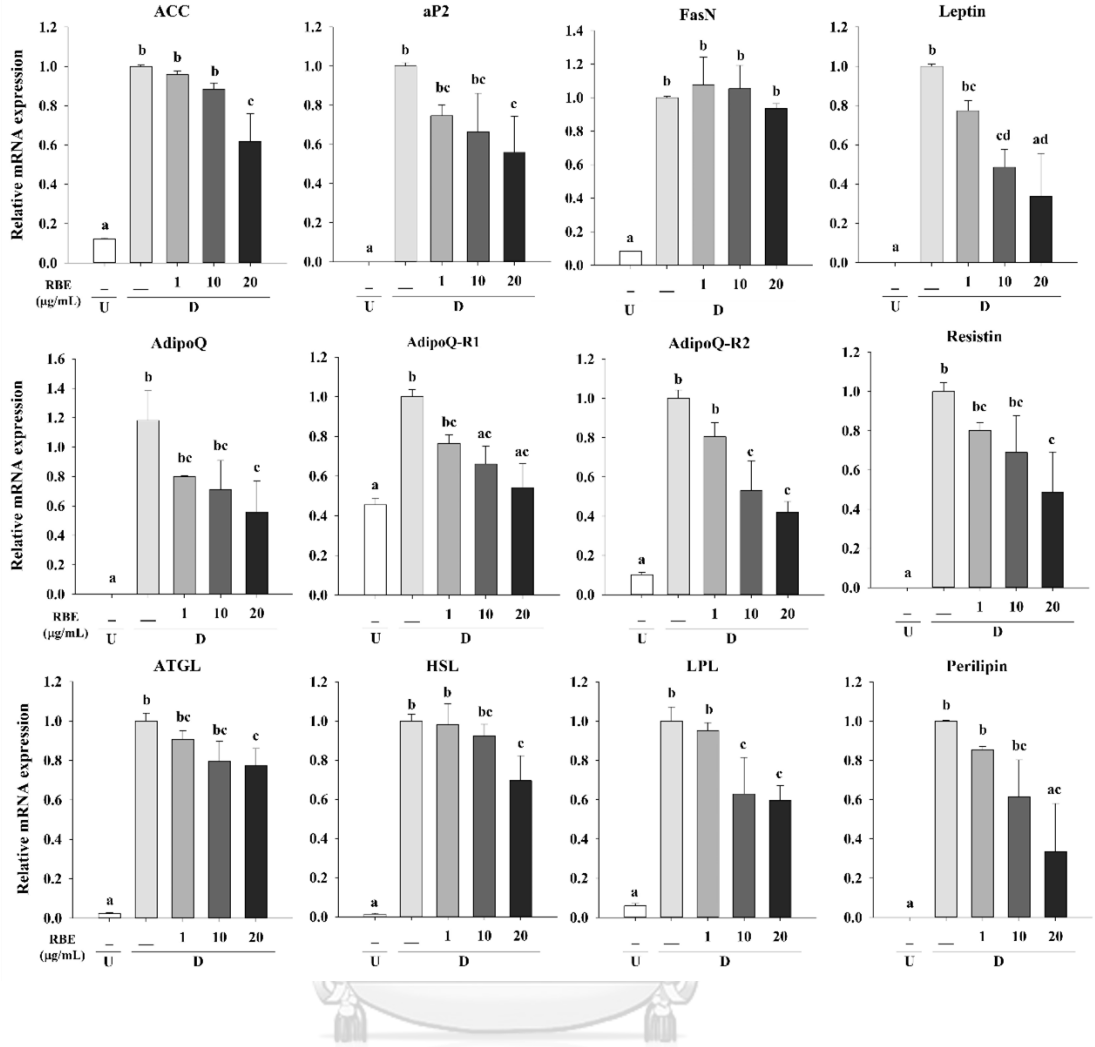


**Figure 30** The effects of Riceberry rice extract (RBE) on adipogenic gene expression. Results are presented as mean ± SEM from the three independent experiments. Groups with different letters are significantly different ($P < 0.05$). Data was normalized with β-actin. U = undifferentiated cells. D = differentiated cells.

4.2.6 RBE decreased glucose uptake by downregulating Glut4 expression.

To investigate the effects of RBE on adipocyte function, glucose uptake was examined. After 8 days of treatment, RBE at 10 and 20 μg/mL reduced glucose uptake by 16% compared to differentiated control cells (Figure 31). In addition, RBE (20 μg/mL) downregulated glucose transporter 4 (Glut4) mRNA expression compared to differentiated control cells but had no effect on insulin receptor (InsR) mRNA expression (Figure 32).

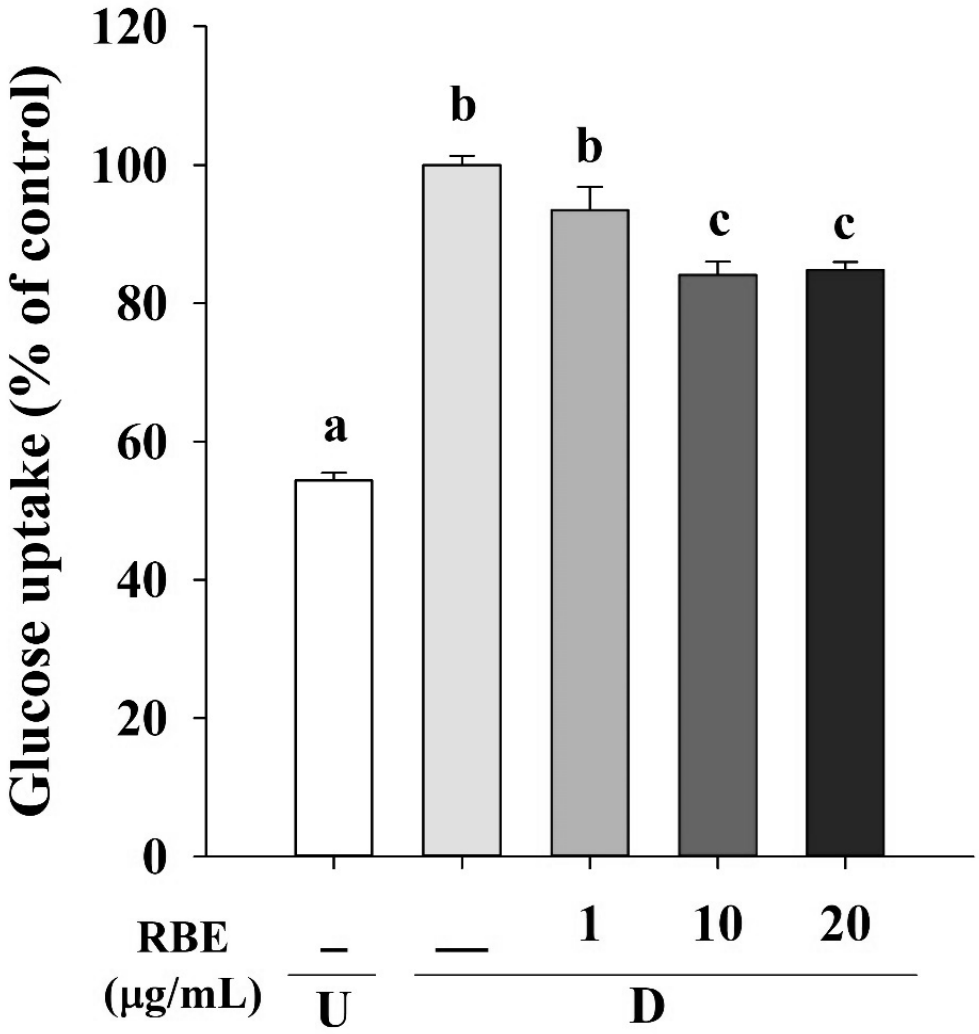




**Figure 31** The effects of Riceberry rice extract (RBE) on glucose uptake in adipocytes. Results are presented as mean ± SEM from the three independent experiments. Groups with different letters are significantly different ($P < 0.05$). U = undifferentiated cells. D = differentiated cells.

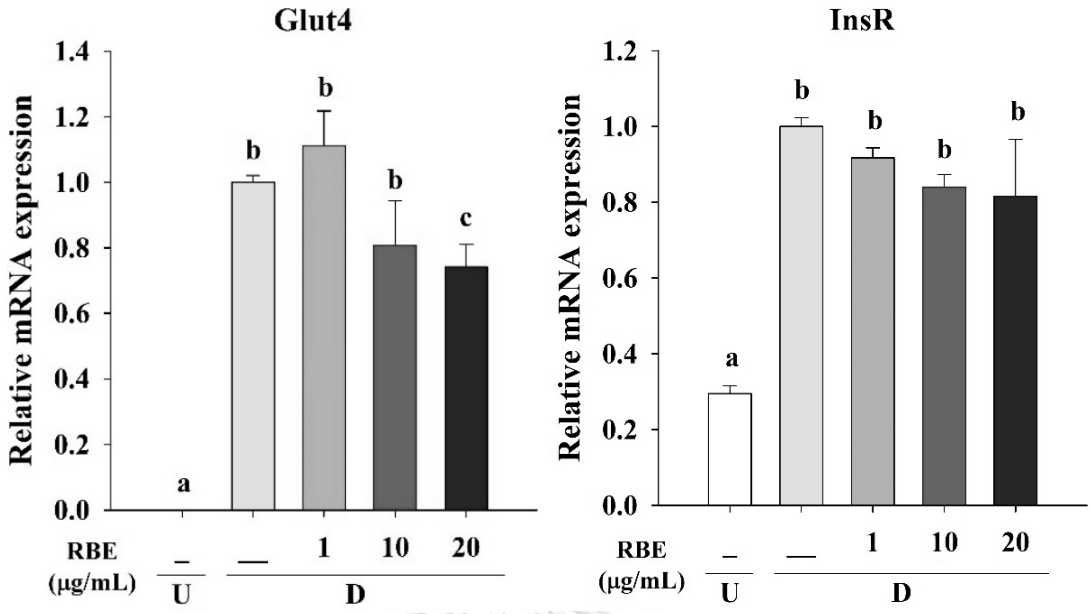


**Figure 32** The effects of Riceberry rice extract (RBE) on Glut4 and InsR expression. Results are presented as mean ± SEM from the three independent experiments. Groups with different letters are significantly different ($P < 0.05$). Data was normalized with β-actin. U = undifferentiated cells. D = differentiated cells.

4.2.7 RBE stimulated lipolysis in adipocytes.

The effect of RBE on lipolysis were examined in differentiated cells. The results showed that RBE increased basal lipolysis after treatment for 3 h. RBE at 20 μg/mL stimulated isoproterenol-induced lipolysis by 35% compared to the untreated cells (Figure 33).

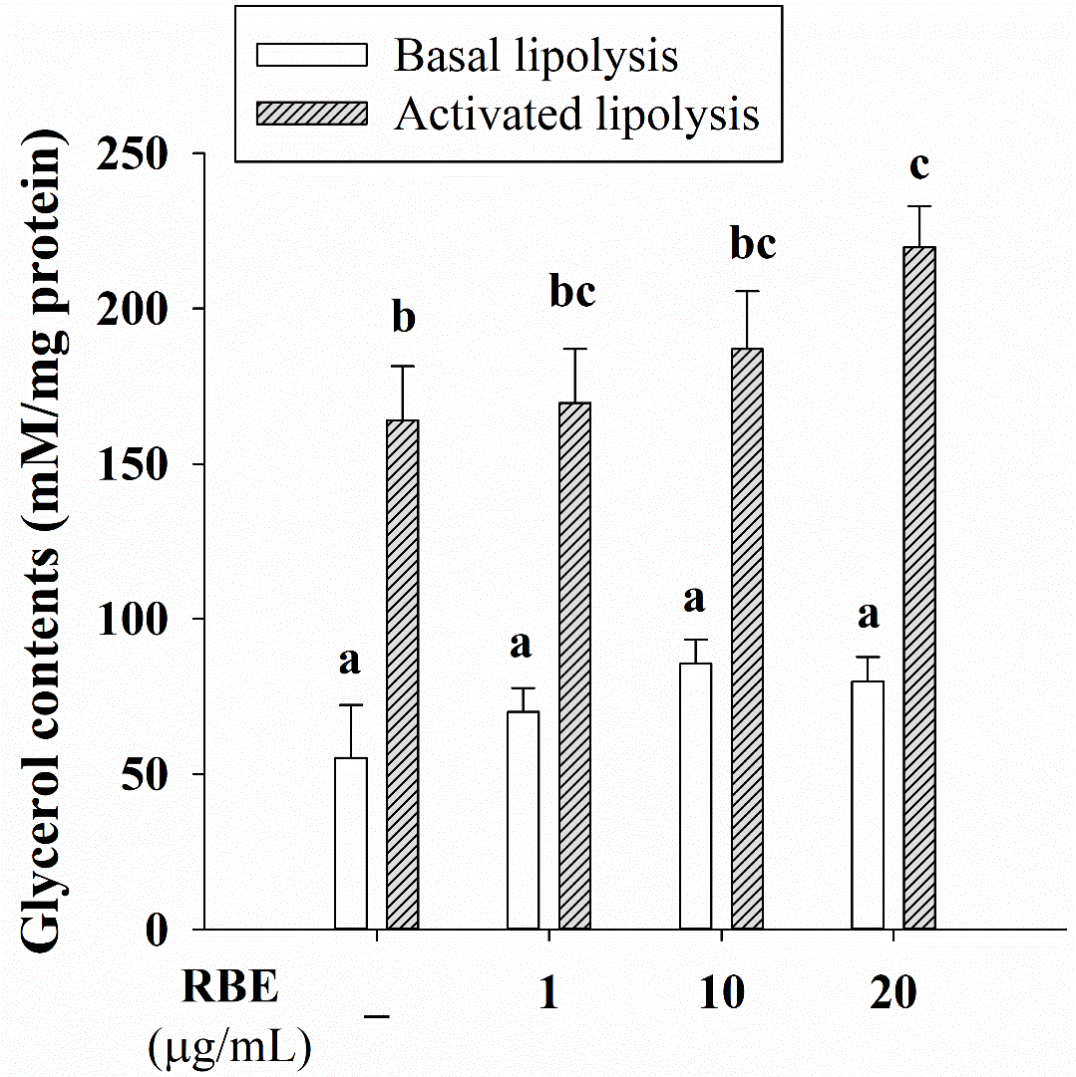




**Figure 33** The effects of Riceberry rice extract (RBE) on lipolysis in adipocytes. Results are presented as mean ± SEM from the three independent experiments. Groups with different letters are significantly different ($P < 0.05$).

4.2.8 RBE does not increase intracellular calcium signals in preadipocytes.

Intracellular calcium signaling is necessary for adipogenic differentiation. Therefore, we tested whether this signaling mechanism was involved in the RBE effects in preadipocytes. Stimulation of cells with RBE (1-20 μg/mL) failed to increase intracellular calcium signals (Figure 34).

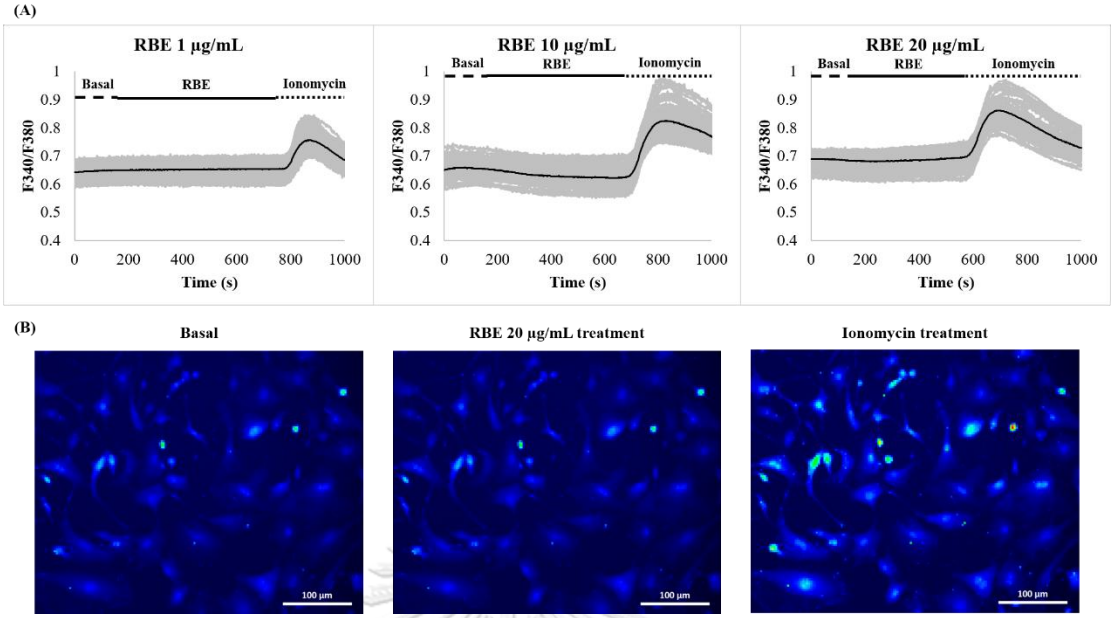


**Figure 34** Average calcium signals in response to Riceberry rice extract (RBE) in preadipocytes.

(A) Calcium signals of preadipocytes during the stimulation with RBE at 1, 10, and 20 µg/mL and ionomycin as a positive control. Results are presented as average traces from individual cells. Black lines = average. Grey lines = individual cells. (B) Images of fluorescence emission from cells at basal, during RBE treatment and ionomycin treatment. Data represent 81-140 cells/experiment from three replicates.

4.2.9 Cyanidin (Cy) and cyanidin-3-rutinoside (C3R) increased intracellular calcium signals in 3T3-L1 preadipocytes.

Based on the previous results, RBE failed to increase intracellular calcium signals in preadipocytes. Hence, we tested whether purified phytochemical compounds in RBE based on the UHPLC-MS/MS data could increase calcium signals. Figure 35 shows that coumaric acid (CA), protocatechuic acid (PCA), and C3G at 100 μM failed to increase intracellular calcium signals. However, stimulation of cells with 100 μM Cy and C3R increased intracellular calcium signals in preadipocytes (Figure 35). Ferulic acid (FA, 100 μM) did not increase intracellular calcium but showed autofluorescence (Figure 35).

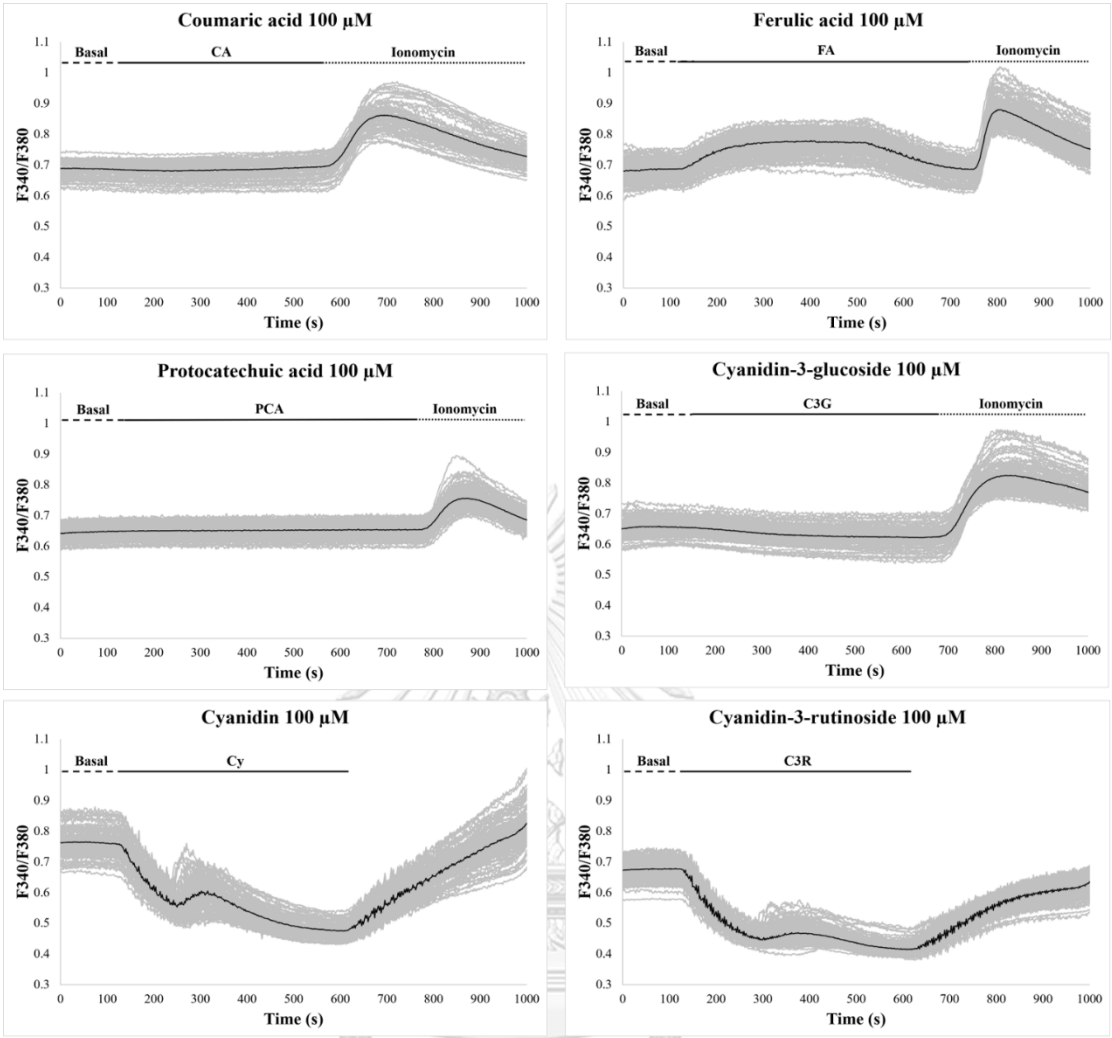




**Figure 35** Average calcium signals in response to coumaric acid (CA), ferulic acid (FA), protocatechuic acid (PCA), cyanidin-3-glucoside (C3G), cyanidin (Cy), and cyanidin-3-rutinoside (C3R).

Results are presented as average traces from individual cells. Black lines = average. Grey lines = individual cells (n = 49-90 cells/experiment).

4.2.10 Cyanidin (Cy) and cyanidin-3-rutinoside (C3R) induced calcium release from the endoplasmic reticulum.

To investigate the calcium sources for the Cy and C3R responses, experiments were performed under different calcium conditions. As shown in Figure 36 and 37, 100 μM Cy and C3R still increased calcium signals under extracellular calcium free buffer. Depletion of intracellular calcium stores in the ER with thapsigargin (TG), abolished the Cy and C3R responses in preadipocytes (Figure 36 and 37). Under extracellular calcium free with TG condition, Cy and C3R responses is completely abolished (Figure 36 and 37). These results suggested that Cy and C3R induced calcium release from the endoplasmic reticulum.

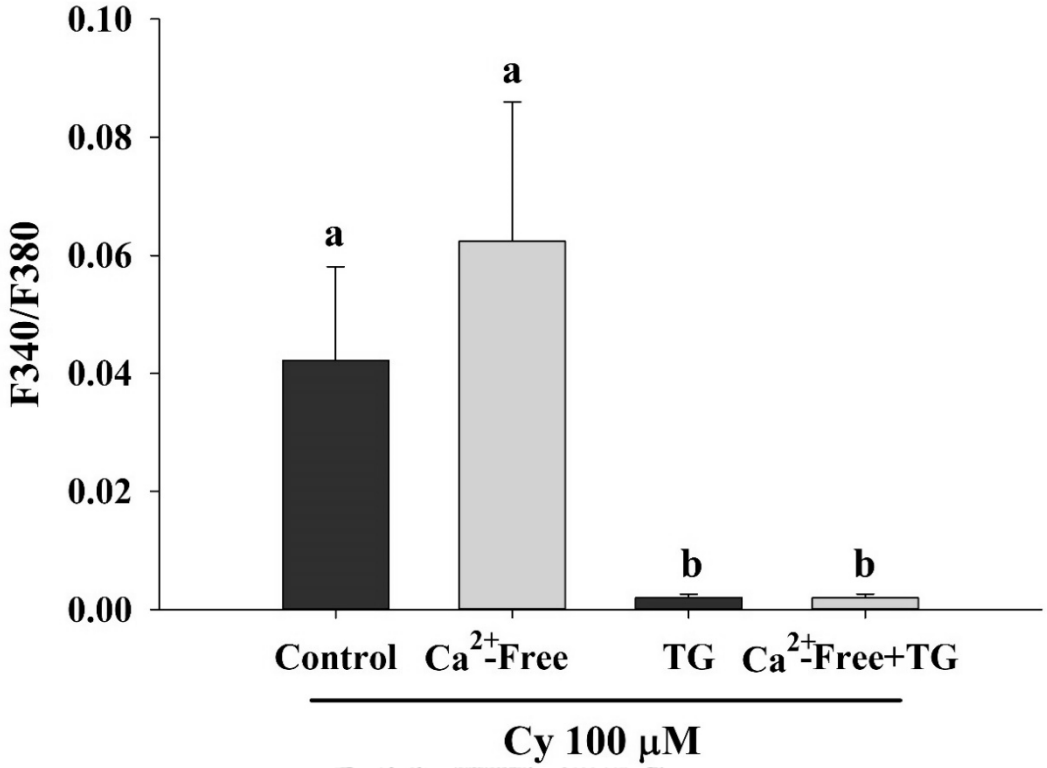


**Figure 36** The effects of cyanidin (Cy) on intracellular calcium signals under different calcium conditions.

Results are presented as mean ± SEM from the three independent experiments (n = 77-175 cells/group). Groups with different letters are significantly different ($P < 0.05$).

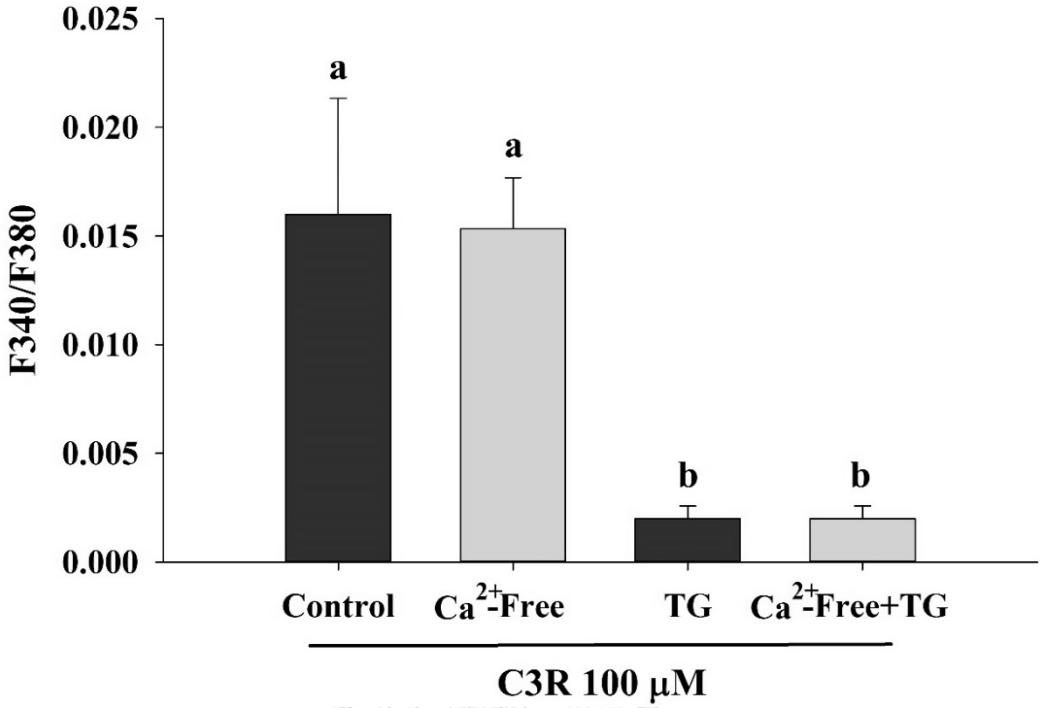


**Figure 37** The effects of cyanidin-3-rutinoside (C3R) on intracellular calcium signals under different calcium conditions.

Results are presented as mean ± SEM from the three independent experiments (n = 120-205 cells/group). Groups with different letters are significantly different ($P < 0.05$).

### 4.3 Cyanidin-3-rutinoside (C3R) stimulated insulin secretion from pancreatic β-cells

4.3.1 RBE does not increase intracellular calcium signals in INS-1 cells.

Calcium signals are required for insulin secretion from pancreatic β-cells. We investigated whether RBE and other phytochemical compounds utilized intracellular calcium signaling in pancreatic INS-1 cells. The results showed that RBE 100 μg/mL, C3G, protocatechuic acid (PCA), and coumaric acid (CA) at 100 μM failed to increase intracellular calcium signals (Figure 38). Ferulic acid (FA) did not induce intracellular calcium signals but emitted autofluorescence (Figure 38). However, stimulation of cells with 100 μM C3R increased intracellular calcium signals (Figure 38).

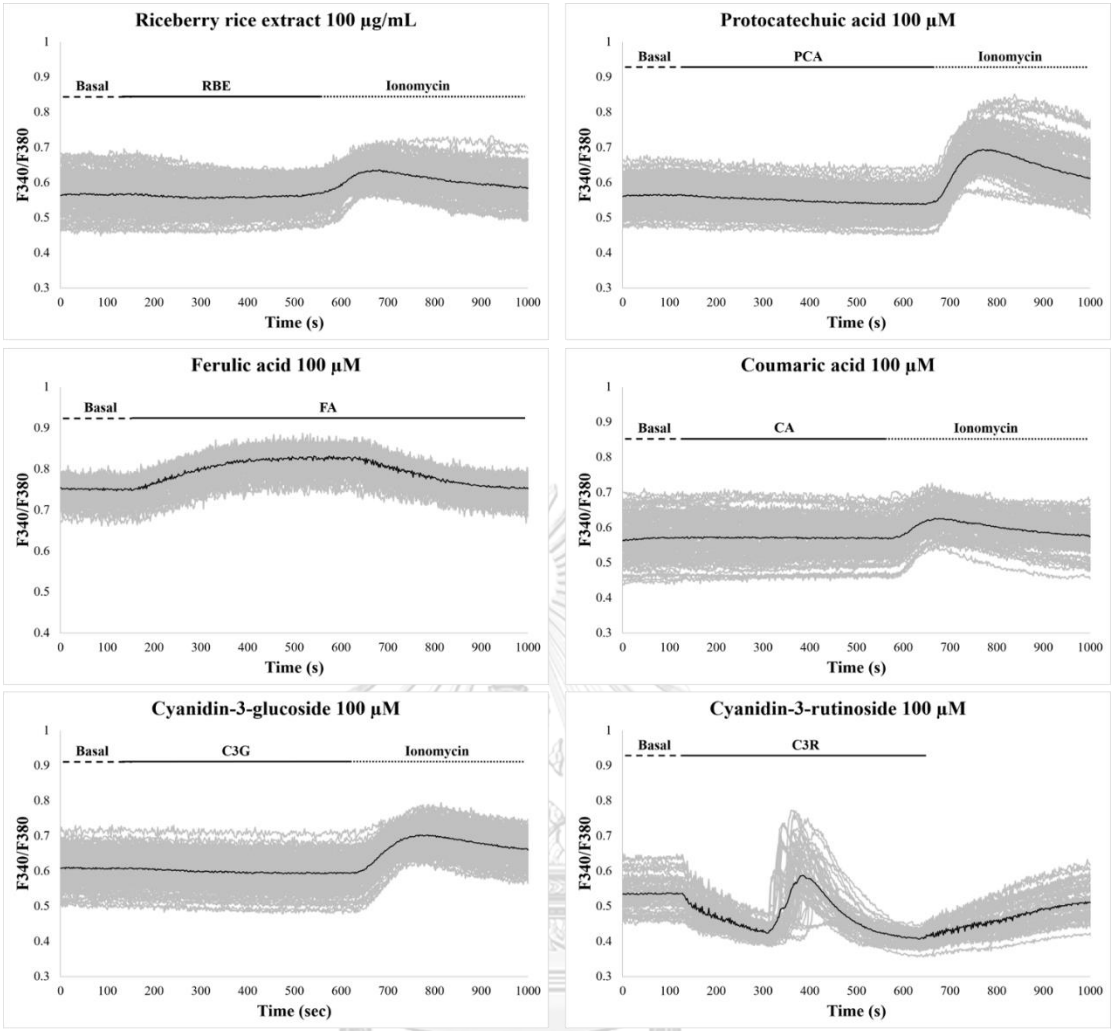




**Figure 38** Average calcium signals in response to Riceberry rice extract (RBE), protocatechuic acid (PCA), ferulic acid (FA), coumaric acid (CA), cyanidin-3-glucoside (C3G) and cyanidin-3-rutinoside (C3R).

Results are presented as average traces from individual cells. Black lines = average. Grey lines = individual cells (n = 88-140 cells/experiments).

4.3.2 C3R increased intracellular calcium signals in INS-1 cells.

Based on the UHPLC-MS/MS data, quercetin-3-rutinoside or rutin was one of the phytochemical compounds in Riceberry rice extract (RBE). We investigated whether C3R, glycoside form of rutin utilized intracellular calcium signaling in INS-1 cells. The results showed that stimulation of cells with C3R (30-300 μM) increased intracellular calcium in a concentration-dependent manner (Figure 39). The peak response for each concentration is shown in Figure 40.

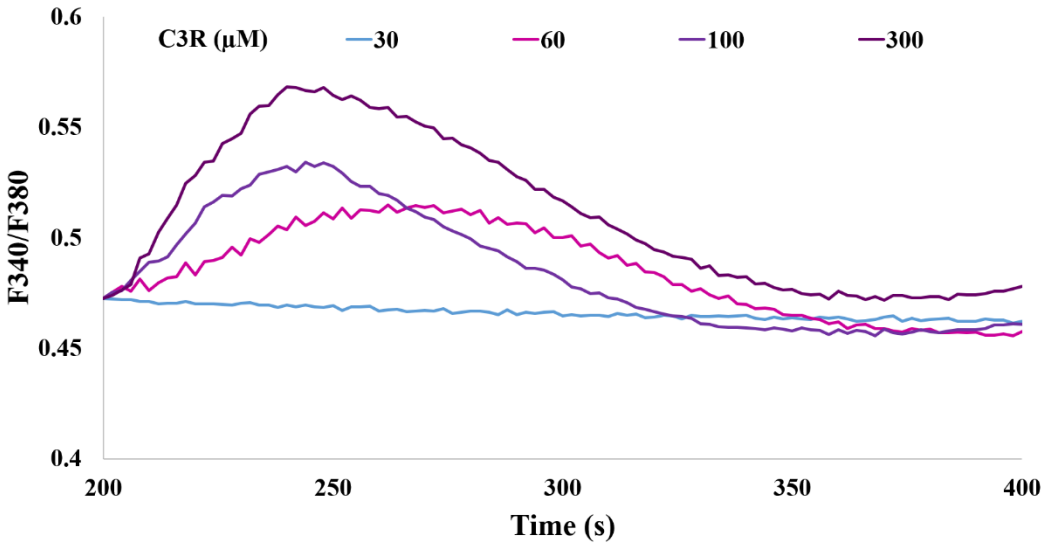


**Figure 39** Average calcium signals in response to cyanidin-3-rutinoside (C3R). Results are presented as average traces from the three independent experiments (n = 127-210 cells/group).

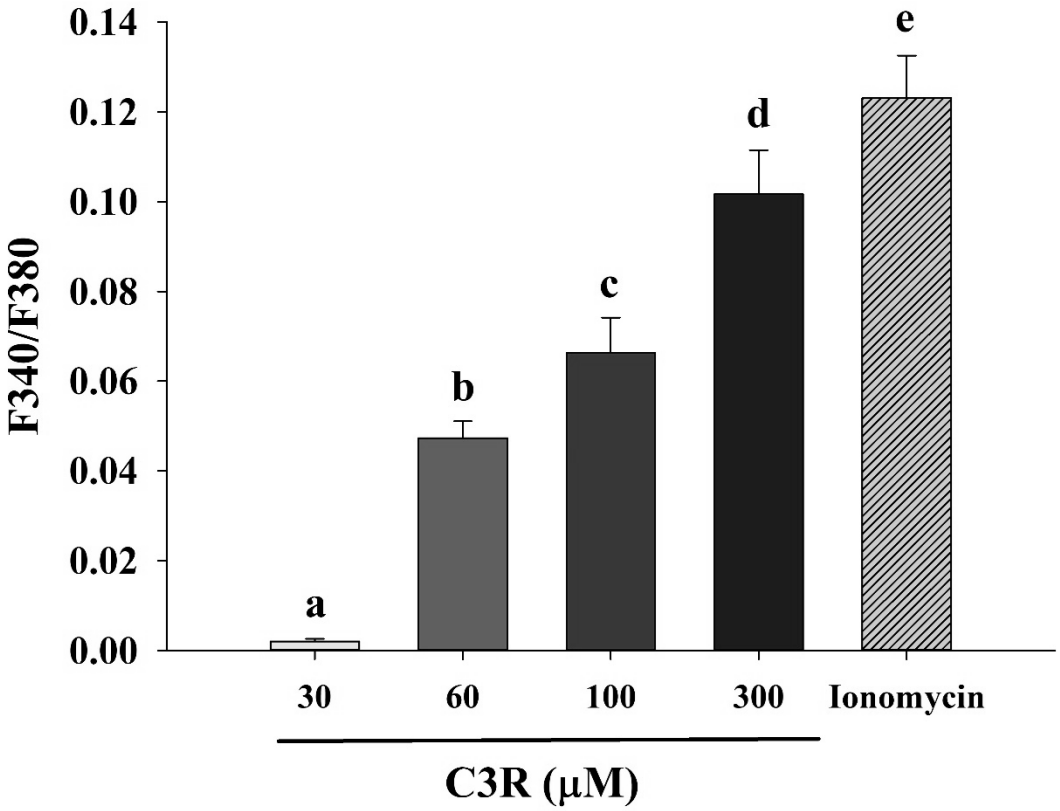


**Figure 40** Average calcium peak responses to cyanidin-3-rutinoside (C3R).

Results are presented as mean ± SEM from three independent experiments (n = 127-210 cells/group). Groups with different letters are significantly different ($P < 0.05$).

4.3.3 C3R stimulated insulin secretion.

To investigate whether C3R stimulated insulin secretion, cells were treated with C3R (1-300 μM). The results showed that C3R at 60, 100, and 300 μM increased insulin secretion by 6-fold, 11-fold, and 7-fold increase, respectively compared to basal (Figure 41). Meanwhile, stimulation of cells with 20 mM KCl as a positive control resulted in a 3-fold increase. Maximal insulin secretion was obtained with 100 μM C3R that was 3.5-fold greater than KCl treatment (Figure 41). C3R concentrations up to 100 μM did not induce cell cytotoxicity after 24 h (Figure 42). Therefore, 100 μM C3R was selected for further experiments.

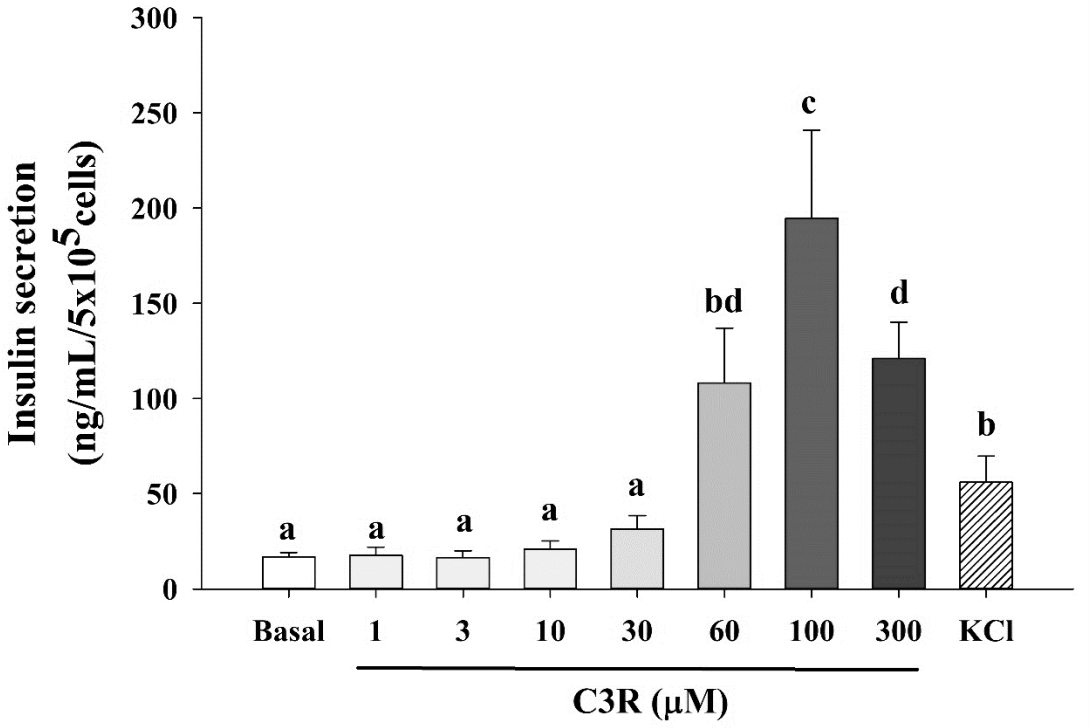


**Figure 41** The effect of cyanidin-3-rutinoside (C3R) on insulin secretion.

Results are presented as mean ± SEM from the three independent experiments. Groups with different letters are significantly different ($P < 0.05$).

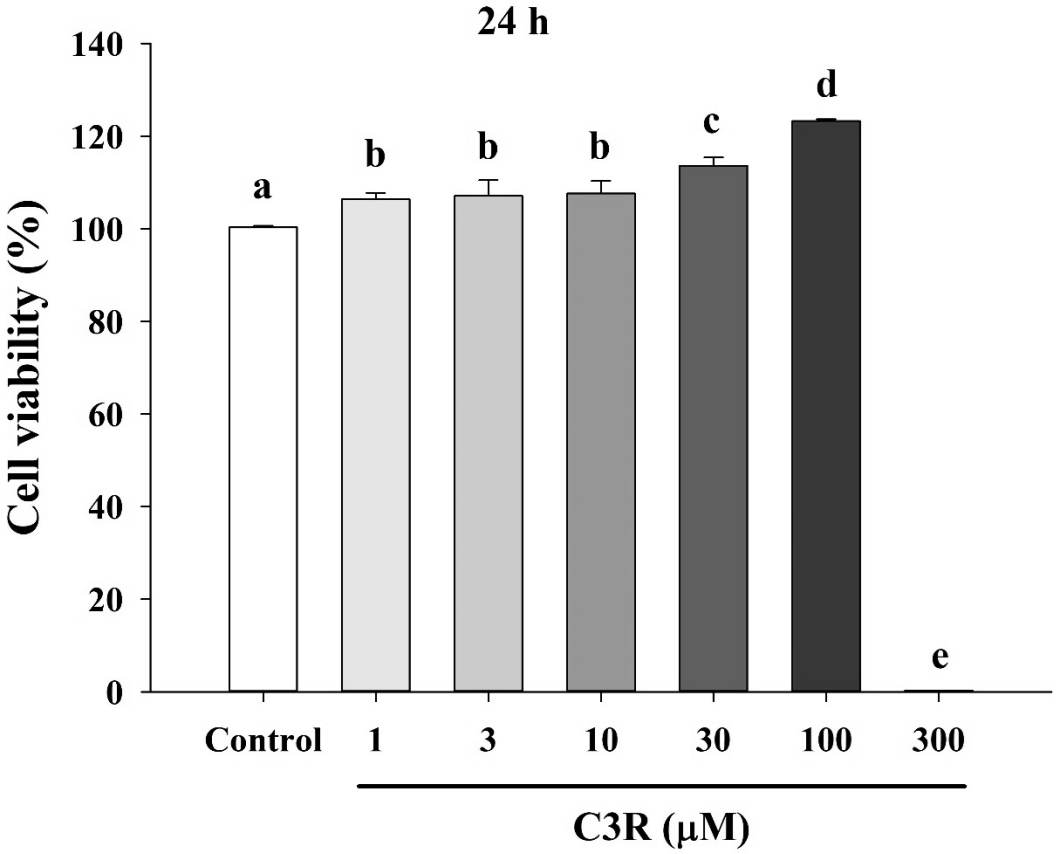


**Figure 42** The effects of cyanidin-3-rutinoside (C3R) on cell viability after 24 h of treatment.

Results are presented as mean ± SEM from the three independent experiments. Groups with different letters are significantly different ($P < 0.05$).

4.3.4 C3R activates the PLC-$IP_3$ pathway.

The PLC-$IP_3$ pathway is one mechanism to regulate intracellular calcium signaling. Hence, we tested whether this signaling mechanism was involved in the C3R effects. Pretreatment of cells with 10 μM U73122, a PLC inhibitor, inhibited the intracellular calcium signals by 100 μM C3R compared to control cells (Figure 43 and 44), but not in the presence of 10 μM U73343 (an inactive analogue of U73122) (Figure 43). Moreover, pretreatment of cells with 2-APB, an $IP_3$ receptor blocker in the ER, inhibited the C3R responses in a concentration-dependent manner (Figure 45). The results suggested that the PLC-$IP_3$ pathway is involved in calcium signals in response to C3R stimulation.

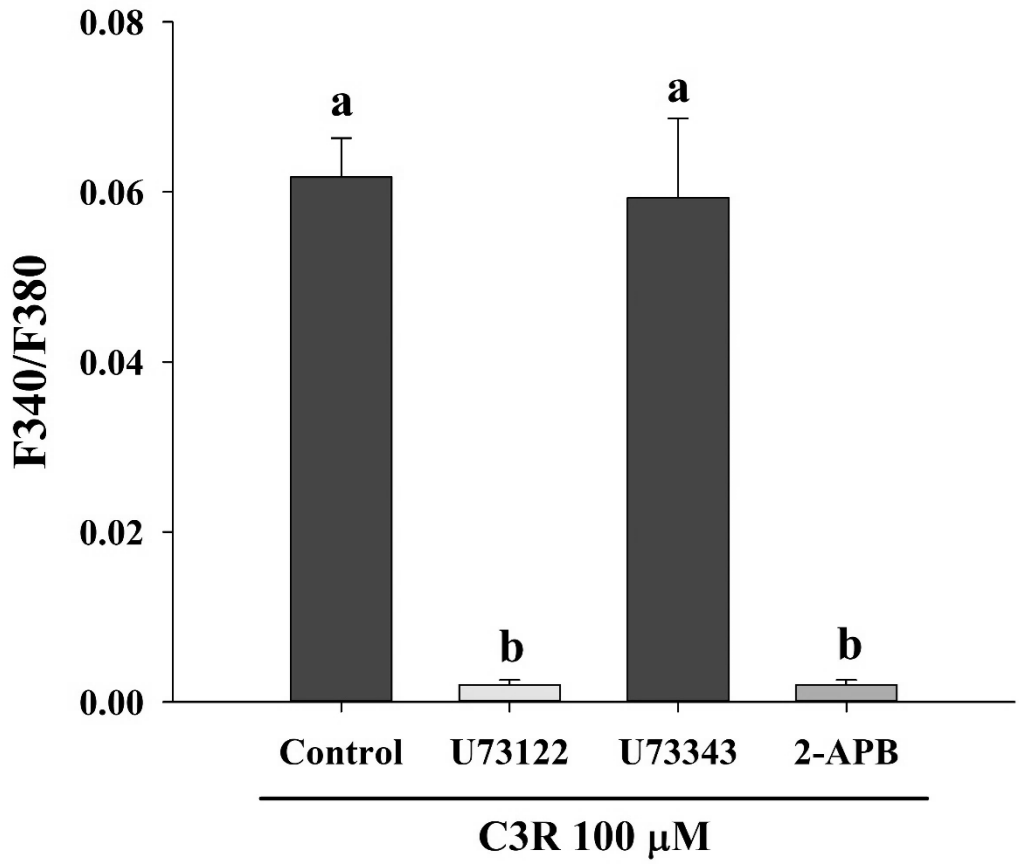


**Figure 43** The PLC-$IP_3$ pathway is required for intracellular calcium signals by cyanidin-3-rutinoside (C3R).

Results are presented as mean ± SEM from three independent experiments (n = 66-218 cells/group). Groups with different letters are significantly different ($P < 0.05$).

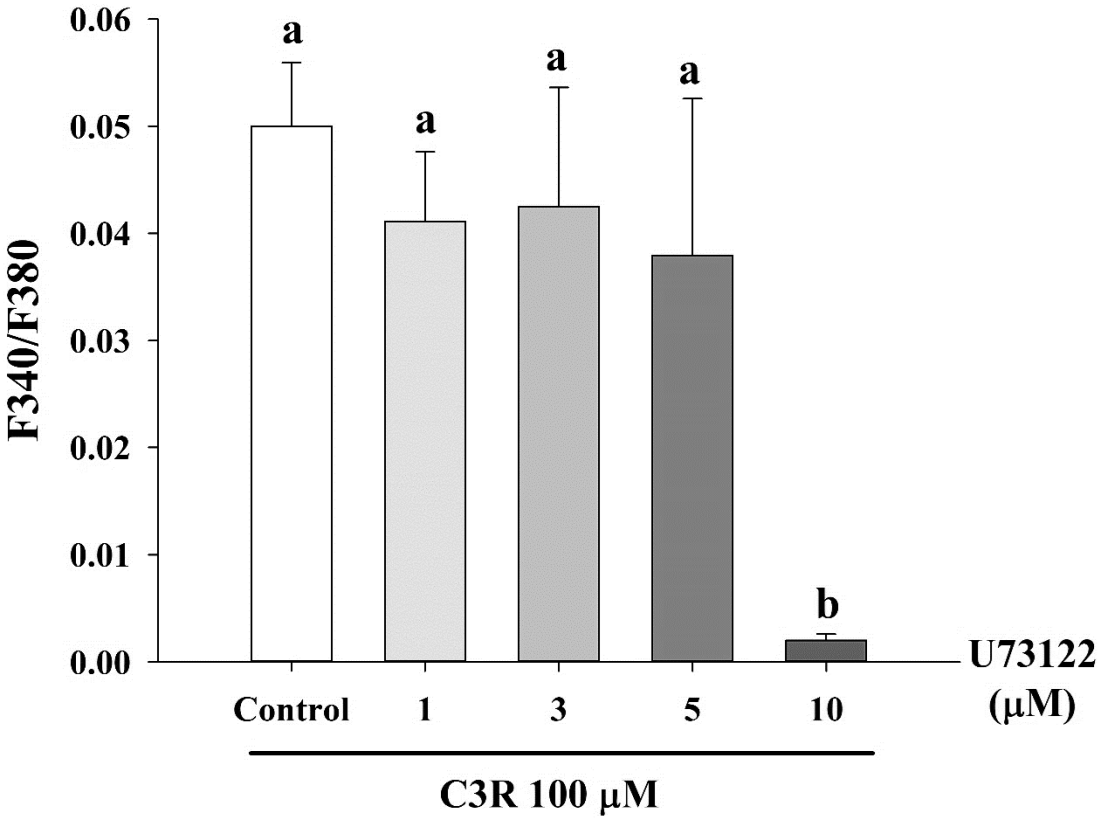


**Figure 44** Pretreatment of cells with the PLC inhibitor (U73122) inhibited intracellular calcium signals by cyanidin-3-rutinoside (C3R).

Results are presented as mean ± SEM from three independent experiments (n = 100-218 cells/group). Groups with different letters are significantly different ($P < 0.05$).

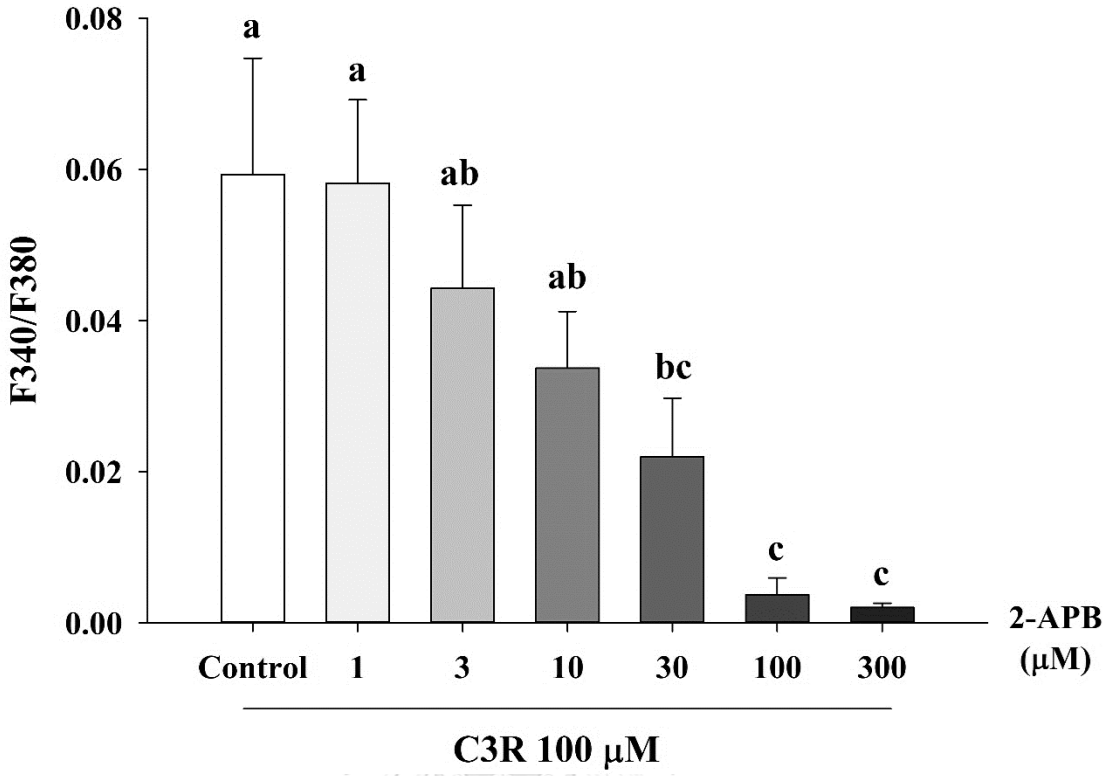


Figure 45 Pretreatment of cells with $IP_3$ receptor blocker (2-APB) inhibited intracellular calcium signals by cyanidin-3-rutinoside (C3R).

Results are presented as mean ± SEM from three independent experiments (n = 93-215 cells/group). Groups with different letters are significantly different ($P < 0.05$).

4.3.5 C3R activated L-type voltage-dependent calcium channels (VDCCs).

In pancreatic β-cells, extracellular calcium influx through VDCCs are required for insulin secretion. Therefore, nimodipine, the L-type VDCCs blocker was used to test whether C3R induced calcium influx through this channel. Pretreatment of cells with nimodipine (1-150 μM) inhibited the intracellular calcium signals in responses to 100 μM C3R (Figure 46). The results suggested that C3R induced calcium influx through L-type VDCCs.

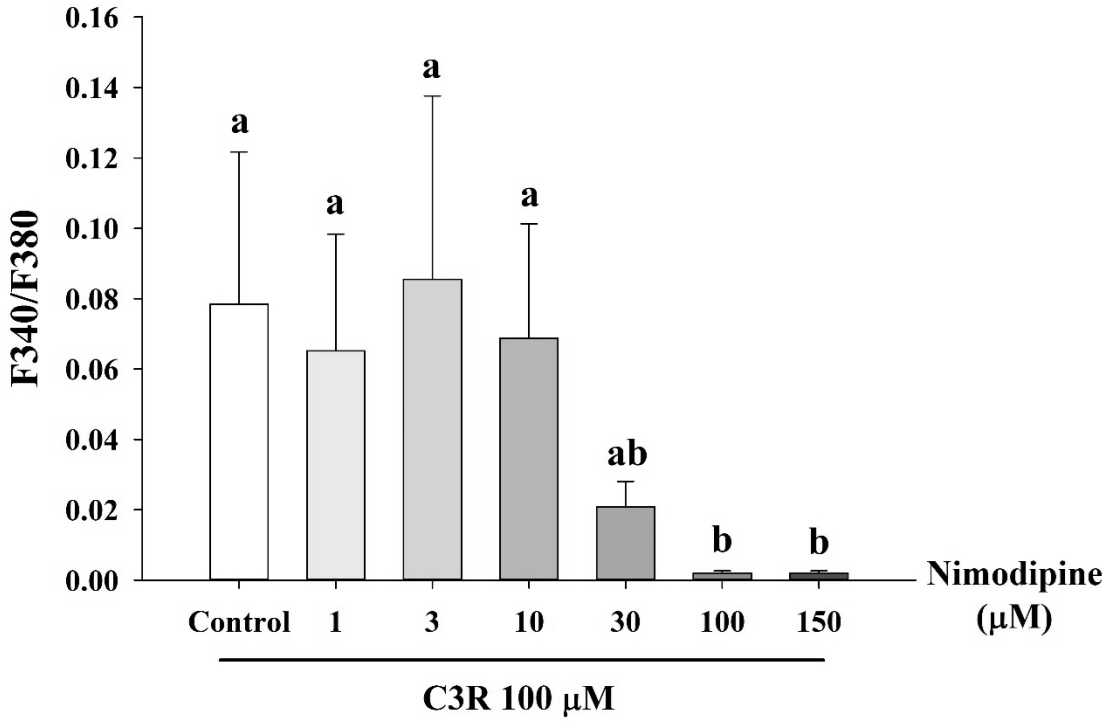


**Figure 46** Pretreatment of cells with nimodipine inhibited intracellular calcium signals by cyanidin-3-rutinoside (C3R).

Results are presented as mean ± SEM from three independent experiments (n = 50-225 cells/group). Groups with different letters are significantly different ($P < 0.05$).

4.3.6 Source of calcium for C3R signals.

To investigate the calcium sources for the C3R responses, experiments were performed under extracellular calcium free buffer and/or after depletion the intracellular calcium stores in the endoplasmic reticulum (ER). Removal of extracellular calcium reduced the calcium signals in response to C3R (100 μM) compared to the control group in calcium containing buffer (Figure 47). Depletion of calcium stores with thapsigargin (TG), did not affect the C3R responses. Under extracellular calcium free with TG, C3R responses were abolished (Figure 47). The effect of C3R on insulin secretion was also examined under similar experimental conditions. The results showed that after intracellular calcium stores depletion, C3R (100 μM) increased insulin secretion compared to control cells (Figure 48). Meanwhile, C3R failed to increase insulin secretion under extracellular calcium free conditions with or without TG treatment (Figure 48). The results suggested that calcium influx from extracellular space is required for insulin secretion during C3R stimulation.

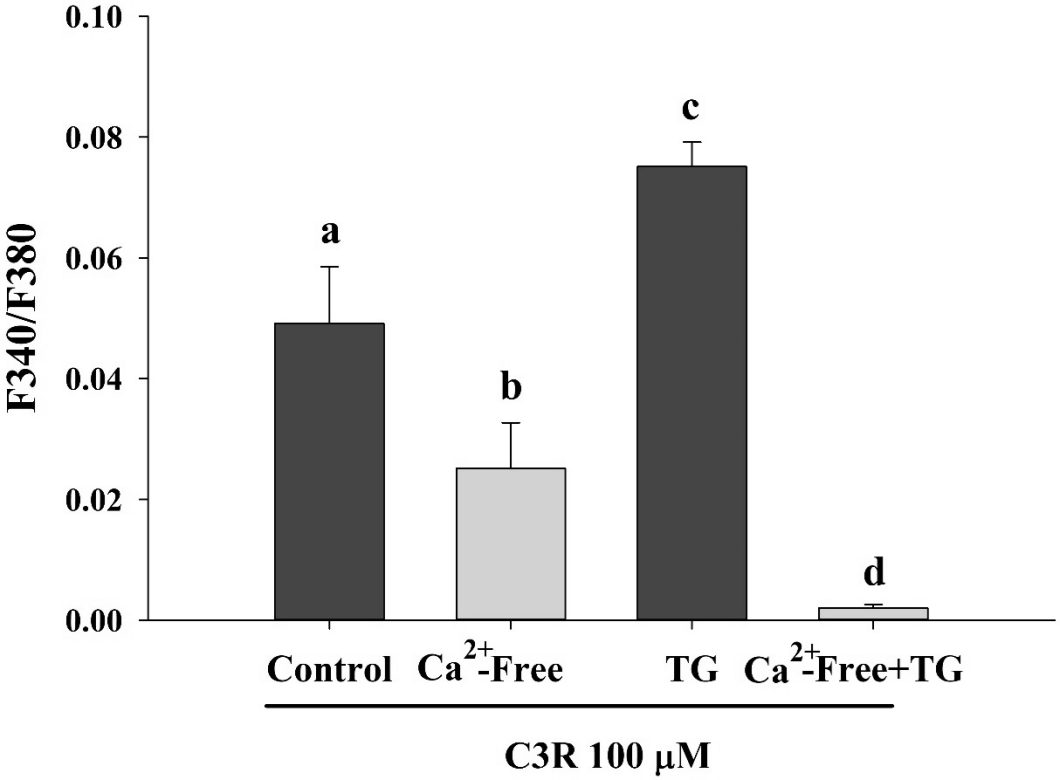


**Figure 47** The effect of cyanidin-3-rutinoside (C3R) on intracellular calcium signals under different calcium conditions.

Results are presented as mean ± SEM from three independent experiments (n = 147-202 cells/group). Groups with different letters are significantly different ($P < 0.05$).

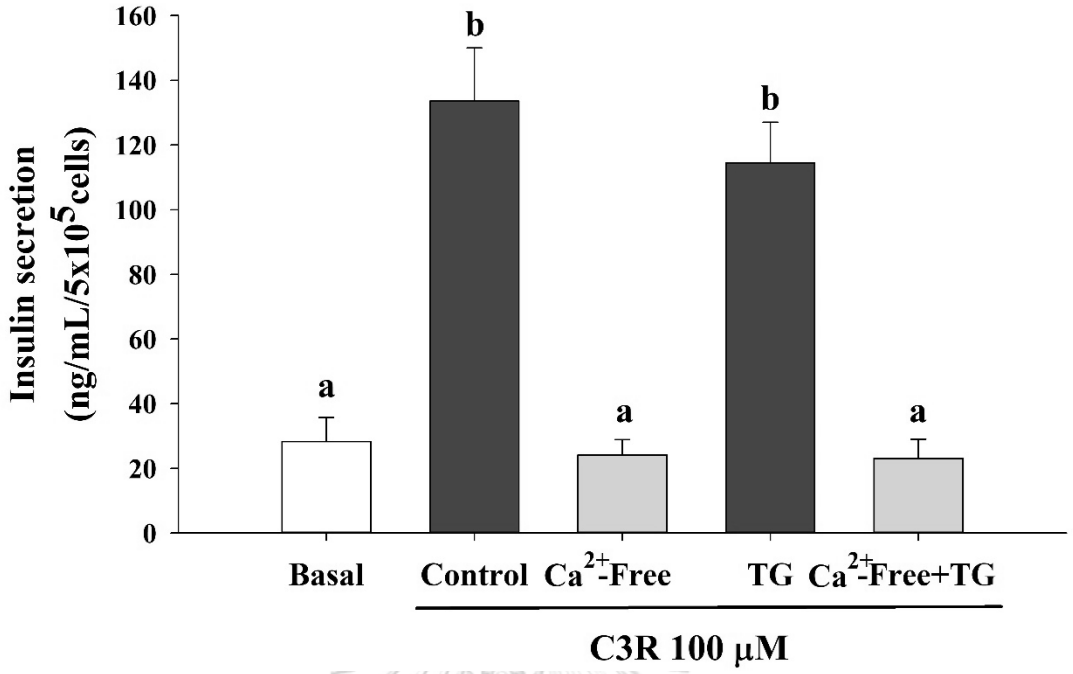


**Figure 48** The effect of cyanidin-3-rutinoside (C3R) on insulin secretion under different calcium conditions.

Results are presented as mean ± SEM from three independent experiments. Groups with different letters are significantly different ($P < 0.05$).

4.3.7 C3R upregulated insulin secretion genes.

Finally, the effects of C3R on mRNA expression of genes involved in the glucose-induced insulin secretion pathway were examined. After treatment with 100 μM C3R for 6 h, the results showed that C3R upregulated the expression of Glut2 and $Kir_{6.2}$ genes compared to untreated cells (Figure 49). However, C3R did not affect the expression of Ins, $Cav_{1.2}$, and GK genes (Figure 49).

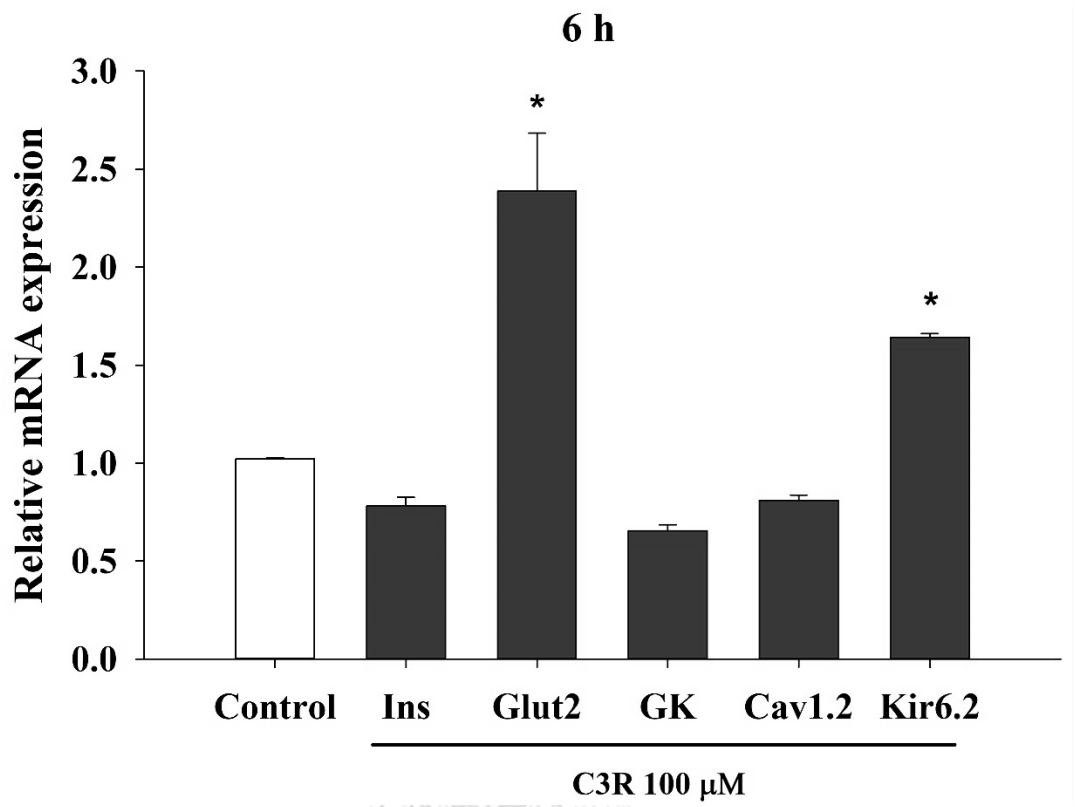


**Figure 49** The effects of cyanidin-3-rutinoside (C3R) on insulin secretion related gene expression.

Results are presented as mean ± SEM from three independent experiments. * $P < 0.05$ when compared to control. Data was normalized with β-actin.

# Chapter V
# Discussion

## 5.1 Phytochemical composition of Riceberry rice extract (RBE)

The present study is the first identification of the phytochemical composition in RBE using UHPLC-MS/MS. The results showed that RBE contained phenolic acids (ferulic acid and caffeic acid), flavonoids (quercetin-3-rutinoside or rutin and taxifolin), and anthocyanins (C3G, P3G, and petunidin-3-glucoside). In comparison to other pigmented rice extract such as Black rice (Jang *et al*., 2015), RBE contained C3G as a major anthocyanin as well. The total phenolic contents and anthocyanins concentration in RBE were similar to those reported by Anuyahong *et al*., 2020 using water extraction. However, the phytochemical content in our extract were lower than studies with ethanol extraction (Arjinajarn *et al*., 2016, Arjinajarn *et al*., 2017), methanol (Leardkamolkarn *et al*., 2011), dichloromethane (Leardkamolkarn *et al*., 2011), or 1% HCl in methanol (Poosri *et al*., 2019). This might be due to their ability to extract other water-insoluble compounds. Moreover, previous studies also purified their extract using solid phase extraction. Apart from anthocyanins, Riceberry rice bran extracted by methanol or dichloromethane contain free fatty acids such as linoleic, oleic, palmitic, myristic, stearic, and arachidic acid, and plant sterols including campesterol, stigmasterol, β-sitosterol, 22,23-dihydrostigmasterol, ergost-4,6,22-trien-3-ol, and cycloartane-type triterpene which are water-insoluble compounds (Leardkamolkarn, *et al*., 2011). In addition, we selected water extraction protocol because it mimics how rice is cooked for consumption.

**5.2 Riceberry rice extract (RBE) inhibited adipogenesis in 3T3-L1 cells**

Obesity is caused by hyperplasia or hypertrophy of fat cells during metabolic syndrome (Rutkowski *et al*., 2015). This study revealed that RBE has the potential to reduce adipose tissue expansion by inhibiting cell proliferation and adipogenesis. Studies show that cell proliferation is inhibited by cell cycle arrest during adipogenesis (Aguilar *et al*., 2010). We found that RBE has anti-proliferative effect by decreasing preadipocyte number without cytotoxicity. Flow cytometry assay revealed that RBE induced cell cycle arrest by increasing cells at the G0/G1 and G2/M phase. Moreover, RBE also reduced the total cell number without causing cytotoxicity during preadipocyte differentiation. These findings are consistent with reports with black soybean anthocyanins in 3T3-L1 cells (Kim *et al*., 2012).

During differentiation, preadipocytes which have fibroblast-like shape begins to differentiate into round-shape adipocytes with lipid droplet accumulation (Luo and Liu, 2016). RBE decreased adipocyte number and triglyceride accumulation in a concentration-dependent manner. Adipogenesis is controlled by a cascade of transcription factors including PPARγ and C/EBPs (Camp *et al*., 2002, Sarjeant and Stephens, 2012). In the early phase of adipogenesis, dexamethasone and IBMX upregulate the expression of C/EBPδ and C/EBPβ, respectively (Rosen and MacDougald, 2006). After that, C/EBPβ and C/EBPδ, mediate the expression of PPARγ and C/EBPα which are key regulators of adipogenesis. In addition, the expression of PPARγ and C/EBPα is also upregulated by insulin via the PI3K-Akt signaling pathway (Lowe *et al*., 2011). Moreover, C/EBPγ, a member of the C/EBP family inactivates C/EBPβ by heterodimerization to inhibit adipogenesis (Rosen and MacDougald, 2006). Our results indicated that RBE inhibited adipogenesis by downregulating PPARγ and C/EBPα and upregulating C/EBPγ in both early and late phase of adipogenesis. The effect of RBE on Akt1 pathway was determined. It was found that RBE did not influence Akt1 phosphorylation, indicating that the anti-adipogenic effect of RBE is not mediated by the Akt1 pathway. Another alternative mechanism could be inhibition of the MEK-ERK and Akt1 pathways that downregulate C/EBPβ, PPARγ, and C/EBPα expression (Maki *et*

*al*., 2017). It would be interesting for further study to investigate other underlying mechanisms of anti-adipogenic effect of RBE.

The roles of these transcription factors are regulation of adipogenic genes expression during adipocyte development and biosynthesis including lipogenesis, glucose uptake, adipokines secretion, and lipolysis (Lowe *et al*., 2011). Triglyceride is produced from glucose and free fatty acid through the lipogenesis pathway. The first rate-limiting enzyme of lipogenesis is ACC, which converts acetyl CoA to malonyl CoA. Then, fatty acids are produced by FasN, another rate-limiting enzyme of lipogenesis. After that, free fatty acids are transported by aP2 to generate triglyceride (Guo *et al*., 2009). In addition, lipid droplets also require proteins such as perilipin (structural proteins) and lipases enzyme (LPL, HSL, and ATGL) (Guo *et al*., 2009). Our study revealed that RBE downregulated adipogenic gene expression leading to a decrease in triglyceride accumulation. Adipose tissue also acts as an endocrine organ by secreting adipokines that regulate nutrient metabolism. There are three major adipokines including adiponectin, leptin, and resistin which are involved in metabolic syndrome (Zhang *et al*., 2015). Our study revealed that these adipokines were downregulated by RBE during adipogenic differentiation. Interestingly, adiponectin receptors (AdipoQ-R1 and AdipoQ-R2) were downregulated by RBE as well. Based on insulin-sensitivity of adipocytes, glucose uptake is another important function of adipocytes in response to insulin and promote adipogenesis. After binding to insulin receptors, insulin activates the PI3K-Akt pathway to promote Glut4 expression and translocation in adipocytes (Ducluzeau *et al*., 2002). Our study showed that RBE reduced glucose uptake in 3T3-L1 adipocytes by downregulating Glut4 mRNA expression. These findings are consistent with studies using anthocyanin-rich extract such as blue pea flower (Chayaratanasin *et al*., 2019), blueberry (Song *et al*., 2013), and cranberry (Kowalska *et al*., 2014, Kowalska *et al*., 2015) to inhibit adipogenesis.

Another way to reduce hypertrophic adipocyte is triglyceride breakdown through lipolysis. Lipolysis consists of basal lipolysis and activated lipolysis by isoproterenol or catecholamine (Jocken and Blaak, 2008). The β3-adrenergic receptor belongs to the G-

protein coupled receptor that promotes lipolysis via the cAMP-PKA pathway (Jocken and Blaak, 2008). Our results by which RBE enhanced isoproterenol-stimulated lipolysis are consistent with blue pea flower extract reports (Chayaratanasin *et al*., 2019).

The anti-obesity effect of RBE by inhibiting preadipocyte proliferation and differentiation are consistent with studies in anthocyanin-rich plants. Particularly, black rice (*Oryza sativa L*.) extract inhibits adipogenesis by suppressing PPARγ, C/EBPα, aP2, and LPL gene expression in mesenchymal C3H10T1/2 cells. Interestingly, C3G and P3G are the potential anti-adipogenic compounds in black rice (Jang *et al*., 2015). In addition to anthocyanins, phenolic compounds in RBE such as caffeic acid, ferulic acid, and rutin or quercetin-3-rutinoside could be effective to inhibit adipogenesis (Hsu and Yen, 2007). Rutin inhibits adipogenesis by downregulating PPARγ, C/EBPα, aP2, FasN, and LPL expression (Choi *et al*., 2006, Han *et al*., 2016). Coffee extract which contains caffeic acid has anti-adipogenic effects by downregulating adipogenic genes expression including PPARγ, C/EBPα, aP2, Glut4, adiponectin, and LPL (Maki *et al*., 2017). Previous study revealed that ferulic acid can bind to PPARγ leading to conformational changes and reduces gene expression for FasN, aP2, perilipin1, adiponectin, and LPL (Aranaz *et al*., 2019). The binding ability of phenolic compounds in RBE to PPARγ could be one mechanism for its anti-adipogenic effects. These findings suggest that the anti-obesity action of RBE may be due to the anthocyanins (C3G and P3G) and phenolic compounds (rutin, caffeic acid, and ferulic acid).

Intracellular calcium signaling is one mechanism that can regulate adipocyte cell cycle and function (Hu *et al*., 2009, Turovsky *et al*., 2012). Real-time calcium imaging revealed that RBE does not increase intracellular calcium in preadipocytes. These findings indicated that the anti-adipogenic effect of RBE are not mediated through calcium signaling. The anti-adipogenic effect of coffee extract is mediated by interrupting insulin signaling. Coffee extract suppresses the insulin receptor substrate 1 (IRS1) protein expression and promote protein degradation (Maki *et al*., 2017). Anthocyanins isolated from the fruit of *Vitis colgnetiae Pulliat* inhibits adipogenesis in 3T3-L1 cells by downregulating PPARγ, C/EBPα, C/EBPβ, aP2, leptin and FasN via the

AMPK pathway (Han *et al*., 2018). Blueberry peel extract and juice extract has anti-adipogenic effects in 3T3-L1 cells by downregulating PPARγ and C/EBPβ and decreasing the Akt signaling and enhancing the AMPK signaling (Song *et al*., 2013, Sánchez-Villavicencio *et al*., 2017).

In addition to RBE, we investigated whether other phenolic compounds increased intracellular calcium signals in preadipocytes. Our results revealed that C3G, ferulic acid, coumaric acid, and protocatechuic acid had no effect on the intracellular calcium signaling. However, Cy and C3R increased intracellular calcium by stimulating calcium release from the endoplasmic reticulum. These findings are different from studies in pancreatic β-cells where Cy (Suantawee *et al*., 2017) and C3R activates calcium influx through L-type VDCCs. It because preadipocytes are non-excitable cells that could not generate action potential to activate VDCCs. Hence, the calcium signals in preadipocytes are required the ligand-binding pathway such as the PLC-$IP_3$ pathway (Mears, 2004, Islam, 2010). Based on our findings, it would be interesting to investigate the effects and mechanisms of Cy and C3R on cell proliferation and differentiation through the intracellular calcium signaling in preadipocytes.

In summary, RBE inhibited preadipocyte proliferation by inducing cell cycle arrest and downregulating major transcription factors and adipogenic gene expression. Moreover, RBE decreased glucose uptake by downregulating Glut4 expression and enhancing isoproterenol-activated lipolysis in adipocytes. The proposed mechanism is shown in Figure 50.

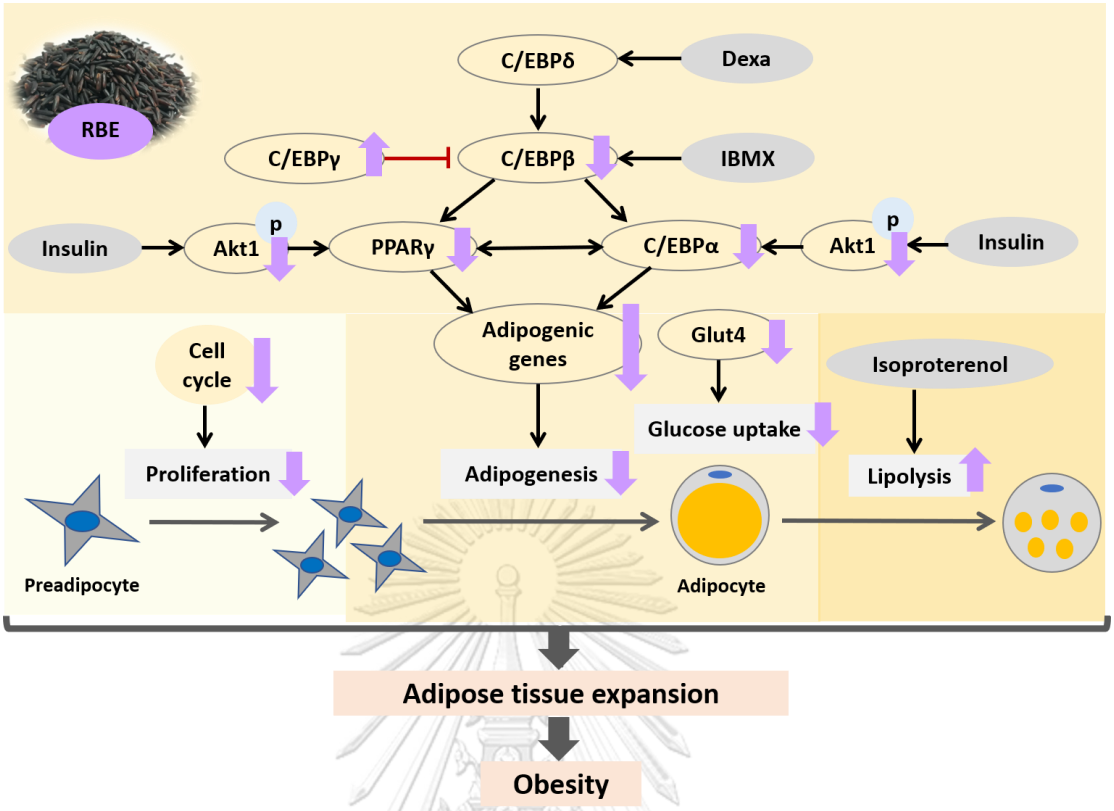


Figure 50 Proposed mechanism of Riceberry rice extract (RBE) in 3T3-L1 preadipocytes.

**5.3 Cyanidin-3-rutinoside (C3R) stimulated insulin secretion from pancreatic INS-1 cells**

Hyperglycemia is one of the hallmarks for metabolic syndrome (Grundy *et al*., 2004). Improving β-cell function by stimulating insulin secretion is an effective approach to treat hyperglycemia (Prentki and Nolan, 2006). Insulin secretion is regulated by intracellular calcium signaling in β-cells (Mears, 2004). Hence, we investigated the effect of RBE and other phenolic compounds on intracellular calcium signaling for the first time. The results demonstrated that RBE, C3G, ferulic acid, coumaric acid, and protocatechuic acid had no effects on intracellular calcium signals. However, C3R which is synthesized from rutin or quercetin-3-rutinoside presenting in Riceberry rice increased intracellular calcium signals in β-cells. Therefore, we also examined its effect on insulin secretion. The results indicated that C3R improved cell function by stimulating insulin secretion from INS-1 cells with no evidence of cytotoxicity at concentrations up to 100 μM. The increase in C3R concentration increased insulin secretion levels. However, cells treated with C3R 300 μM showed less insulin levels compared to 100 μM. It is due to C3R 300 μM is toxic to the cells. This is an agreement with studies in MIN-6 cells where C3R also improved glucose-stimulated insulin secretion by upregulating GK and ATP accumulation (Zheng *et al*., 2016). In addition to insulin secretion, C3R preserves β-cells mass by preventing cell apoptosis. Studies in INS-1 cells show that C3R protects against apoptosis by reducing pro-apoptotic protein expression (e.g., Bax, cytochrome c, caspase 9, and caspase 3), and increasing Bcl-2, an anti-apoptotic protein expression (Choi *et al*., 2018).

In our study, C3R increased intracellular calcium signals in a concentration-dependent manner. These results are consistent with other compounds such as Cy (Suantawee *et al*., 2017), quercetin (Bardy *et al*., 2013, Kittl, Beyreis *et al*., 2016), and rutin (quercetin-3-rutinoside) (Kappel *et al*., 2013). The PLC-$IP_3$ pathway is one mechanism to regulate intracellular calcium signals and activation of G protein-coupled receptors also regulation of pancreatic β-cells. For example, GPR40 stimulates insulin secretion by inducing calcium release from the ER via the PLC-$IP_3$ pathway (Ahren, 2009). U73122 (a PLC inhibitor) and 2-APB (a selective $IP_3$ receptor blocker) were used

to test whether the PLC-$IP_3$ pathway was involved in the C3R response. The experiments confirmed that this is the case for C3R signaling. These findings are similar to those by rutin or quercetin-3-rutinoside (Kappel *et al*., 2013).

Voltage-dependent calcium channels (VDCCs) are required for calcium influx and insulin secretion from pancreatic β-cells (Mears, 2004). The L-type VDCCs blocker, nimodipine, confirmed that C3R induces calcium influx through VDCCs. These findings are consistent with other flavonoids such as Cy (Suantawee *et al*., 2017), quercetin (Bardy *et al*., 2013, Kittl *et al*., 2016), rutin (quercetin-3-rutinoside) (Kappel *et al*., 2013), and *p*-methoxycinnamic acid (Adisakwattana *et al*., 2011).

There is main two sources for intracellular calcium signals: calcium influx from extracellular space and calcium release from intracellular stores such as the ER (Nowycky and Thomas, 2002). The results showed that C3R induced calcium signals under extracellular calcium free condition. It is possible that C3R may induce calcium release from other intracellular calcium stores: mitochondria and Golgi apparatus, apart from the ER. Our findings suggested that C3R induced calcium signals by promoting calcium influx through L-type VDCCs and activating the PLC-$IP_3$ pathway. These findings are quite different from Cy which promotes calcium influx only (Suantawee *et al*., 2017). It is possible that the core structure of Cy stimulates calcium channels on cell membrane whereas the rutinoside structure on C3R may activate the PLC-$IP_3$ pathway or Gq-coupled receptors in the cell membrane. This supported by the study with rutin that activates both calcium influx through L-type VDCCs and the PLC pathway in rat pancreatic islets (Kappel *et al*., 2013). There is another underlying mechanism by which C3R activates calcium influx through L-type VDCCs and the PLC-$IP_3$ pathway. It is possible that C3R may activates VDCCs via the PLC/PKC-dependent pathway. After hydrolysis of $PIP_2$ by PLC enzyme, DAG is generated and induce L-type VDCCs opening leading to calcium influx and insulin secretion (Shigeto *et al*., 2017, Suzuki *et al*., 2006). In addition, insulin secretion experiments under different calcium conditions confirmed that calcium influx from extracellular space is the main source for insulin secretion during C3R stimulation.

The present study also investigated the effect of C3R on the expression of genes necessary for glucose-induced insulin secretion. Lack of Glut2 expression in diabetic animals causes hyperglycemia (Orci *et al*., 1990, Bonny *et al*., 1997). The ATP-sensitive potassium channel ($K_{ATP}$) consists of two major subunits, $Kir_{6.2}$ and SUR1 (Velasco *et al*., 2016). Downregulation of $Kir_{6.2}$ inhibits $K_{ATP}$ currents and calcium influx and insulin secretion in HIT-T15 cells (Chen *et al*., 2010). Our results showed that C3R upregulated mRNA expression for Glut2 and $Kir_{6.2}$ genes. These findings are consistent with previous report for cyanidin in INS-1 cells (Suantawee *et al*., 2017). However, our findings are different from studies in MIN-6 cells where C3R also upregulates the GK (Zheng *et al*., 2016). It might be explained by the variation among cell lines. In addition, based on its bioavailability, C3R can identify in blood as intact form after oral consumption (Matsumoto *et al*., 2001). Therefore, it is possible to see these effects of C3R on pancreatic β-cells function. However, further studies in different cell lines, animal models, or clinical trial should be performed to better understand of C3R's effects on insulin secretion.

In summary, C3R stimulated insulin secretion by activating calcium influx through L-type voltage-dependent calcium channels (VDCCs), activating the PLC-$IP_3$ pathway, and upregulated Glut2 and $Kir_{6.2}$ gene expression. The proposed mechanism is shown in Figure 51.

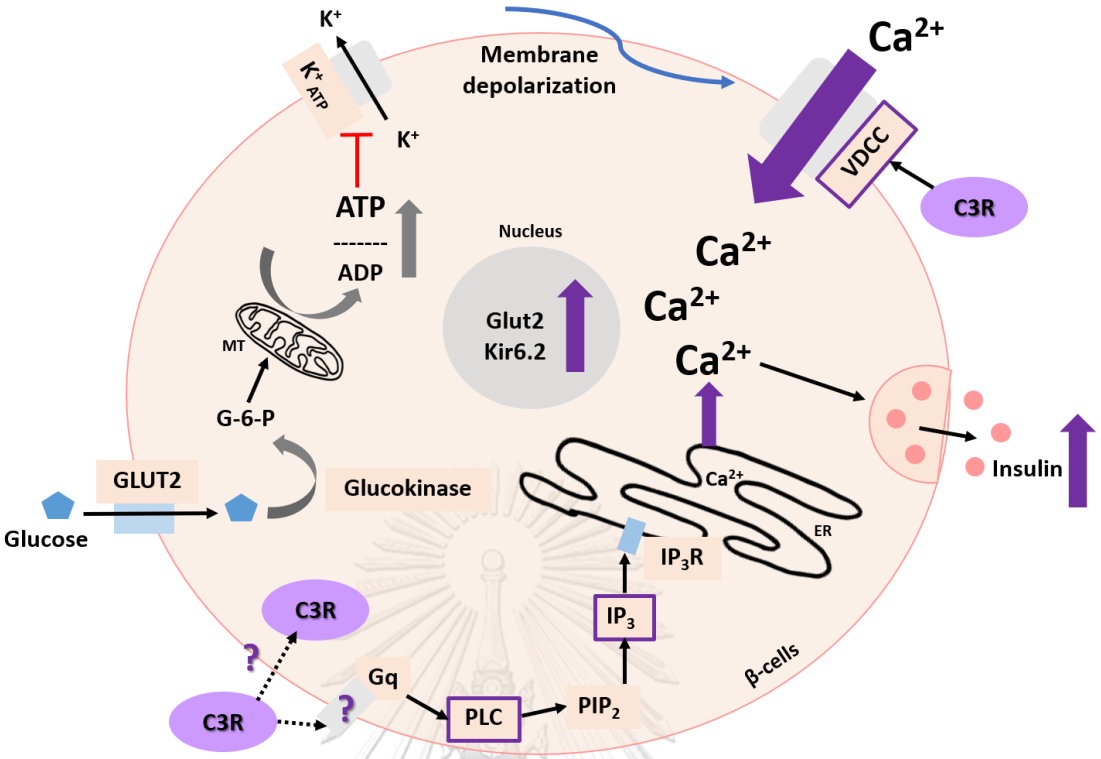


**Figure 51** Proposed mechanism for cyanidin-3-rutinoside (C3R) stimulation of insulin secretion from pancreatic β-cells

# Chapter VI
# Conclusion

Cyanidin-3-glucoside (C3G) and peonidin-3-glucoside (P3G) are the major anthocyanins of Riceberry rice extract (RBE). Other phenolic compounds such as petunidin-3-glucoside, caffeic acid, taxifolin, quercetin-3-rutinoside (rutin) and ferulic acid are present. The study revealed that RBE inhibits cell proliferation and differentiation of preadipocytes. RBE decreased cell number by inducing cell cycle arrest without causing cytotoxicity. During adipogenesis, RBE modulated the mRNA expression of adipogenic transcription factors by upregulating C/EBPγ but downregulating PPARγ, C/EBPα, C/EBPβ along with their target genes associated with the reduction of adipocyte number and triglyceride accumulation. In addition, RBE reduced glucose uptake by downregulating Glut4 expression and stimulating isoproterenol-induced lipolysis. These findings suggest that RBE could potentially be used as an anti-obesity agent.

Riceberry rice extract alone or some of its components could not induce insulin secretion from pancreatic β-cells. However, we found that cyanidin-3-rutinoside (C3R), a glycoside-derivative of rutin, stimulated insulin secretion by promoting calcium influx through L-type voltage-dependent calcium channels (VDCCs) and activating the PLC-$IP_3$ pathway. Furthermore, C3R upregulated glucose-induced insulin secretion genes Glut2 and $Kir_{6.2}$ without cytotoxicity. These findings suggest that C3R could potentially be used as an anti-hyperglycemic agent.

Taken together, these findings support the beneficial effects of anthocyanins on the prevention of obesity, diabetes, and metabolic syndrome.

# REFERENCES

"Hyperglycemia (High Blood Glucose)." Retrieved 8/3/2019, from http://www.diabetes.org/living-with-diabetes/treatment-and-care/blood-glucose-control/hyperglycemia.html.

"ข้าวไรซ์เบอร์รี่ - Riceberry." from http://dna.kps.ku.ac.th/index.php/news-articles-rice-rsc-rgdu-knowledge/rice-breeding-lab/riceberry-variety.

Adisakwattana, S., W. H. Hsu and S. Yibchok-Anun (2011). "Mechanisms of *p*-methoxycinnamic acid-induced increase in insulin secretion." Horm Metab Res 43(11): 766-773.

Adisakwattana, S., N. Ngamrojanavanich, K. Kalampakorn, W. Tiravanit, S. Roengsumran and S. Yibchok-Anun (2004). "Inhibitory activity of cyanidin-3-rutinoside on α-glucosidase." J Enzyme Inhib Med Chem 19(4): 313-316.

Adisakwattana, S., S. Yibchok-Anun, P. Charoenlertkul and N. Wongsasiripat (2011). "Cyanidin-3-rutinoside alleviates postprandial hyperglycemia and its synergism with acarbose by inhibition of intestinal α-glucosidase." J Clin Biochem Nutr 49(1): 36-41.

Aekplakorn, W., V. Chongsuvivatwong, P. Tatsanavivat and P. Suriyawongpaisal (2011). "Prevalence of metabolic syndrome defined by the International Diabetes Federation and National Cholesterol Education Program criteria among Thai adults." Asia Pac J Public Health 23(5): 792-800.

Aguilar, V., J.-S. Annicotte, X. Escote, J. Vendrell, D. Langin and L. Fajas (2010). "Cyclin G2 regulates adipogenesis through PPARγ coactivation." Endocrinology 151(11): 5247-5254.

Ahren, B. (2009). "Islet G protein-coupled receptors as potential targets for treatment of type 2 diabetes." Nat Rev Drug Discov 8(5): 369-385.

Akkarachiyasit, S., S. Yibchok-Anun, S. Wacharasindhu and S. Adisakwattana (2011). "In vitro inhibitory effects of cyandin-3-rutinoside on pancreatic α-amylase and its combined effect with acarbose." Molecules 16(3): 2075-2083.

Andrikopoulos, S. (2010). "Obesity and Type 2 diabetes: Slow down!—Can metabolic deceleration protect the islet beta cell from excess nutrient-induced damage?" Mol Cell Endocrinol 316(2): 140-146.

Anuyahong, T., C. Chusak and S. Adisakwattana (2020). "Incorporation of anthocyanin-rich riceberry rice in yogurts: Effect on physicochemical properties, antioxidant activity and in vitro gastrointestinal digestion." LWT 129: 109571.

Anuyahong, T., C. Chusak, T. Thilavech and S. Adisakwattana (2020). "Postprandial effect of yogurt enriched with anthocyanins from riceberry rice on glycemic response and antioxidant capacity in healthy adults." Nutrients 12(10): 2930.

Aranaz, P., D. Navarro-Herrera, M. Zabala, I. Miguéliz, A. Romo-Hualde, M. López-Yoldi, J. A. Martínez, J. L. Vizmanos, F. I. Milagro and C. J. González-Navarro (2019). "Phenolic compounds inhibit 3T3-L1 adipogenesis depending on the stage of differentiation and their binding affinity to PPARγ." Molecules 24(6): 1045.

Arjinajarn, P., N. Chueakula, A. Pongchaidecha, K. Jaikumkao, V. Chatsudthipong, S. Mahatheeranont, O. Norkaew, N. Chattipakorn and A. Lungkaphin (2017). "Anthocyanin-rich Riceberry bran extract attenuates gentamicin-induced hepatotoxicity by reducing oxidative stress, inflammation and apoptosis in rats." Biomed Pharmacother 92: 412-420.

Arjinajarn, P., A. Pongchaidecha, N. Chueakula, K. Jaikumkao, V. Chatsudthipong, S. Mahatheeranont, O. Norkaew, N. Chattipakorn and A. Lungkaphin (2016). "Riceberry bran extract prevents renal dysfunction and impaired renal organic anion transporter 3 (Oat3) function by modulating the PKC/Nrf2 pathway in gentamicin-induced nephrotoxicity in rats." Phytomedicine 23(14): 1753-1763.

Azzini, E., J. Giacometti and G. L. Russo (2017). "Antiobesity effects of anthocyanins in preclinical and clinical studies." Oxid Med Cell Longev 2017: 1-11.

Bagur, R. and G. Hajnóczky (2017). "Intracellular $Ca^{2+}$ sensing: role in calcium homeostasis and signaling." Mol Cell 66(6): 780-788.

Balamurugan, R., S. E. Vendan, A. Aravinthan and J.-H. Kim (2015). "Isolation and structural characterization of 2R, 3R taxifolin 3-O-rhamnoside from ethyl acetate extract of *Hydnocarpus alpina* and its hypoglycemic effect by attenuating hepatic key enzymes of glucose metabolism in streptozotocin-induced diabetic rats." Biochimie 111: 70-81.

Bardy, G., A. Virsolvy, J. F. Quignard, M. A. Ravier, G. Bertrand, S. Dalle, G. Cros, R. Magous, S. Richard and C. Oiry (2013). "Quercetin induces insulin secretion by direct

activation of L-type calcium channels in pancreatic beta cells." Br J Pharmacol 169(5): 1102-1113.

Bensellam, M., D. R. Laybutt and J.-C. Jonas (2012). "The molecular mechanisms of pancreatic β-cell glucotoxicity: recent findings and future research directions." Mol Cell Endocrinol 364(1-2): 1-27.

Berridge, M. J. (2012). "Module 9: Cell Cycle and Proliferation." Cell Signal Biol 6.

Bhattacharya, S., N. Oksbjerg, J. F. Young and P. B. Jeppesen (2014). "Caffeic acid, naringenin and quercetin enhance glucose-stimulated insulin secretion and glucose sensitivity in INS-1E cells." Diabetes Obes Metab 16(7): 602-612.

Bito, M., T. Tomita, M. Komori, T. Taogoshi, Y. Kimura and K. Kihira (2013). "The mechanisms of insulin secretion and calcium signaling in pancreatic β-cells exposed to fluoroquinolones." Biol Pharm Bull 36(1): 31-35.

Bolsoni-Lopes, A. and M. I. C. Alonso-Vale (2015). "Lipolysis and lipases in white adipose tissue–an update." Arch Endocrinol Metab 59(4): 335-342.

Bonny, C., R. Roduit, S. Gremlich, P. Nicod, B. Thorens and G. Waeber (1997). "The loss of GLUT2 expression in the pancreatic β-cells of diabetic db/db mice is associated with an impaired DNA-binding activity of islet-specific *trans*-acting factors." Mol Cell Endocrinol 135(1): 59-65.

Bootman, M. D., K. Rietdorf, H. Hardy, Y. Dautova, E. Corps, C. Pierro, E. Stapleton, E. Kang and D. Proudfoot (2012). "Calcium signalling and regulation of cell function." eLS. John Wiley & Sons 1-14.

Boucher, J., A. Kleinridders and C. R. Kahn (2014). "Insulin receptor signaling in normal and insulin-resistant states." Cold Spring Harb Perspect Biol 6(1): a009191.

Brewer, P. D., E. N. Habtemichael, I. Romenskaia, C. C. Mastick and A. C. F. Coster (2014). "Insulin-regulated Glut4 translocation membrane protein trafficking with six distinctive steps." J Biol Chem 289(25): 17280-17298.

Camp, H. S., D. Ren and T. Leff (2002). "Adipogenesis and fat-cell function in obesity and diabetes." Trends Mol Med 8(9): 442-447.

American Diabetes Association (2011). "Diagnosis and classification of diabetes mellitus." Diabetes care 34(Supplement 1): S62-S69.

Castro-Acosta, M. L., L. Smith, R. J. Miller, D. I. McCarthy, J. A. Farrimond and W. L. Hall (2016). "Drinks containing anthocyanin-rich blackcurrant extract decrease postprandial blood glucose, insulin and incretin concentrations." J Nutr Biochem 38: 154-161.

Chang, W.-T., C.-H. Wu and C.-L. Hsu (2015). "Diallyl trisulphide inhibits adipogenesis in 3T3-L1 adipocytes through lipogenesis, fatty acid transport, and fatty acid oxidation pathways." J Funct Foods 16: 414-422.

Chayaratanasin, P., A. Caobi, C. Suparpprom, S. Saenset, P. Pasukamonset, N. Suanpairintr, M. A. Barbieri and S. Adisakwattana (2019). "*Clitoria ternatea* flower petal extract inhibits adipogenesis and lipid accumulation in 3T3-L1 preadipocytes by downregulating adipogenic gene expression." Molecules 24(10): 1894.

Chen, C.-C., W.-T. Chuang, A.-H. Lin, C.-W. Tsai, C.-S. Huang, Y.-T. Chen, H.-W. Chen and C.-K. Lii (2016). "Andrographolide inhibits adipogenesis of 3T3-L1 cells by suppressing C/EBPβ expression and activation." Toxicol Appl Pharmacol 307: 115-122.

Chen, F., D. Zheng, Y. Xu, Y. Luo, H. Li, K. Yu, Y. Song, W. Zhong and Y. Ji (2010). "Down-regulation of Kir6. 2 affects calcium influx and insulin secretion in HIT-T15 cells." J Pediatr Endocrinol Metab 23(7): 709-717.

Chen, K., L. Zhao, H. He, X. Wan, F. Wang and Z. Mo (2014). "Silibinin protects β cells from glucotoxicity through regulation of the Insig-1/SREBP-1c pathway." Int J Mol Med 34(4): 1073-1080.

Cheng, H., A. Beck, P. Launay, S. A. Gross, A. J. Stokes, J.-P. Kinet, A. Fleig and R. Penner (2007). "TRPM4 controls insulin secretion in pancreatic β-cells." Cell Calcium 41(1): 51-61.

Cheng, H., S. Yibchok-Anun, S.-C. Park and W. H. Hsu (2002). "Somatostatin-induced paradoxical increase in intracellular $Ca^{2+}$ concentration and insulin release in the presence of arginine vasopressin in clonal HIT-T15 β-cells." Biochem 364(1): 33-39.

Choe, S. S., J. Y. Huh, I. J. Hwang, J. I. Kim and J. B. Kim (2016). "Adipose tissue remodeling: its role in energy metabolism and metabolic disorders." Front Endocrinol 7: 30.

Choi, I., Y. Park, H. Choi and E. H. Lee (2006). "Anti-adipogenic activity of rutin in 3T3-L1 cells and mice fed with high-fat diet." Biofactors 26(4): 273-281.

Choi, K.-H., M. H. Park, H. A. Lee and J.-S. Han (2018). "Cyanidin-3-rutinoside protects INS-1 pancreatic β cells against high glucose-induced glucotoxicity by apoptosis." Z Naturforsch C J Biosci 73(7-8): 281-289.

Chusak, C., P. Pasukamonset, P. Chantarasinlapin and S. Adisakwattana (2020). "Postprandial glycemia, insulinemia, and antioxidant status in healthy subjects after ingestion of bread made from anthocyanin-rich riceberry rice." Nutrients 12(3): 782.

Clapham, D. E. (1995). "Calcium signaling." Cell 80(2): 259-268.

Dolgacheva, L. P., M. V. Turovskaya, V. V. Dynnik, V. P. Zinchenko, N. V. Goncharov, B. Davletov and E. A. Turovsky (2016). "Angiotensin II activates different calcium signaling pathways in adipocytes." Arch Biochem Biophys 593: 38-49.

Ducluzeau, P.-H., L. M. Fletcher, H. Vidal, M. Laville and J. M. Tavare (2002). "Molecular mechanisms of insulin-stimulated glucose uptake in adipocytes." Diabetes Metab 28: 85-92.

Dumitraşcu, L., E. Enachi, N. Stănciuc and I. Aprodu (2019). "Optimization of ultrasound assisted extraction of phenolic compounds from cornelian cherry fruits using response surface methodology." CYTA J Food 17(1): 814-823.

Duncan, R. E., M. Ahmadian, K. Jaworski, E. Sarkadi-Nagy and H. S. Sul (2007). "Regulation of lipolysis in adipocytes." Annu Rev Nutr 27: 79-101.

Elhabiri, M., P. Figueiredo, A. Fougerousse and R. Brouillard (1995). "A convenient method for conversion of flavonols into anthocyanins." Tetrahedron Lett 36(26): 4611-4614.

Engin, A. B. and A. Engin (2017). “Obesity and lipotoxicity,” Adv Exp Med Biol 960.

Fasshauer, M. and R. Paschke (2003). "Regulation of adipocytokines and insulin resistance." Diabetologia 46(12): 1594-1603.

FDA U.S. (2015). Diabetes medicines, FDA Office of women's health.

FDA U.S. (2018). Diabetes medicines, FDA Office of women's health.

Fernandes, I., A. Faria, C. Calhau, V. de Freitas and N. Mateus (2014). "Bioavailability of anthocyanins and derivatives." J Funct Foods 7: 54-66.

Francisco Bonamichi, B. D. S., E. Bezerra Parente, R. B. dos Santos, R. Beltzhoover, J. Lee and J. E. Nunes Salles (2018). "The Challenge of Obesity Treatment: A Review of Approved Drugs and New Therapeutic Targets." J Obes Eat Disord 4(1): 1-10.

Fu, Z. and D. Liu (2009). "Long-term exposure to genistein improves insulin secretory function of pancreatic β-cells." Eur J Pharmacol 616(1-3): 321-327.

Gaggini, M., F. Carli and A. Gastaldelli (2017). "The color of fat and its central role in the development and progression of metabolic diseases." Horm Mol Biol Clin Investig 31(1): 1-14.

Garralda-Del-Villar, M., S. Carlos-Chillerón, J. Diaz-Gutierrez, M. Ruiz-Canela, A. Gea, M. A. Martínez-González, M. Bes-Rastrollo, L. Ruiz-Estigarribia, S. N. Kales and A. Fernández-Montero (2019). "Healthy lifestyle and incidence of metabolic syndrome in the SUN cohort." Nutrients 11(1): 65.

Ghosh, D. (2005). "Anthocyanins and anthocyanin-rich extracts in biology and medicine: biochemical, cellular, and medicinal properties." Curr Top Nutraceutical Res 3(2): 113-124.

Gonçalves, A. C., M. Rodrigues, A. O. Santos, G. Alves and L. R. Silva (2018). "Antioxidant status, antidiabetic properties and effects on Caco-2 cells of colored and non-colored enriched extracts of sweet cherry fruits." Nutrients 10(11): 1688.

Gowd, V., Z. Jia and W. Chen (2017). "Anthocyanins as promising molecules and dietary bioactive components against diabetes – A review of recent advances." Trends Food Sci Technol 68: 1-13.

Graham, D. J., J. A. Staffa, D. Shatin, S. E. Andrade, S. D. Schech, L. La Grenade, J. H. Gurwitz, K. A. Chan, M. J. Goodman and R. Platt (2004). "Incidence of hospitalized rhabdomyolysis in patients treated with lipid-lowering drugs." Jama 292(21): 2585-2590.

Grundy, S. M., H. B. Brewer Jr, J. I. Cleeman, S. C. Smith Jr and C. Lenfant (2004). "Definition of metabolic syndrome: report of the National Heart, Lung, and Blood Institute/American Heart Association conference on scientific issues related to definition." Circulation 109(3): 433-438.

Grundy, S. M., J. I. Cleeman, S. R. Daniels, K. A. Donato, R. H. Eckel, B. A. Franklin, D. J. Gordon, R. M. Krauss, P. J. Savage, S. C. J. C. Smith Jr, J. A. Spertus and F. Costa (2005). "Diagnosis and management of the metabolic syndrome: an American Heart Association/National Heart, Lung, and Blood Institute scientific statement." Circulation 112(17): 2735-2752.

Grundy, S. M. (2016). "Metabolic syndrome update." Trends Cardiovasc Med 26(4): 364-373.

Guo, Y., K. R. Cordes, R. V. Farese and T. C. Walther (2009). "Lipid droplets at a glance." J Cell Sci 122(6): 749-752.

Han, M. H., H. J. Kim, J.-W. Jeong, C. Park, B. W. Kim and Y. H. Choi (2018). "Inhibition of adipocyte differentiation by anthocyanins isolated from the fruit of *Vitis coignetiae* pulliat is associated with the activation of AMPK signaling pathway." Toxicol Res 34(1): 13-21.

Han, Y.-H., J.-Y. Kee, J. Park, D.-S. Kim, S. Shin, D.-H. Youn, J. W. Kang, Y. Jung, Y.-M. Lee, J.-H. Park, S.-J. Kim, J.-Y. Um and S.-H. Hong (2016). "Lipin1-mediated repression of adipogenesis by rutin." Am J Chin Med 44(3): 565-578.

Hannan, J. M. A., L. Marenah, L. Ali, B. Rokeya, P. R. Flatt and Y. H. A. Abdel-Wahab (2006). "*Ocimum sanctum* leaf extracts stimulate insulin secretion from perfused pancreas, isolated islets and clonal pancreatic β-cells." J Endocrinol 189(1): 127-136.

Hasnain, S. Z., J. B. Prins and M. A. McGuckin (2016). "Oxidative and endoplasmic reticulum stress in β-cell dysfunction in diabetes." J Mol Endocrinol 56(2): R33-R54.

Hassimotto, N. M. A., M. I. Genovese and F. M. Lajolo (2008). "Absorption and metabolism of cyanidin-3-glucoside and cyanidin-3-rutinoside extracted from wild mulberry (*Morus nigra* L.) in rats." Nutr Res 28(3): 198-207.

Hausman, D. B., M. DiGirolamo, T. J. Bartness, G. J. Hausman and R. J. Martin (2001). "The biology of white adipocyte proliferation." Obes Rev 2(4): 239-254.

He, Y., W. Niu, C. Xia and B. Cao (2016). "Daidzein reduces the proliferation and adiposeness of 3T3-L1 preadipocytes via regulating adipogenic gene expression." J Funct Foods 22: 446-453.

Hong, S. H., J.-I. Heo, J.-H. Kim, S.-O. Kwon, K.-M. Yeo, A. M. Bakowska-Barczak, P. Kolodziejczyk, O.-H. Ryu, M.-K. Choi, Y.-H. Kang, S. S. Lim, H.-W. Suh, S.-O. Huh and J.-Y. Lee (2013). "Antidiabetic and Beta cell-protection activities of purple corn anthocyanins." Biomol Ther 21(4): 284-289.

Hsieh, Y.-H. and S.-Y. Wang (2013). "Lucidone from *Lindera erythrocarpa* Makino fruits suppresses adipogenesis in 3T3-L1 cells and attenuates obesity and consequent metabolic disorders in high-fat diet C57BL/6 mice." Phytomedicine 20(5): 394-400.

Hsu, C.-L. and G.-C. Yen (2007). "Effects of flavonoids and phenolic acids on the inhibition of adipogenesis in 3T3-L1 adipocytes." J Agric Food Chem 55(21): 8404-8410.

Hu, R., M.-L. He, H. Hu, B.-X. Yuan, W.-J. Zang, C.-P. Lau, H.-F. Tse and G.-R. Li (2009). "Characterization of calcium signaling pathways in human preadipocytes." J Cell Physiol 220(3): 765-770.

Hu, Y.-C., D.-M. Hao, L.-X. Zhou, Z. Zhang, N. Huang, M. Hoptroff and Y.-H. Lu (2014). "2′, 4′-Dihydroxy-6′-methoxy-3′, 5′-dimethylchalcone protects the impaired insulin secretion induced by glucotoxicity in pancreatic β-cells." J Agric Food Chem 62(7): 1602-1608.

Islam, M. S. (2010). “The islets of Langerhans,” Adv Exp Med Biol 654.

James, D. E. (2005). "MUNC-ing around with insulin action." J Clin Investig 115(2): 219-221.

Jang, W.-S., C.-R. Seo, H. H. Jang, N.-J. Song, J.-K. Kim, J.-Y. Ahn, J. Han, W. D. Seo, Y. M. Lee and K. W. Park (2015). "Black rice (*Oryza sativa* L.) extracts induce osteoblast differentiation and protect against bone loss in ovariectomized rats." Food Funct 6(1): 265-275.

Jayaprakasam, B., S. K. Vareed, L. K. Olson and M. G. Nair (2005). "Insulin secretion by bioactive anthocyanins and anthocyanidins present in fruits." J Agric Food Chem 53(1): 28-31.

Jittorntrum, B., R. Chunhabundit, R. Kongkachuichai, S. Srisala and Y. Visetpanit (2009). "Cytoprotective and cytotoxic effects of rice bran extracts on $H_2O_2$-induced oxidative damage in human intestinal Caco-2 cells." Thai J Toxicol 24(2): 92-100.

Jocken, J. W. E. and E. E. Blaak (2008). "Catecholamine-induced lipolysis in adipose tissue and skeletal muscle in obesity." Physiol Behav 94(2): 219-230.

Kamboj, A., R. Gupta, A. Rana and R. Kaur (2015). "Application and analysis of the Folin Ciocalteu method for the determination of the total phenolic content from extracts of *Terminalia bellerica*." European J Biomed 2(3): 201-215.

Kang, J. W., D. Nam, K. H. Kim, J.-E. Huh and J.-D. Lee (2013). "Effect of gambisan on the inhibition of adipogenesis in 3T3-L1 adipocytes." Evid Based Complement Alternat Med 2013: 1-11.

Kappel, V. D., M. J. S. Frederico, B. G. Postal, C. P. Mendes, L. H. Cazarolli and F. R. M. B. Silva (2013). "The role of calcium in intracellular pathways of rutin in rat pancreatic islets: potential insulin secretagogue effect." Eur J Pharmacol 702(1-3): 264-268.

Karpe, F. and K. E. Pinnick (2015). "Biology of upper-body and lower-body adipose tissue—link to whole-body phenotypes." Nat Rev Endocrinol 11(2): 90-100.

Kassi, E., P. Pervanidou, G. Kaltsas and G. Chrousos (2011). "Metabolic syndrome: definitions and controversies." BMC Med 9(1): 48.

Khoo, H. E., A. Azlan, S. T. Tang and S. M. Lim (2017). "Anthocyanidins and anthocyanins: colored pigments as food, pharmaceutical ingredients, and the potential health benefits." Food Nutr Res 61(1): 1361779.

Kim, H.-K., J. N. Kim, S. N. Han, J.-H. Nam, H.-N. Na and T. J. Ha (2012). "Black soybean anthocyanins inhibit adipocyte differentiation in 3T3-L1 cells." Nutr Res 32(10): 770-777.

Kim, S. Y., H.-R. Wi, S. Choi, T. J. Ha, B. W. Lee and M. Lee (2015). "Inhibitory effect of anthocyanin-rich black soybean testa (*Glycine max* (L.) Merr.) on the inflammation-induced adipogenesis in a DIO mouse model." J Funct Foods 14: 623-633.

Kittl, M., M. Beyreis, M. Tumurkhuu, J. Fürst, K. Helm, A. Pitschmann, M. Gaisberger, S. Glasl, M. Ritter and M. Jakab (2016). "Quercetin stimulates insulin secretion and reduces the viability of rat INS-1 beta-cells." Cell Physiol Biochem 39(1): 278-293.

Kongkachuichai, R., P. Prangthip, R. Surasiang, J. Posuwan, R. Charoensiri, A. Kettawan and A. Vanavichit (2013). "Effect of Riceberry oil (deep purple oil; *Oryza sativa* Indica) supplementation on hyperglycemia and change in lipid profile in Streptozotocin (STZ)-induced diabetic rats fed a high fat diet." Int Food Res J 20(2): 873-882.

Kowalska, K., A. Olejnik, J. Rychlik and W. Grajek (2014). "Cranberries (*Oxycoccus quadripetalus*) inhibit adipogenesis and lipogenesis in 3T3-L1 cells." Food Chem 148: 246-252.

Kowalska, K., A. Olejnik, J. Rychlik and W. Grajek (2015). "Cranberries (*Oxycoccus quadripetalus*) inhibit lipid metabolism and modulate leptin and adiponectin secretion in 3T3-L1 adipocytes." Food Chem 185: 383-388.

Krebs, J., L. B. Agellon and M. Michalak (2015). "$Ca^{2+}$ homeostasis and endoplasmic reticulum (ER) stress: An integrated view of calcium signaling." Biochem Biophys Res Commun 460(1): 114-121.

Leardkamolkarn, V., W. Thongthep, P. Suttiarporn, R. Kongkachuichai, S. Wongpornchai and A. Wanavijitr (2011). "Chemopreventive properties of the bran extracted from a newly-developed Thai rice: The Riceberry." Food Chem 125(3): 978-985.

Lee, B., M. Lee, M. Lefevre and H.-R. Kim (2014). "Anthocyanins inhibit lipogenesis during adipocyte differentiation of 3T3-L1 preadipocytes." Plant Foods Hum Nutr 69(2): 137-141.

Lee, D., J. Ham, K. S. Kang and H.-J. Lee (2016). "Cyanidin 3-*O*-glucoside isolated from *Lonicera caerulea* fruit improves glucose response in INS-1 cells by improving insulin secretion and signaling." Bull Korean Chem Soc 37(12): 2015-2018.

Lee, D., J. S. Lee, J. Sezirahiga, H. C. Kwon, D. S. Jang and K. S. Kang (2020). "Bioactive phytochemicals isolated from *Akebia quinata* enhances glucose-stimulated insulin secretion by inducing PDX-1." Plants 9(9): 1087.

Lee, H., J. Kim, J. Y. Park, K. S. Kang, J. H. Park and G. S. Hwang (2017). "Processed *Panax ginseng*, sun ginseng, inhibits the differentiation and proliferation of 3T3-L1 preadipocytes and fat accumulation in *Caenorhabditis elegans*." J Ginseng Res 41(3): 257-267.

Lee, J., R. W. Durst and R. E. Wrolstad (2005). "Determination of total monomeric anthocyanin pigment content of fruit juices, beverages, natural colorants, and wines by the pH differential method: collaborative study." J AOAC Int 88(5): 1269-1278.

Lee, J. S., Y. R. Kim, J. M. Park, Y. E. Kim, N. I. Baek and E. K. Hong (2015). "Cyanidin-3-glucoside isolated from mulberry fruits protects pancreatic β-cells against glucotoxicity-induced apoptosis." Mol Med Rep 11(4): 2723-2728.

Lee, W. K., S. T. Kao, I.-M. Liu and J.-T. Cheng (2006). "Increase of insulin secretion by ginsenoside Rh2 to lower plasma glucose in Wistar rats." Clin Exp Pharmacol Physiol 33(1-2): 27-32.

Leney, S. E. and J. M. Tavaré (2009). "The molecular basis of insulin-stimulated glucose uptake: signalling, trafficking and potential drug targets." J Endocrinol 203(1): 1-18.

Li, S., C. Bouzar, C. Cottet-Rousselle, I. Zagotta, F. Lamarche, M. Wabitsch, M. Tokarska-Schlattner, P. Fischer-Posovszky, U. Schlattner and D. Rousseau (2016). "Resveratrol inhibits lipogenesis of 3T3-L1 and SGBS cells by inhibition of insulin signaling and mitochondrial mass increase." Biochim Biophys Acta 1857(6): 643-652.

Liu, D., W. Zhen, Z. Yang, J. D. Carter, H. Si and K. A. Reynolds (2006). "Genistein acutely stimulates insulin secretion in pancreatic β-cells through a cAMP-dependent protein kinase pathway." Diabetes 55(4): 1043-1050.

Liu, L. and N. A. Clipstone (2007). "Prostaglandin F2α inhibits adipocyte differentiation via a Gαq-Calcium-Calcineurin-Dependent signaling pathway." J Cell Biochem 100(1): 161-173.

Lowe, C. E., S. O'Rahilly and J. J. Rochford (2011). "Adipogenesis at a glance." J Cell Sci 124(16): 2681-2686.

Luna-Vital, D. A. and E. G. de Mejia (2018). "Anthocyanins from purple corn activate free fatty acid-receptor 1 and glucokinase enhancing *in vitro* insulin secretion and hepatic glucose uptake." PloS one 13(7): e0200449.

Luo, L. and M. Liu (2016). "Adipose tissue in control of metabolism." J Endocrinol 231(3): R77-R99.

Maki, C., M. Funakoshi-Tago, R. Aoyagi, F. Ueda, M. Kimura, K. Kobata, K. Tago and H. Tamura (2017). "Coffee extract inhibits adipogenesis in 3T3-L1 preadipocyes by interrupting insulin signaling through the downregulation of IRS1." PloS one 12(3): e0173264.

Manaharan, T., C. H. Ming and U. D. Palanisamy (2013). "*Syzygium aqueum* leaf extract and its bioactive compounds enhances pre-adipocyte differentiation and 2-NBDG uptake in 3T3-L1 cells." Food Chem 136(2): 354-363.

Marquez, M. P., F. Alencastro, A. Madrigal, J. L. Jimenez, G. Blanco, A. Gureghian, L. Keagy, C. Lee, R. Liu, L. Tan, K. Deignan, B. Armstrong and Y. Zhao (2017). "The role of cellular proliferation in adipogenic differentiation of human adipose tissue-derived mesenchymal stem cells." Stem Cells Dev 26(21): 1578-1595.

Martino, H. S. D., M. M. dos Santos Dias, G. Noratto, S. Talcott and S. U. Mertens-Talcott (2016). "Anti-lipidaemic and anti-inflammatory effect of açai (*Euterpe oleracea* Martius) polyphenols on 3T3-L1 adipocytes." J Funct Foods 23: 432-443.

Matsukawa, T., M. O. Villareal and H. Isoda (2016). "The type 2 diabetes-preventive effect of cyanidin-3-glucoside on adipocytes." J Sustain Agr 11(1): 31-35.

Matsumoto, H., H. Inaba, M. Kishi, S. Tominaga, M. Hirayama and T. Tsuda (2001). "Orally administered delphinidin 3-rutinoside and cyanidin 3-rutinoside are directly absorbed in rats and humans and appear in the blood as the intact forms." J Agric Food Chem 49(3): 1546-1551.

Mears, D. (2004). "Regulation of insulin secretion in islets of Langerhans by $Ca^{2+}$ channels." J Membr Biol 200(2): 57-66.

Meier, U. and A. M. Gressner (2004). "Endocrine regulation of energy metabolism: review of pathobiochemical and clinical chemical aspects of leptin, ghrelin, adiponectin, and resistin." Clin Chem 50(9): 1511-1525.

Meldolesi, J. (2008). "Inhibition of adipogenesis: a new job for the ER $Ca^{2+}$ pool." J Cell Biol 182(1): 11-13.

Neal, J. W. and N. A. Clipstone (2002). "Calcineurin mediates the calcium-dependent inhibition of adipocyte differentiation in 3T3-L1 cells." J Biol Chem 277(51): 49776-49781.

Nowycky, M. C. and A. P. Thomas (2002). "Intracellular calcium signaling." J Cell Sci 115(19): 3715-3716.

Orci, L., M. Ravazzola, D. Baetens, L. Inman, M. Amherdt, R. G. Peterson, C. B. Newgard, J. H. Johnson and R. H. Unger (1990). "Evidence that down-regulation of β-cell glucose transporters in non-insulin-dependent diabetes may be the cause of diabetic hyperglycemia." Proc Natl Acad Sci 87(24): 9953-9957.

Pękal, A. and K. Pyrzynska (2014). "Evaluation of aluminium complexation reaction for flavonoid content assay." Food Anal Methods 7(9): 1776-1782.

Pepin, É., A. Al-Mass, C. Attané, K. Zhang, J. Lamontagne, R. Lussier, S. R. M. Madiraju, E. Joly, N. B. Ruderman, R. Sladek, M. Prentki and M.-L. Peyot (2016). "Pancreatic β-cell dysfunction in diet-induced obese mice: roles of AMP-kinase, protein kinase Cε, mitochondrial and cholesterol metabolism, and alterations in gene expression." PloS one 11(4): e0153017.

Pongchaiyakul, C., T. V. Nguyen, E. Wanothayaroj, N. Karusan and V. Klungboonkrong (2007). "Prevalence of metabolic syndrome and its relationship to weight in the Thai population." J Med Assoc Thai 90(3): 459-467.

Poosri, S., T. Thilavech, P. Pasukamonset, C. Suparpprom and S. Adisakwattana (2019). "Studies on Riceberry rice (*Oryza sativa* L.) extract on the key steps related to carbohydrate and lipid digestion and absorption: A new source of natural bioactive substances." NFS J 17: 17-23.

Posuwan, J., P. Prangthip, V. Leardkamolkarn, U. Yamborisut, R. Surasiang, R. Charoensiri and R. Kongkachuichai (2013). "Long-term supplementation of high pigmented rice bran oil (*Oryza sativa* L.) on amelioration of oxidative stress and histological changes in streptozotocin-induced diabetic rats fed a high fat diet; Riceberry bran oil." Food Chem 138(1): 501-508.

Prangthip, P., R. Surasiang, R. Charoensiri, V. Leardkamolkarn, S. Komindr, U. Yamborisut, A. Vanavichit and R. Kongkachuichai (2013). "Amelioration of hyperglycemia, hyperlipidemia, oxidative stress and inflammation in steptozotocin-induced diabetic rats fed a high fat diet by riceberry supplement." J Funct Foods 5(1): 195-203.

Prentki, M. and C. J. Nolan (2006). "Islet β cell failure in type 2 diabetes." J Clin Investig 116(7): 1802-1812.

Pruszyńska-Oszmałek, E., P. A. Kołodziejski, M. Sassek and J. H. Sliwowska (2017). "Kisspeptin-10 inhibits proliferation and regulates lipolysis and lipogenesis processes in 3T3-L1 cells and isolated rat adipocytes." Endocrine 56(1): 54-64.

Rabe, K., M. Lehrke, K. G. Parhofer and U. C. Broedl (2008). "Adipokines and insulin resistance." Mol Med 14(11-12): 741-751.

Rahman, N., M. Jeon and Y.-S. Kim (2016). "Delphinidin, a major anthocyanin, inhibits 3T3-L1 pre-adipocyte differentiation through activation of Wnt/β-catenin signaling." BioFactors 42(1): 49-59.

Rerksuppaphol, L. and S. Rerksuppaphol (2014). "Prevalence of metabolic syndrome in Thai children: a cross-sectional study." J Clin Diagn Res 8(4): PC04-PC07.

Rosen, E. D. and O. A. MacDougald (2006). "Adipocyte differentiation from the inside out." Nat Rev Mol Cell Biol 7(12): 885-896.

Różańska, D. and B. Regulska-Ilow (2018). "The significance of anthocyanins in the prevention and treatment of type 2 diabetes." Adv Clin Exp Med 27(1): 135-142.

Ruginǎ, D., Z. Diaconeasa, C. Coman, A. Bunea, C. Socaciu and A. Pintea (2015). "Chokeberry anthocyanin extract as pancreatic β-cell protectors in two models of induced oxidative stress." Oxid Med Cell Longev 2015: 1-10.

Rutkowski, J. M., J. H. Stern and P. E. Scherer (2015). "The cell biology of fat expansion." J Cell Biol 208(5): 501-512.

Saklayen, M. G. (2018). "The global epidemic of the metabolic syndrome." Curr Hypertens Rep 20(2): 12.

Sánchez-Villavicencio, M. L., M. Vinqvist-Tymchuk, W. Kalt, C. Matar, F. J. A. Aguilar, M. d. C. E. Villanueva and P. S. Haddad (2017). "Fermented blueberry juice extract and its specific fractions have an anti-adipogenic effect in 3 T3-L1 cells." BMC Complement Altern Med 17(1): 24.

Sarjeant, K. and J. M. Stephens (2012). "Adipogenesis." Cold Spring Harb Perspect Biol 4(9): a008417.

Sarni-Manchado, P., E. Le Roux, C. Le Guernevé, Y. Lozano and V. Cheynier (2000). "Phenolic composition of litchi fruit pericarp." J Agric Food Chem 48(12): 5995-6002.

Schnell, S., M. Schaefer and C. Schöfl (2007). "Free fatty acids increase cytosolic free calcium and stimulate insulin secretion from β-cells through activation of GPR40." Mol Cell Endocrinol 263(1-2): 173-180.

Seo, M.-J., H.-S. Choi, H.-J. Jeon, M.-S. Woo and B.-Y. Lee (2014). "Baicalein inhibits lipid accumulation by regulating early adipogenesis and m-TOR signaling." Food Chem Toxicol 67: 57-64.

Sergeev, I. N. (2009). "1, 25-Dihydroxyvitamin D3 induces $Ca^{2+}$-mediated apoptosis in adipocytes via activation of calpain and caspase-12." Biochem Biophys Res Commun 384(1): 18-21.

Shi, H., Y.-D. Halvorsen, P. N. Ellis, W. O. Wilkison and M. B. Zemel (2000). "Role of intracellular calcium in human adipocyte differentiation." Physiol Genomics 3(2): 75-82.

Shi, X.-l., Y.-Z. Ren and J. Wu (2011). "Intermittent high glucose enhances apoptosis in INS-1 cells." Exp Diabetes Res 2011: 1-7.

Shigeto, M., C. Y. Cha, P. Rorsman and K. Kaku (2017). "A role of PLC/PKC-dependent pathway in GLP-1-stimulated insulin secretion." J Mol Med 95(4): 361-368.

Somintara, S., V. Leardkamolkarn, P. Suttiarporn and S. Mahatheeranont (2016). "Anti-tumor and immune enhancing activities of rice bran gramisterol on acute myelogenous leukemia." PloS one 11(1): e0146869.

Song, Y., H. J. Park, S. N. Kang, S.-H. Jang, S.-J. Lee, Y.-G. Ko, G.-S. Kim and J.-H. Cho (2013). "Blueberry peel extracts inhibit adipogenesis in 3T3-L1 cells and reduce high-fat diet-induced obesity." PloS one 8(7): e69925.

Suantawee, T., S. T. Elazab, W. H. Hsu, S. Yao, H. Cheng and S. Adisakwattana (2017). "Cyanidin stimulates insulin secretion and pancreatic β-cell gene expression through activation of l-type voltage-dependent $Ca^{2+}$ channels." Nutrients 9(8): 814.

Sun, C.-D., B. Zhang, J.-K. Zhang, C.-J. Xu, Y.-L. Wu, X. Li and K.-S. Chen (2012). "Cyanidin-3-glucoside-rich extract from Chinese bayberry fruit protects pancreatic β cells and ameliorates hyperglycemia in streptozotocin-induced diabetic mice." J Med Food 15(3): 288-298.

Surasiang R., P. Prangthip, A. Kettawan, R. Charoensiri, U. Yamborisut, R. Kongkachuichai (2011). Effect of cold press rice berry oil (*dark violet oil*) on blood glucose, insulin level and oxidative stress in high fat diet fed to streptozotocin-induced diabetic rats. The 20th National Graduate Research Conference. Mahidol University, Salaya.

Suzuki, Y., H. Zhang, N. Saito, I. Kojima, T. Urano and H. Mogami (2006). "Glucagon-like peptide 1 activates protein kinase C through $Ca^{2+}$-dependent activation of phospholipase C in insulin-secreting cells." J Biol Chem 281(39): 28499-28507.

Tang, C., P. Han, A. I. Oprescu, S. C. Lee, A. V. Gyulkhandanyan, G. N. Chan, M. B. Wheeler and A. Giacca (2007). "Evidence for a role of superoxide generation in glucose-induced β-cell dysfunction in vivo." Diabetes 56(11): 2722-2731.

Tansey, J. T., C. Sztalryd, E. M. Hlavin, A. R. Kimmel and C. Londos (2004). "The central role of perilipin A in lipid metabolism and adipocyte lipolysis." IUBMB life 56(7): 379-385.

Tchernof, A. and J.-P. Després (2013). "Pathophysiology of human visceral obesity: an update." Physiol Rev 93(1): 359-404.

Teerawattananon, Y. and A. Luz (2017). “Obesity in Thailand and its economic cost estimation.” ADB Institute 703.

Thilavech, T., S. Ngamukote, M. Abeywardena and S. Adisakwattana (2015). "Protective effects of cyanidin-3-rutinoside against monosaccharides-induced protein glycation and oxidation." Int J Biol Macromol 75: 515-520.

Thilavech, T., S. Ngamukote, D. Belobrajdic, M. Abeywardena and S. Adisakwattana (2016). "Cyanidin-3-rutinoside attenuates methylglyoxal-induced protein glycation and DNA damage via carbonyl trapping ability and scavenging reactive oxygen species." BMC Complement Altern Med 16(138): 1-10.

Thiranusornkij, L., P. Thamnarathip, A. Chandrachai, D. Kuakpetoon and S. Adisakwattana (2019). "Comparative studies on physicochemical properties, starch hydrolysis, predicted glycemic index of Hom Mali rice and Riceberry rice flour and their applications in bread." Food Chem 283: 224-231.

Tran, T. D. N., S. Yao, W. H. Hsu, J. M. Gimble, B. A. Bunnell and H. Cheng (2015). "Arginine vasopressin inhibits adipogenesis in human adipose-derived stem cells." Mol Cell Endocrinol 406: 1-9.

Tran, T. D. N., O. Zolochevska, M. L. Figueiredo, H. Wang, L.-J. Yang, J. M. Gimble, S. Yao and H. Cheng (2014). "Histamine-induced $Ca^{2+}$ signalling is mediated by TRPM4 channels in human adipose-derived stem cells." Biochem 463(1): 123-134.

Tsuda, T. (2012). "Anthocyanins as functional food factors—chemistry, nutrition and health promotion—." J Food Sci Technol 18(3): 315-324.

Turovsky, E. A., N. P. Kaimachnikov, M. V. Turovskaya, A. V. Berezhnov, V. V. Dynnik and V. P. Zinchenko (2012). "Two mechanisms of calcium oscillations in adipocytes." Biochem (Mosc) Suppl Ser A Membr Cell Biol 6(1): 26-34.

Turovsky, E. A., M. V. Turovskaya, V. P. Zinchenko, V. V. Dynnik and L. P. Dolgacheva (2016). "Insulin induces $Ca^{2+}$ oscillations in white fat adipocytes via PI3K and PLC." Biochem (Mosc) Suppl Ser A Membr Cell Biol 10(1): 53-59.

Tzeng, T.-F. and I.-M. Liu (2013). "6-Gingerol prevents adipogenesis and the accumulation of cytoplasmic lipid droplets in 3T3-L1 cells." Phytomedicine 20(6): 481-487.

Velasco, M., C. M. Díaz-García, C. Larqué and M. Hiriart (2016). "Modulation of ionic channels and insulin secretion by drugs and hormones in pancreatic beta cells." Mol Pharmacol 90(3): 341-357.

Wang, R., B. C. McGrath, R. F. Kopp, M. W. Roe, X. Tang, G. Chen and D. R. Cavener (2013). "Insulin secretion and $Ca^{2+}$ dynamics in β-cells are regulated by PERK (EIF2AK3) in concert with calcineurin." J Biol Chem 288(47): 33824-33836.

Wang, W. and P. Seale (2016). "Control of brown and beige fat development." Nat Rev Mol Cell Biol 17(11): 691-702.

Watanabe, Y., Y. Nagai and K. Takatsu (2013). "Activation and regulation of the pattern recognition receptors in obesity-induced adipose tissue inflammation and insulin resistance." Nutrients 5(9): 3757-3778.

WHO expert consultation (2004). "Appropriate body-mass index for Asian populations and its implications for policy and intervention strategies." Lancet 363(9403): 157-163.

World Health Organization (2000). “Obesity: preventing and managing the global epidemic.” WHO Techical Report Series 894.

Worrall, D. S. and J. M. Olefsky (2002). "The effects of intracellular calcium depletion on insulin signaling in 3T3-L1 adipocytes." Mol Endocrinol 16(2): 378-389.

Youl, E., G. Bardy, R. Magous, G. Cros, F. Sejalon, A. Virsolvy, S. Richard, J. F. Quignard, R. Gross, P. Petit, D. Bataille and C. Oiry (2010). "Quercetin potentiates insulin secretion and protects INS-1 pancreatic β-cells against oxidative damage via the ERK1/2 pathway." Br J Pharmacol 161(4): 799-814.

Yuenyongchaiwat, K., D. Pipatsitipong and P. Sangprasert (2017). "The prevalence and risk factors of metabolic syndrome a suburban community in Pathum Thani province, Thailand." SJST 39(6): 787-792.

Zhang, J., K. H. O. Pronyuk, O. V. Kuliesh and S. Chenghe (2015). "Adiponectin, resistin and leptin: possible markers of metabolic syndrome." Endocrinal Metab Syndr 4(4): 2161-1017.10002.

Zhang, Y. and D. Liu (2011). "Flavonol kaempferol improves chronic hyperglycemia-impaired pancreatic beta-cell viability and insulin secretory function." Eur J Pharmacol 670(1): 325-332.

Zhang, Z., X. Kou, K. Fugal and J. McLaughlin (2004). "Comparison of HPLC methods for determination of anthocyanins and anthocyanidins in bilberry extracts." J Agric Food Chem 52(4): 688-691.

Zhang, L. L., D. Y. Liu, L. Q. Ma, Z. D. Luo, T. B. Cao, J. Zhong, Z. C. Yan, L. J. Wang, Z. G. Zhao, S. J. Zhu, M. Schrader, F. Thilo, Z. M. Zhu and M. Tepel (2007). "Activation of transient receptor potential vanilloid type-1 channel prevents adipogenesis and obesity." Circ Res 100(7): 1063-1070.

Zheng, Y.-C., H. He, X. Wei, S. Ge and Y.-H. Lu (2016). "Comparison of regulation mechanisms of five mulberry ingredients on insulin secretion under oxidative stress." J Agric Food Chem 64(46): 8763-8772.

# VITA

| | |
|---|---|
| NAME | Phutthida Kongthitilerd |
| DATE OF BIRTH | 11 August 1993 |
| PLACE OF BIRTH | Bangkok, Thailand |
| INSTITUTIONS ATTENDED | Bachelor's degree of Science with first class honor (Major: Nutrition and Dietetics and Minor: Weight Control) in 2016 from Faculty of Allied Health Sciences, Chulalongkorn University, Bangkok, Thailand.<br>Research scholar in Department of Comparative Biomedical Sciences, School of Veterinary Medicine at Louisiana State University, Baton Rouge, LA, USA. September 2019 – February 2021 |
| HOME ADDRESS | Bangkok, Thailand |
| PUBLICATION | Kongthitilerd P, Suantawee T, Cheng H, Thilavech T, Marnpae M, Adisakwattana S. Anthocyanin-enriched Riceberry rice extract inhibits cell proliferation and adipogenesis in 3T3-L1 preadipocytes by downregulating adipogenic transcription factors and their targeting genes. Nutrients, 2020, 12(2480). |